A fresh soil health perspective: Soil health dynamics and improved measurement techniques

Ayush Joshi Gyawali

Dissertation submitted to the faculty of the Virginia Polytechnic Institute and State University in partial fulfillment of the requirements for the degree of

Doctor of Philosophy
In
School of Plant and Environmental Science

Committee:
Ryan D. Stewart
Michael S. Strickland
Wade E. Thomason
Steven C. Hodges

April 16, 2019
Blacksburg, Virginia

Keywords: Soil health indicators, temporal dynamics, aggregate stability, inexpensive tool, CO_2 measurement

A fresh soil health perspective: Soil health dynamics and improved measurement techniques

Ayush Joshi Gyawali

ACADEMIC ABSTRACT

Encouraging greater implementation of conservation agriculture practices such as reduced tillage and cover crops may require better understanding of the effect of these practices on soil health. The overall objective of this study was to quantify soil health dynamics due to conservation agriculture practices and address methodological gaps in terms of measuring soil health parameters. We developed five sites across the state of Virginia; each site had replicated plots with combinations of reduced tillage versus disk tillage and wintertime cover crops versus no cover crops as experimental treatments. Soil and plant samples were collected 1-2 times per year for 3 years, and were analyzed for 30 soil health parameters. The parameters were first evaluated to determine if any consistently detected treatment differences. We then quantified the temporal dynamics of the eight most responsive soil health parameters, while considering influences of soil water content at time of tillage, cover crop biomass, and previous land management history.

Of the analyzed parameters, only 2-4 mm aggregate stability and magnesium showed high responsiveness and consistency in identifying tillage and cover crop effects. None of the parameters detected treatment differences in all sites or at all times, yet samples collected after high biomass cover crops or after tillage in wet conditions tended to show significant treatment differences for multiple indicators. The previous history of management in each site may have affected trends in aggregate stability, but did not appear to influence other indicators.

As soil aggregate stability was found to be the most important soil health parameter, our third study developed an improved method for measuring soil aggregate stability. This new method, Integrated Aggregate Stability (IAS), interprets aggregate stability using a laser diffraction machine. Overall, IAS showed higher correlation with the wet sieving method (R^2 = 0.49 to 0.59) than widely used median aggregate size (d50) (R^2 = 0.09 to 0.27). IAS can also quantify stability of macro- and micro-sized aggregates, which d50 cannot. When comparing between IAS and wet sieving, IAS requires considerably less time and sample amounts.

Our fourth study focused on creating an inexpensive yet accurate tool for measuring soil respiration, as microbial assessments based on respiration rates have great potential for detecting rapid changes in soil health. Using an Arduino-based infrared gas analyzer (IRGA) sensor, we developed the Soil Microbial Activity Assessment Contraption (SMAAC) for less than $150. Our results show that SMAAC provided consistent readings with a commercial IRGA unit when tested using three different configurations.

Altogether, the research presented in this dissertation identifies important soil health parameters and quantifies their temporal and between-site dynamics. Using this narrower set of indicators can help producers and practitioners save resources when conducting measurements to assess soil health effects of agricultural practices. Further, this work also provides improved measurement techniques for useful soil health parameters like aggregate stability and soil respiration. These findings and innovations should help to encourage greater adoption of agricultural management practices that build and preserve soil health.

A fresh soil health perspective: Soil health dynamics and improved measurement techniques

Ayush Joshi Gyawali

GENERAL AUDIENCE ABSTRACT

If we want to make sure that ample and safe food is available to future generations, then it is time that we produce food without damaging the soil. Many widely used soil management techniques like tillage and leaving the field bare can harm the soil and decrease productivity in the long run. One potential technique to produce food while protecting the soil and environment is conservation agriculture, which can include reduced tillage and cover cropping. Reduced tillage is a technique in which we grow food without majorly disturbing the soil, while cover crops are planted when cash crops are not in the field in order to improve or sustain the soil.

Understanding the soil-related benefits of conservation agriculture practices is important to encourage farmers to adopt these practices. In this study we tested the effects on soils of reduced tillage and cover crop practices versus conventional tillage and bare soil practices, using five locations across Virginia. We also developed improved methods for measuring two informative soil parameters.

We found that, when looking at all of our five sites, the stability of soil aggregates, the rate at which water enters soil, and the nutrients in surface soils were all affected by the type of management that the soils were subjected to. Reduced tillage increased stability of soil aggregates when compared with conventional till. This increased stability of aggregates indicators lower potential for surface water runoff, erosion, and flooding when we practice reduced tillage. Cover cropping also increased stability of soil aggregates, especially when the cover crops attained substantial above-ground mass. Soil nutrients (which are essential for plants to grow) were also overall higher in the surface soil layers under no-till.

Since the stability of soil aggregates was found to be an important benefit of CA practices, we also perceived a need for a better method for measuring stability of these aggregates. In response, we developed a new index called Integrated Aggregate Stability (IAS). IAS was found to give similar results as established methods, but the time required to get IAS result is about 10 minutes, whereas the time required for established methods like wet sieving is around 2 days. IAS measurements are therefore both accurate and quick to perform.

We also focused on developing an inexpensive tool for measuring soil respiration. Soil respiration-based measurements help us to understand the activity of microbes in the soil. These microbes are very important for soils to function. Our tool, Soil Microbial Activity Assessment Contraption (SMAAC), was very consistent with a currently used tool and shows high potential for future use.

Altogether, we found that no-tillage and cover cropping can increase stability of soil aggregates even within 1-3 years of starting those practices. No-till can also increase nutrient concentrations in the top soil layer. The tools and innovations developed in this study have the potential to increase the ability of farmers to assess soil health and also encourage greater adoption of conservation agriculture practices.

Acknowledgement

I would like to thank my committee members, and especially my advisor Dr. Ryan Stewart, for their patience, encouragement and all the support they have given me throughout my time here at Virginia Tech. Without them I would not have gotten through this roller coaster ride known as Ph. D. My committee members supported me and encouraged me when the roller coaster was stagnating in the bottom sections. Without such committee members, I would not have been able to finish this roller coaster ride and get ready for other interesting rides in the amusement park called Science. I would also like to take this opportunity to thank my parents in Nepal for their continuous love and support. My parents make me feel important, which instills a huge amount of confidence in me. This confidence has helped me to get through even in the worst of times. My lab mates, Jesse Radolinski and Jingjing Chen, were always really helpful both for work or to go outside and have fun. I also received lot of laboratory and field help from undergraduate students: Matt DeAngelo, Ben Spencer, Mayanni McCourty, Victoria Schluszas, Jonathan Grubb, Camille VanSkiver, Alexis Gillmore, and Aaron Cleveland were all really helpful for my work. I would like to acknowledge all the staff here in the School of Plant and Environmental Sciences, and also staff working and helping graduate students at the AREC and other fields. Without these staff, getting all of the field as well as laboratory work done for my Ph. D. would have been impossible. I would like to mention a few names here: Dr. Mark Reiter, Dr. David Reed, Julia Burger, Brandon Lester, Patricia Donovan, Brooks Saville, Jr., and Athena Tilley were all very helpful at various stages of my Ph.D. I would also like to thank Christopher Brown and Dr. Tim Durham for helping me set up and manage the plots in Ferrum. Likewise, Mike Phillips helped me to set up and manage the plots in Harrisonburg, while also filling me up with enthusiasm about soil every time I met him. Besides the technical staff, my friends here at Virginia Tech have also helped me in each and every step. I never felt as being away from home, this felt like home because of them. Lastly, I would also like to thank my Nepalese community in Blacksburg. They have been always supportive and I am sure they will continue to help all Nepalese folks in need. I would like to thank all these folks from the bottom of my heart. Thanks!!!!

Table of Contents

Chapter 1. Introduction

Conservation agriculture, which is an approach that attempts to optimize both the productive (in terms of yield) and protective (in terms of environment) aspects of agriculture, has been suggested as a way to increase sustainability and security in our food supply by various non-governmental organizations (Kassam, et al., 2009) and governmental agencies (Akram-Lodhi, 2008). A variety of conservation agriculture practices exist, with the most common being use of reduced tillage, cover crops during fallow periods, and crop rotations (Friedrich, et al., 2012). Reduced till is a conservation agriculture practice where soil tillage is reduced or eliminated compared to traditional cultivation methods (Uri, 2000). In the case of no-till farming, soil disturbance is often limited to seed planting (e.g., cash or cover crops), though subsoiling may be used to break up subsurface compaction layers (Jin, et al., 2006). Another popular conservation agriculture practice is use of cover crops. Cover crops are the plants that are cultivated in the field after the harvest of one cash crop and before the planting of another cash crop (Fageria, et al., 2005), with the primary goal of providing benefits to the soil such as reduced erosion (Hartwig and Ammon, 2002). Cover crops are often terminated using herbicides and left in the field as residue, but can also be mechanically rolled or crimped (Davis, 2010), harvested for forage or grazed (Sulc and Tracy, 2007), or even tilled into the soil (Halde, et al., 2015).

Conservation agriculture practices be costly to producers in terms of new equipment and extra input costs. Reduced-till can cause short-term declines in yield (Kladivko, et al., 1986, Ogle, et al., 2012, Pittelkow, et al., 2015). Together these factors have limited the producer adoption of these practices (Krueger, et al., 2011, Snapp, et al., 2005). It is therefore important to

understand and quantify any benefits of these practices of soil function and soil health, which may help to encourage producer adoption.

Soil health refers to the capacity of soil to sustain plant and animal productivity and preserve agroecosystem function, and is represented by integrated soil biological, physical and chemical properties (Doran and Zeiss, 2000). Conservation agricultural practices can have positive effect on soil health, particularly over periods of many years. For example Hernanz, et al. (2002) observed that after more than a decade of treatment application, soil organic carbon was higher in no-till fields compared to conventional till ones. By contrast, short term benefits in soil health that can result from conservation agricultural practices are not well quantified. Quantification of soil health indicators also involves addressing temporal (Hu, et al., 2018), spatial (Cardoso, et al., 2013, Zuber and Villamil, 2016) and history of management variations (Jangid, et al., 2011) in parameter values. Consequently, the concept of soil health as a motivating factor to encourage adoption of conservation agricultural practices faces two main challenges: 1) soil health parameters that consistently respond to conservation agricultural practices must be identified, and 2) short-term (i.e., < 3 years) soil health benefits must be quantified. Overcoming these challenges can help encourage to farmers to adopt conservation agriculture practices despite concerns of associated costs.

This dissertation addressed the first challenge in Chapter 2, where the aim was to identify a smaller set of soil health parameters that are responsive and show consistent effects to conservation agricultural practice like reduced tillage and cover crops. In that study we developed five experimental sites across Virginia: Our imposed treatments were 1) reduced tillage with cover crops, 2) reduced tillage without cover crops, 3) conventional tillage with cover crops, and 4) conventional tillage without cover crops. Treatments were put in place

September 2015 and soil and plant samples were taken April 2016 and April 2017. A total of 30 soil health parameters were measured. A multivariate approach was used to detect for treatment differences, visualize the differences and determine the parameters driving the treatment differences observed. These multivariate approach were used instead of multiple univariate analysis (e.g., multiple analyses of variations, multiple regressions) because univariate approaches can be hindered by problems of multicollinearity between different parameters, which makes the underlying assumptions of independence invalid. Using information from our multivariate approach, two new indices were developed to quantify the responsiveness, Proportional Response (PR), and consistency, Consistency Parameter (CP), of soil health parameters. These indices were developed as no index was found that could quantify the responsiveness and consistency of soil health parameters.

The dissertation addressed the second challenge in Chapter 3, where the aim was to quantify temporal dynamics in eight parameters identified as being responsive in Chapter 2. Both chapters used data from the same set of experimental plots; however, in contrast to the earlier chapter, Chapter 3 focused on trends in individual parameters, and included more data points (five sampling times) for all eight parameters. In Chapter 3 we examined how differences in soil texture, cover crop biomass, and water content at time of tillage may help explain variability in indicator responses, including why specific sampling times showed pronounced effects of reduced till and cover crops across parameter types. Lastly, our five sites had different management histories prior to the start of the study, providing the opportunity to evaluate the influence of initial soil health on the subsequent trends of different parameters.

The results of both Chapter 2 and Chapter 3 suggested that soil aggregate stability is a parameter with high importance to soil health. However, soil aggregate stability is often

measured using a set of sieves repeatedly passed through water. This approach has many drawbacks, including a lack of repeatability (Amézketa, 1999), inadequate ability to quantify or regulate input energy, limited number of sieve sizes (Rawlins, et al., 2013), and bias towards larger aggregates sizes (Tisdall and Oades, 1982). As a result, Chapter 4 focused on developing an improved method for soil aggregate stability. This method uses laser diffraction-based size measurements to compare aggregated versus dispersed samples. Using laser diffraction with a built-in ultrasonic unit allows for controlled energy inputs, which can be used to evaluate aggregate stability across a range of conditions. We then developed a new indicator to interpret these results called Integrated Aggregate Stability (IAS), which corrects for the underlying particle size distribution of the soil. We then compared aggregate stability measurements for three different soils that were collected using both the proposed indicator and the established wet sieve method, before concluding the chapter with examples of how this indicator can be used to study aggregate stability dynamics as a function of applied energy.

Finally, the results in Chapters 2 and 3 suggested that soil biological indicators did not respond consistently to the imposed treatments. One possible reason for this finding is that biological parameters may fluctuate on shorter time-scales than chemical or physical properties (Cardoso, et al., 2013, Kibblewhite, et al., 2007, Ritz, et al., 2009). To understand the effects of conservation agriculture practices on soil microbial communities and soil biological functioning, we need the ability to conduct such measurements at finer temporal scales and with sufficient number of replicates to properly sample across spatial variation. Current methods to assess soil respiration use gas chromatography (McGowen, et al., 2018) or infrared gas analyzers (IRGAs). IRGA-based measurements have also been used to study microbial community composition (Fierer, et al., 2003), which represents one of the important properties related to soil function

(Mukhopadhyay, et al., 2014). However, these widely used soil respiration techniques are often expensive, putting them beyond the means of many practitioners, and power-intensive, limiting their usefulness in the field. In Chapter 5 I discussed an inexpensive Arduino-powered and IRGA-based CO_2 measurement device that we developed to address the above-mentioned shortcomings. The device is called the Soil Microbial Activity Assessment Contraption (SMAAC), and can be constructed for less than $150, providing the promise of widespread usage if successfully developed. SMAAC performance was verified by comparing its measurements with those from a commercial field-portable IRGA system.

In total, the research encompassed in this dissertation aimed to accurately and consistently quantify short-term soil health benefits due to conservation agriculture. The innovations in methodology and understanding represented in this work may help to encourage farmers to adopt more conservation agriculture practices, as we together move towards a sustainable world.

Chapter 2. A multivariate approach to quantify responsiveness and consistency of soil health parameters

To be submitted to *Soil and Tillage Research*

2.1 Abstract

Quantifying soil health requires measuring a large set of soil physical, chemical and biological properties, yet limits in time and funding often mean that it is not possible to measure all recommended parameters. The main objective of this research was to identify a smaller set of soil health parameters that show consistent responses to conservation agricultural practice like reduced tillage and cover crops. The treatments (reduced tillage with cover crops, reduced tillage without cover crops, conventional tillage with cover crops and conventional tillage without cover crops) were installed in September 2015 in five sites across the state of Virginia. Soil and plant samples and measurements taken in April 2016 and April 2017 were used to quantify a total of 30 soil health parameters. A multivariate approach was then used to detect treatment differences and determine the parameters driving those differences. Using information from our multivariate approach, we developed two new indices to quantify the responsiveness, Proportional Response (PR), and consistency, Consistency Parameter (CP), of measured soil health parameters. The results showed that the surface soil layers had a greater number of significant differences in parameter values between treatments compared the subsurface layers. Tillage effects were observed faster (within 0.5 years of treatments) than cover crop effects, which only appeared after 1.5 years. In terms of PR, field-saturated hydraulic conductivity, aggregate stability, soil phosphorous, potassium, calcium, magnesium, boron, and cation exchange capacity were found to be the most responsive soil health parameters. Aggregate stability and magnesium parameters also showed high CP values. Soil aggregate stability correlates to a wide range of soil functions, suggesting that parameter may be among the most use for quantifying soil health.

2.2 Introduction

More than 10 billion people may inhabit the planet by 2050 (Lutz, et al., 2017); meeting the food demands of this rapidly growing and increasingly wealthy population will require agricultural intensification (Foley, et al., 2011). Agricultural intensification based on intensive tillage and residue loss can negatively affect surrounding agroecosystems (Keesstra, et al., 2016, Tilman, et al., 2001) and may cause yield declines over long periods (Friedrich, et al., 2012, Rusinamhodzi, et al., 2011). To address these concerns, conservation agriculture was developed. Conservation agriculture is an approach that attempts to optimize both the productive (in terms of yield) and protective (in terms of environment) aspects of agriculture. The most common conservation agricultural practices are reduced tillage, use of cover crops during fallow periods, and crop rotations (Friedrich, et al., 2012).

Conservation agricultural practices have been evaluated by quantifying their effect on soil health. Soil health refers to the capacity of soil to sustain plant and animal productivity and preserve agroecosystem function, and is represented by integrated soil biological, physical and chemical properties (Doran and Zeiss, 2000). Quantifying soil health typically involves measurement of a large set of soil properties. For example, Stewart et al. (2018) identified 42 types of parameters that have been used to assess effects of agricultural practices on soil health. Due to limited resources such as time and funding, it is often not possible to measure all or even most of these parameters. In this regard, it is important to identify a smaller set of soil health parameters that detects dynamic variations in soil health while conveying information about soil functions and processes. In particularly, it is important to identify soil parameters that have a high and consistent response to management practices (Cardoso, et al., 2013).

Different approaches have been used to identify soil health indicators that are most responsive to conservation agriculture management practices, including using meta-analyses (e.g., Stewart et al., 2018), multiple univariate analyses (Graham, 2003), and expert opinions to weigh scores representing various functions of soil (Karlen, et al., 1994). Meta-analyses have the advantage of identifying trends across many studies, but may not be useful when assessing individual operations. Opinion-based approaches may suffer from bias and can produce non-repeatable results (Andrews, et al., 2002). Multiple univariate analyses (e.g., multiple analyses of variations, multiple regressions) are hindered by problems of multicollinearity between different parameters, which makes the underlying assumptions of independence invalid.

Multivariate analysis represents a more recent approach designed to counter shortcomings of these other methods (Brejda, et al., 2000, Nosrati, 2013, Shukla, et al., 2006, Zuber, et al., 2017). Still, multivariate approaches have not yet been applied to quantify soil health indicator responses to use of cover crops, either alone or in combination with reduced tillage. With agencies such as the U.S. Department of Agriculture Natural Resources and Conservation Service (USDA NRCS) encouraging increased adoption of cover crops and reduced tillage, identifying the most responsive indicators will allow producers to assess the ability of these practices to improve soil health.

In this study we sampled five sets of plots across Virginia over a two-year period, with the goal of evaluating the responsiveness of different soil health indicators to conservation agriculture practices (i.e., reduced tillage and use of overwinter cover crops). The experimental plots included four treatments that combined different tillage and cover crop practices. Our main study objective was to identify single indicators or combinations of indicators that consistently detected treatment differences. By assessing the responsiveness of various indicators and

identifying those with the most consistent ability to detect differences due to soil management, the results of this study will offer producers the ability to better monitor and optimize their practices to improve soil health.

2.3 Methods and Materials

We performed this study at five sites located across the state of Virginia (Figure 2.1).

i)

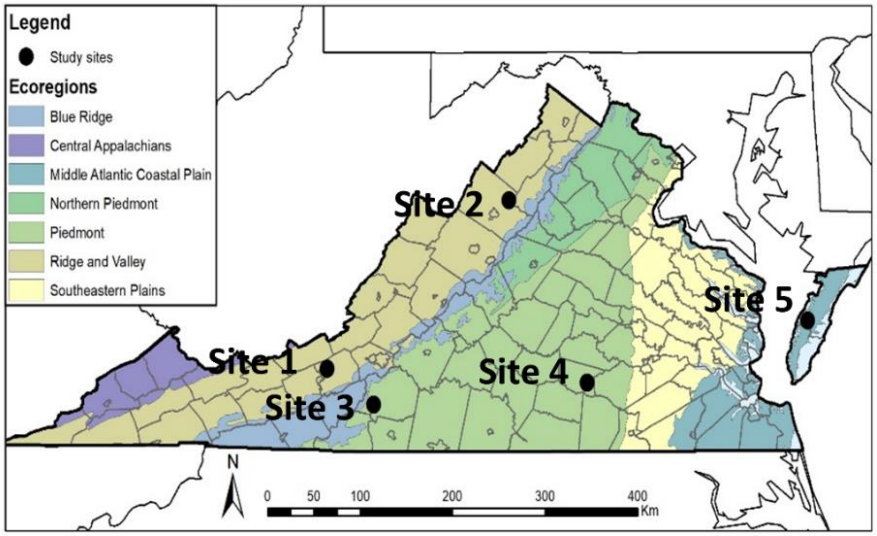

ii)

2014	2015			2016			2017
Sites	July	Sep	Oct	April	May	Sep	April
Site1			Cover crop		Corn		Cover crop
		T		*#	R T	#T	#*
Site 2			Cover crop		Corn		Cover crop
		T		*#	R T	#T	#*
Site 3			Fallow		Corn		Cover crop
		T		*	R T	#T	#*
Site 4			Cover crop		Tobacco		Cover crop
		T		T*#	R	T	#*
Site 5			Cover crop		Corn		Cover crop
		T		*#	R T	T	#*

* Soil sample taken
\# Plant sample taken
R Glyphosate application
T Tillage done on the tilled plots

Figure 2.1: i) Map of Virginia showing site locations, and ii) timeline of cover and cash crop plantings, soil and plant samplings, herbicide application, and tillage.

2.3.1 Description of sites

Site 1 was located in Blacksburg, Virginia, 6 km west of the Virginia Tech campus (37°12'25.3"N 80°29'12.0"W) in a long term no-till corn field. The soil was a Duffield-Ernest-Purdy undifferentiated group: Duffield – *Fine-loamy, mixed, active, mesic Ultic Hapludalfs*; Ernest - *Fine-loamy, mixed, superactive, mesic Aquic Fragiudults*; Purdy - *Fine, mixed, active, mesic Typic Hapludalfs.* (NRCS, 2018).

Site 2 was located in Harrisonburg, Virginia (38°32'46.70"N 78°43'22.17"W). Prior to the start of the experiment, the field was in a no-till corn/cereal crop rotation with winter cover crops. In the year prior to the installation of experimental treatments, the field had been planted with 23 species of cover crops. The soil was a Frederick and Lodi complex – *Fine silt loam, mixed, semiactive, mesic Typic Paleudults* (NRCS, 2018).

Site 3 was located in Ferrum, Virginia (36°55'8.51"N 80° 2'13.24"W). Prior to the experiment, the field was a lightly grazed pasture with fescue. The soil was a Bluemont-Spriggs-Redbrush complex – *Fine-loamy, mixed, superactive, mesic Typic Hapludalfs* (NRCS, 2018).

Site 4 was located in Blackstone, Virginia (37° 5'43.82"N 77°57'40.16"W). The field was previously a non-grazed pasture with fescue. The soil was a Appling coarse sandy loam and Durham coarse sandy loam: Appling coarse sandy loam **–** *Fine, kaolinitic, thermic Typic Kanhapludults*; Durham coarse sandy loam - *Fine-loamy, siliceous, semiactive, thermic Typic Hapludults* (NRCS, 2018).

Site 5 was located in Painter, Virginia (37°35'26.44"N 75°49'18.84"W). The field was most recently managed as a conventional tilled potato field. The soil was a Bojac sandy loam – *Coarse-loamy, mixed, semiactive, thermic Typic Hapludults*. (NRCS, 2018).

2.3.2 Experimental Design

Our experimental design had two factors: tillage and cover cropping. These factors led to four experimental treatments: 1) reduced tillage with winter cover crops (RT CC); 2) reduced tillage without winter cover crops (RT NC); 3) conventional tillage with winter cover crops (CT CC); and 4) conventional tillage without winter cover crops (CT NC). In Sites 1, 2, and 3, we used a split-plot experimental design in which tillage was the whole plot factor and cover cropping was the sub-plot factor. Sites 4 and 5 had a complete randomized design.

We performed disk tillage on the conventional tillage plots every September (after cash crop termination) and every April (after cover crop termination), starting in September 2015. For the reduced tillage treatments, we used no-till for Sites 1-3 and 5 and strip tillage for Site 4, since no-till was not possible in tobacco production. Strip tillage occurred in April after cover crop termination.

We planted the cover crop treatments within relevant plots following tillage each September starting in 2015 (note that Site 3 was not planted in cover crops until September 2016). Our cover crops were a three-way mixture of winter barley (*Hordeum vulgare*), crimson clover (*Trifolium incarnatum*) and tillage radish **(***Raphanus raphanistrum* subsp. *sativus***).**

Sites 1-4 had eight physically replicated plots (two for each treatment), with two subplots within each main plot ($n = 4$). Site 5 had twenty-four physical plots ($n = 4$). Physically replicated plots had the following dimensions: 24.4 m x 30.5 m in Site 1, 6.1 m x 22.9 m in Site 2, 18.3 m x 36.6 m in Site 3, 19.0 m x 25.0 m in Site 4, and 3.05 m x 61.0 m in Site 5.

2.3.3 Soil sampling

In April 2016 and April 2017, we collected loose soil samples from the surface (0-10 cm) and subsurface (10-20 cm) soil layers of the soil profile ($n = 4$ per layer and treatment). We then

split the loose samples into two sub-samples. One sub-sample was air dried for determination of soil aggregate stability and soil chemical parameters, while the other was stored in 4 °C until being tested for soil biological parameters. Note that samples were collected prior to spring tillage, with the exception of Site 4 in April 2016, where tillage took place before sampling (Figure 2.1). We also collected soil core samples at Sites 1-3 to measure bulk density and porosity. Overall we collected 304 loose soil samples and 192 core samples. We then analyzed those samples for a total of 30 soil health parameters, including 12 microbiological parameters, 12 chemical parameters, 6 physical parameters. These parameters represent a combination of field-measured and lab-measured quantities.

2.3.4 Field-measured parameters

Field saturated hydraulic conductivity (K_{fs})

Field-saturated hydraulic conductivity represents the ability of water to intake water under realistic field conditions. We estimated K_{fs} using a minidisk tension infiltrometer (METER Group, Inc.; Pullman, USA), with the tension set to -2 cm. K_{fs} was calculated from the measured infiltration rates using the Zhang (1997) solution, with the α term based on the soil texture for each site. We collected 160 K_{fs} measurements in total.

Soil respiration (SR)

Soil respiration is measurement of CO_2 flux from the soil. This soil respiration is total of heterotrophic microbial plus root respiration. We measured soil respiration using a LI-COR 8100 (LI-COR, Nebraska, USA). To perform the measurements, we installed a 20 cm diameter ring to a depth of approximately 3 cm into the soil. A 2-minute soil CO_2 flux measurement was then obtained from LI-COR 8100. We collected 160 soil respiration measurements over the two-year study period.

2.3.5 Laboratory-measured parameters

Microbial biomass Carbon (MBC) and Microbial Biomass Nitrogen (MBN)

Total (active + inactive) microbial biomass contains mostly microbial C and microbial N. Microbial C can be assessed to determine the sequestering of carbon versus loss of carbon as CO_2. The total microbial biomass was estimated using a modified chloroform fumigation extraction method. Here chloroform was used to lyse the cell membranes of the microbes. Microbial biomass C and N was measured as a difference between C and N in chloroform-fumigated subsamples versus un-fumigated subsamples. The detailed description is presented in Fierer and Schimel (2002) and Fierer and Schimel (2003).

Catabolic Response Profile (CRP) and Microbial Functional Evenness (MFE)

The difference in substrate utilization between microbial communities in the soil is catabolic response profile (CRP). CRP can be quantified using the multiple substrate-induced respiration technique described by Degens and Harris (1997). We used water versus five different organic substrates: glucose, glycine, oxalic acid, cellulose and chitin (Strickland, et al., 2017). CRP quantifies the functional diversity of microbes, based on the relative use of the substrate. Here the use of a substrate is quantified by measuring the CO_2 respiration by an infrared gas analyzer (IRGA; Model LI-7000, Li-Cor Biosciences, Lincoln, NE, USA). The respiration from each of the six substrate was used individually to look for treatment differences.

The information from CRP (six substrates) was also used to calculated Microbial Functional Evenness (MFE) using the Simpson-Yule index: $MFE = 1 / \sum(p_i/t_i)^2$ where p_i is the respiration response due to a substrate and t_i is the total response due to all substrates used (Magurran, 1988, Schipper, et al., 2001). MFE calculated using CRP data was also used to look for treatment differences.

Substrate induced respiration (SIR)

The substrate induced respiration (SIR) technique is used to quantify active microbial biomass (Wardle and Ghani, 1995). Here we followed the procedures of Fierer and Schimel (2003). In our experiment, after a 1-hour pre-incubation with excess autolyzed substrate, we incubated soil slurries for 4 hours at 20 °C. We then measured CO_2 using an infrared gas analyzer (IRGA; Model LI-7000, Li-Cor Biosciences, Lincoln, NE, USA).

Mineralizable carbon (Cmin)

Mineralizable carbon quantifies the rate at which organic matter in the soil will be broken down by the microbes in the soil at optimum temperature and moisture. Mineralizable carbon represents the labile soil carbon pool, and is determined using a static incubation technique for 60 days with periodic determinations of respiration rates (Fierer, et al., 2005). Here, we incubated (20 °C) soil samples in 50 ml tube for 60 days at 60% field capacity. These samples were measured for respiration every week. One day before the measurement, the samples were taken out of the incubator and flushed using CO_2 free air and capped again to obtain accurate respiration rates. The detailed method can be found in Strickland, et al. (2010).

pH

Soil pH (1:1, soil:H2O by volume) was determined on a 3100M benchtop pH meter (OHAUS, Inc., Parsippany, USA).

Elemental analysis

Phosphorous (P), Potassium (K), Calcium (Ca), Magnesium (Mg), Zinc (Zn), Manganese (Mn), Copper (Cu), Iron (Fe), Boron (B), and Aluminum (Al) were analyzed using a Mehlich 1 extracting solution that was analyzed using an ICP-AES (inductively coupled plasma atomic emission spectrometer; CirOS VISION model/Spectro Analytical Instruments/Kleve/Germany).

Soil aggregate stability (AS_2mm, AS_0.25mm, and AS_0.053mm)

We analyzed soil aggregate stability using a modified wet sieve method (Kemper and Rosenau, 1986). Each sample was air-dried and gently sieved through 4 mm sieve. 50 grams of sample was then placed on top of nested sieves: 2, 0.25, and 0.053 mm. The sieve setup with the soil was lowered into the water and submerged for 5 minutes. After 5 minutes, we vertically oscillated the sieves 50 times by hand. The soil remaining in each sieve was dried weighed and corrected for pebbles and sand content. Aggregate stability of each size fraction was quantified as a percentage of the initial sample weight corrected for moisture, pebbles and sand content.

Bulk Density (BD)

Soil bulk density was quantified from the soil cores by weighing the oven-dried soil mass and using the volume of the sampling ring, 231.55 cm^3 (Blake and Hartge, 1986). Particle density was assumed to equal 2.65 g cm^{-3}.

Porosity

Quantification for the intra and inter-aggregate pores in soil is important because the pores play a vital role in water and air movement in soil (Schoenholtz, et al., 2000). Porosity in our study was quantified using intact cores from the field as per Danielson and Sutherland (1986), in which intact cores of known volume were saturated, weighed, then oven-dried and weighed again.

Cover crop and weeds above-ground biomass

Above-ground biomass was quantified for all plots using a 0.3 m x 0.3 m quadrat that was randomly placed within the plots at the time of cover crop maturity (i.e., April 2016 and April 2017; Figure 1). Two samples were collected in each plot and a total of 144 samples for cover crops and any weeds were taken. The biomass was cut at the soil surface, with the

aboveground matter brought to the lab and weighed. After weighing, the sample was dried in a dryer and then weighed again. Using these weights, we calculated the dry biomass per area. Note that the April 2016 sampling in Site 4 occurred after tillage (Figure 2.3.1), so cover crop biomass samples were only collected in the strip till plots. In April 2017, the plant samples were collected prior to tillage, and therefore all plots and treatments were analyzed for above-ground biomass.

Total soil carbon

Total soil carbon was also used as a supplemental information for this chapter. We quantified total soil carbon as fractions of particulate organic matter carbon (POM C) and mineral associated carbon. The fractionation was done using sodium hexa-meta phosphate (Na-HMP) and the percent carbon values were determined using NA1500 CHN Analyzer (Carlo Erba Strumentazione, Milan, Italy). For details please refer to Bradford, et al. (2008) and Strickland, et al. (2010).

2.3.6 Statistical analyses

All statistical analyses were performed using R Version 3.5.0 (R Development Core Team, 2018).

First, soil carbon and cover crop biomass were compared between the five sites using analysis of variance (ANOVA) with Tukey's HSD. Dry cover crop biomass in the cover crop plots were also compared with dry biomass of weeds in the no cover crop plots using Student's t-test.

Next, we conducted multivariate statistics on our 30 quantified soil health parameters. We subsetted the data by site (1-5), sampling depth (top and sub) and sampling time (April 2016 and April 2017), and removed any missing values. In total 20 subsets were obtained; for each subset, we used permutation MANOVA (perMANOVA) with the function *Adonis* in the Vegan

2.5-2 package for R (Oksanen, et al., 2018) to look into overall treatment differences. Whenever interaction effects were observed for the treatments, the *Pairwise.Adonis* function was used as a post hoc test. The assumption of equal dispersion was checked by using the *betadisper* and *anova* functions in R. If any treatment differences were observed by perMANOVA ($P < 0.05$), then non-metric multidimensional scaling (NMDS) plots were made to visualize those differences (Figure 2.2).

To further identify which parameters caused these differences, we used the *envfit* function in the package Vegan 2.5-2. All parameters with $P < 0.05$ in the *envfit* results were included in NMDS plots to analyze the direction(s) corresponding to soil health parameters and treatment differences. For example, Figure 2.2i shows that treatments were different only along NMDS 1, and that 7 soil health parameters showed significance via *envfit* ($P < 0.05$). By contrast, Figure 2.2ii shows that the treatments were different along both NMDS 1 and NMDS 2, with 10 soil health parameters showing significance via *envfit*. NMDS plots showing perMANOVA detected differences and *envfit*-detected parameters are presented in Appendix A.

The function *ordisurf* was used with *nmds* function to get the Pearson's *r* correlation value, which was used to verify that the selected parameters were correlated with treatment differences rather than responding to overall variations in the data. For example in Figure 2.2i, Parameter 6 may have appeared significant because it is responding to the overall variation, yet may not help in detecting treatment differences. When treatments differed primarily along NMDS 1 (Figure 2.2i) then only those parameters that were significantly correlated with NMDS 1 ($|r| \geq 0.5$) were retained. When treatments differed along an axis that corresponded to both NMDS 1 and NMDS 2 (Figure 2.2ii), then only those parameters which were significantly correlated with at least one of the NMDS axes ($|r| \geq 0.5$) were retained. These retained

parameters for each significant treatment detection were used for the calculation of the Proportional Response (PR).

Note that the results presented in the main section of this study (Section 2.4) include all parameters that corresponded to any treatment differences, regardless of whether those differences were due to cover crops, tillage, or interactions between them. Appendix A isolates the parameters that detected cover crop and tillage treatment differences via the perMANOVA analysis.

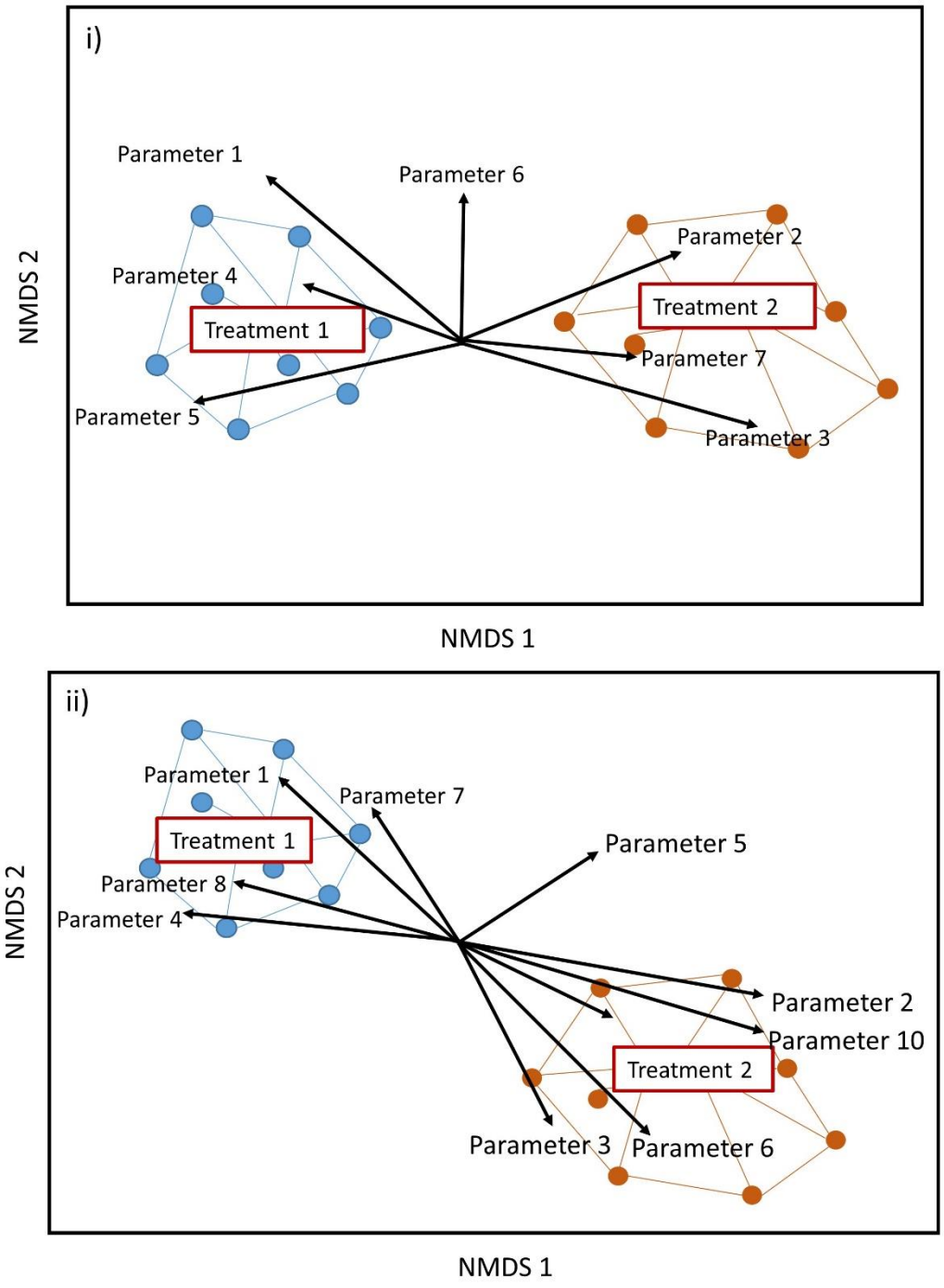

Figure 2.2: Example NMDS plots where the treatment differences are along i) only NMDS 1 versus ii) both NMDS 1 and NMDS 2. The parameters represent soil health indicators that were determined to be significant via the *envfit* function ($P < 0.05$).

2.3.7 Proportional Response (PR) calculation

To quantify the responsiveness of the 30 soil health parameters to the imposed tillage and cover crop treatments, we developed a metric called Proportional Response (PR):

$$PR = N_{td} / N_{total} \quad [2.1]$$

where N_{td} represents the number of instances that the parameter detected significant treatment differences ($P < 0.05$) and N_{total} represents the total number of times that the parameter was used in the perMANOVA analysis. The calculation was done for each soil depth at each site. Since there were two sampling times at five different sites, N_{td} had possible integer values between 0 and 10 for each sampling depth. *PR* values > 0.1 indicate that the parameter detected treatment differences at least once. Higher *PR* values signify parameters that more frequently detected differences between treatments.

2.3.8 Consistency parameter (CP) calculation

We also evaluated the temporal consistency of soil parameters in terms of ranking the four treatments. First, we took the mean values for each parameter based on the combination of sampling date, sampling depth, site and treatment (i.e., every parameter had one mean value per treatment at every site for each sampling date and depth). We then used the Spearman correlation (r_s) to determine rank correlations between parameter values in April 2016 and 2017. The r_s was then used to calculate the consistency parameter, *CP*:

$$CP = \frac{1}{n}\sum_{j=1}^{n} r_{s,j} \quad [2.2]$$

where *j* indexes the study site and n = 5 sites. Note that *CP* can vary from -1 to +1. A *CP* value of +1 indicates that the parameter showed identical treatment rankings and a value of -1 indicates perfectly inversed rankings between the two study years (2016 and 2017) at all five sites.

2.4 Results

2.4.1 Total soil carbon and cover crop biomass

The five sites used for this study had differences in total soil carbon concentrations (Figure 2.3). Site 3 had significantly higher soil carbon than all other sites while Site 5 had significantly lower soil carbon than all sites except Site 4 (ANOVA with Tukey's HSD; $P < 0.05$).

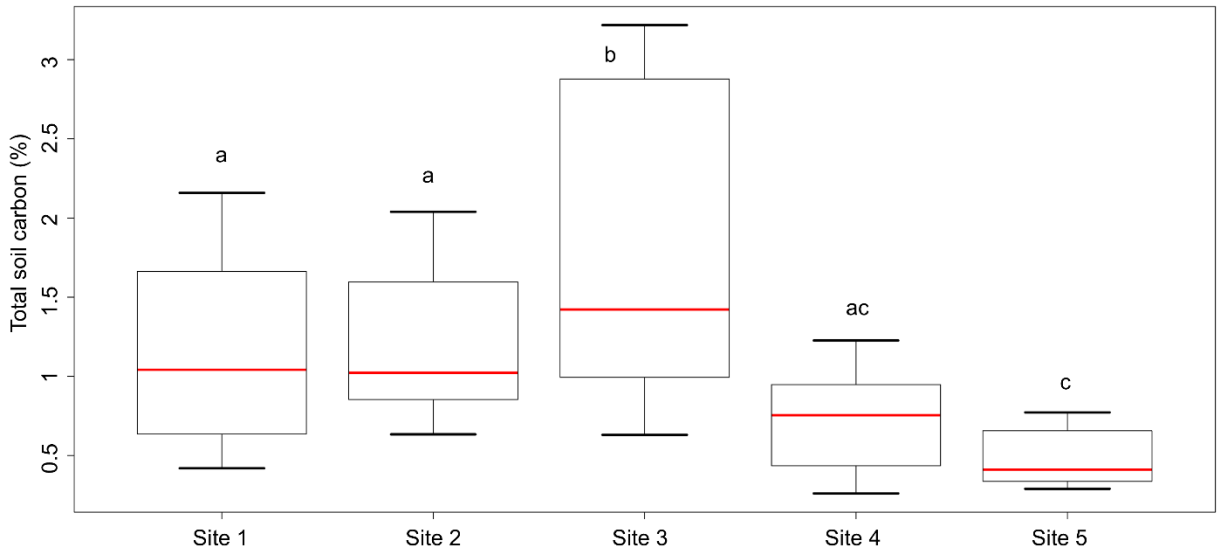

Figure 2.3: Overall soil carbon content (all plots and all soil layers) for each site. Sites associated with different letters are statistically different (ANOVA with Tukey's HSD; $P < 0.05$). Samples were collected in April 2016.

Even though the same cover crop mixture was planted at same seeding rate without fertilization, the resulting cover crop biomass differed between the five sites (Figure 2.4). In April 2017, Sites 2 and 5 had the highest dry cover crop biomass while Sites 1 and 4 had the lowest (ANOVA with Tukey's HSD; $P < 0.05$). In all the five sites, amounts of dry cover crop

biomass in the cover crop plots were significantly higher than dry weed biomass in the no cover crop plots (Student's t-test; $P < 0.05$). In case of Site 4, no biomass was present in the no cover plots.

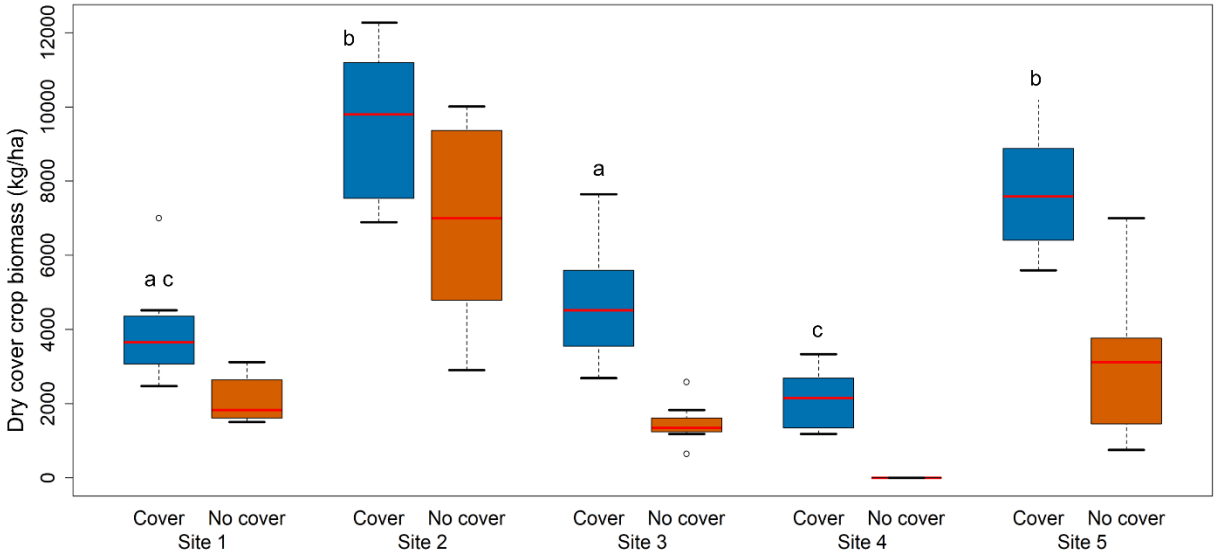

Figure 2.4: Dry biomass in the cover crop (blue) and no cover crop (orange) plots for all five sites for April 2017. Sites associated with different letters are statistically different (ANOVA with Tukey's HSD; $P < 0.05$).

2.4.2 PerMANOVA analysis

The permutational MANOVA (perMANOVA) analysis detected significant treatment differences in four of the five sites ($P < 0.05$; Figure 2.5). During the first sampling event (April 2016), Sites 1 and 4 showed significant tillage effects in the surface soil and Site 2 showed significant interactions between treatments in the subsurface soil. The post hoc test suggested that this interaction was driven primarily by tillage (RT CC > CT CC). During the second year, tillage differences were detected in the surface soils at Sites 1 and 3, and in the subsurface soil at

Site 1. Cover crop treatments also caused significant differences in the surface soils during the second year at Sites 2 and 4. Most treatment differences were observed in the surface soils (6 instances where treatment differences were identified) compared to subsurface soils (2 instances). All of the detected treatment differences shown in Figure 4 was also visualized using NMDS plots in Appendix A (Figures A1-A8).

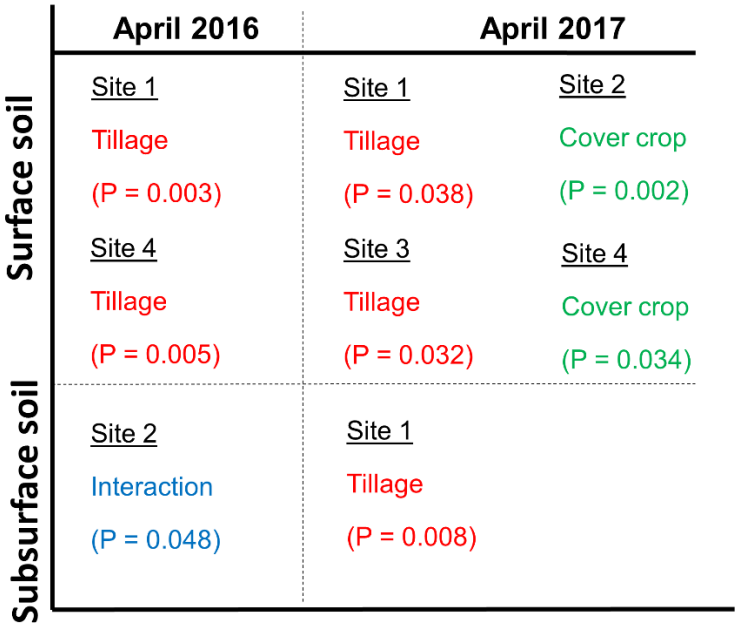

Figure 2.5: A summary of the significant treatment differences quantified using permutational MANOVA.

2.4.3 Proportional response

The proportional response (PR) analysis determined that 23 of 30 parameters had *PR* values > 0.1 in the surface soil samples and 14 out of 25 had *PR* values > 0.1 in the subsoil samples (Figure 2.6), meaning that the soil health parameters detected treatment differences more often in the surface compared to subsurface soil layers. K_{fs}, AS_2mm, P, K, Ca, Mg, B and CEC all had *PR* values of 0.4 or 0.5, meaning that those parameters detected treatment

differences in 40-50% of the sampling times. Further, these soil health indicators were found to detect treatment differences in 4 of the 5 sites, though none of the parameters detected differences in Site 5 (Figure 2.6). Specific parameters that detected cover crop related differences were Cmin, CRP oxalic_acid respiration, AS_0.053mm, K_{fs}, P, K, Ca, Mg, B, Al, and CEC (Figures A7 and A8).

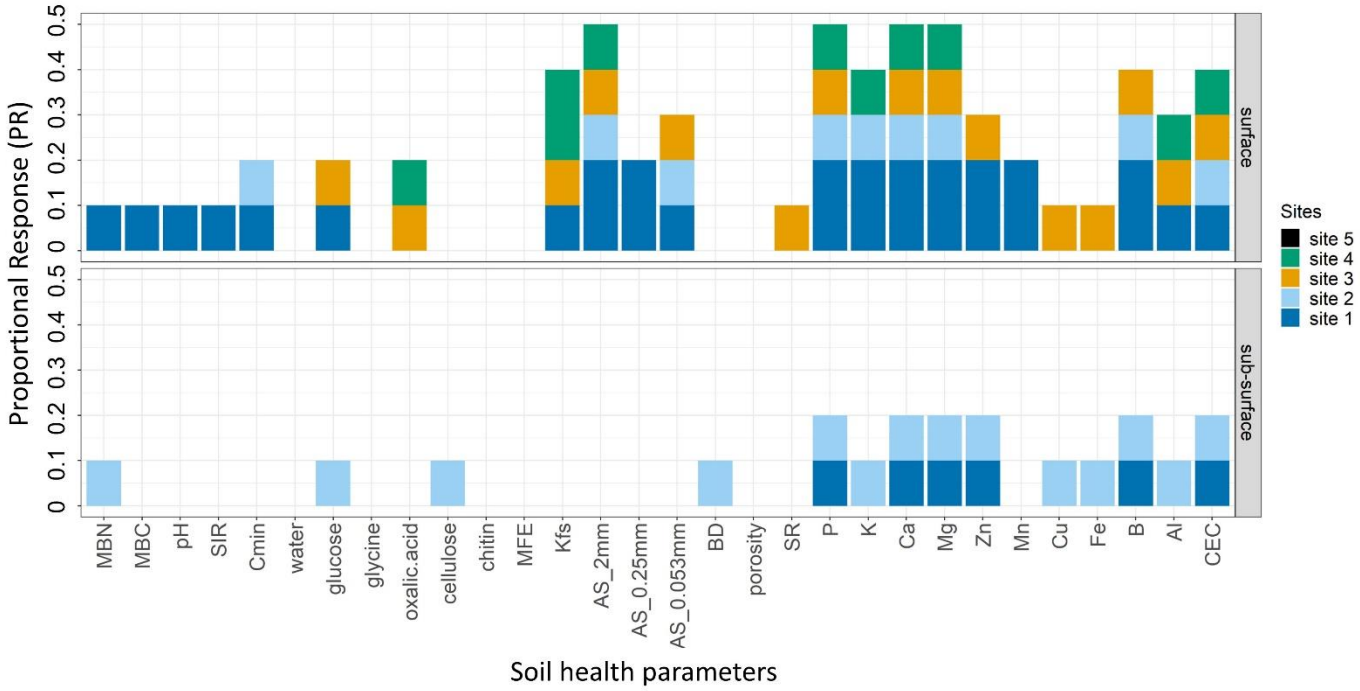

Figure 2.6: Proportional Response (*PR*) values for each measured soil health parameter for all five sites and for both surface and subsurface soil samples. *PR* values are out of a possible maximum of 10 (five sites by two years).

3.4 Soil health parameter consistency

In the surface soil layer, 2 – 4 mm aggregate stability (AS_2mm) was found to have the highest consistency parameter value (*CP* = 0.49; Figure 2.7). Soil respiration as chitin as substrate (chitin) was observed to have the lowest *CP* value (*CP* = -0.42). In case of the subsurface soils, respiration with cellulose as the substrate (cellulose) was found to have highest *CP* value, 0.67, while soil potassium (K) had the lowest *CP* value, -0.27.

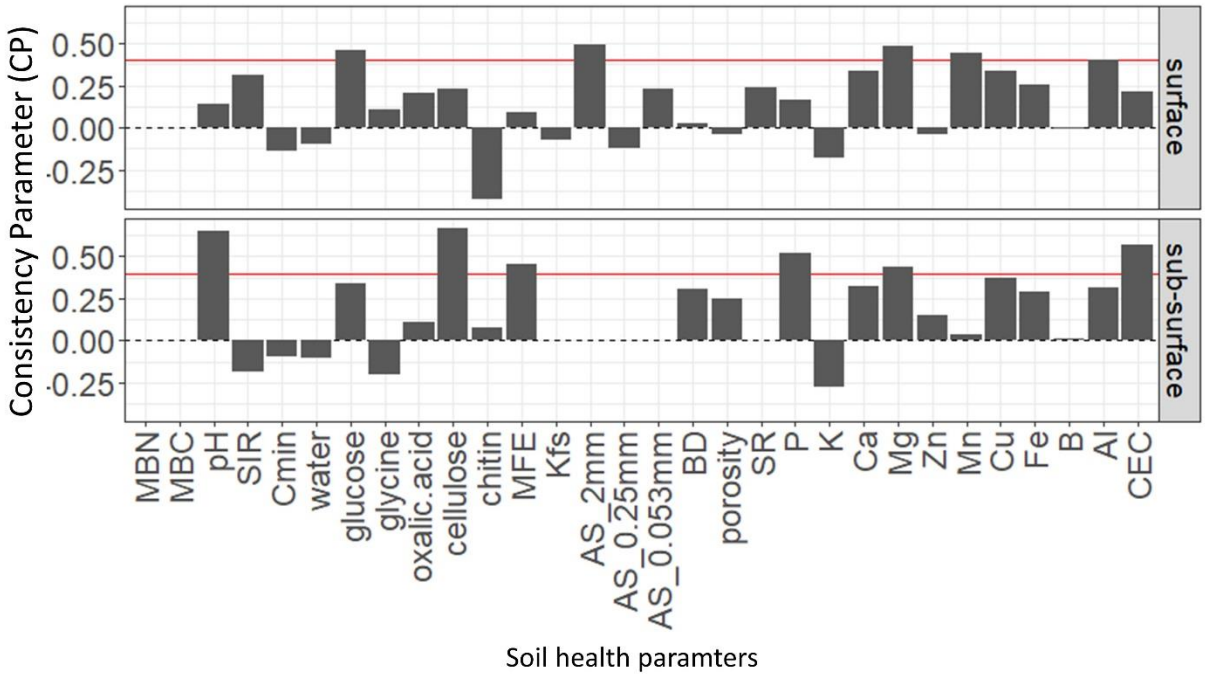

Figure 2.7: Consistency Parameter (*CP*) for all measured soil health parameters for all five sites, separated between surface and subsurface soil samples. The red line represents CP value of 0.4.

2.5 Discussion

2.5.1 Tillage and cover crop treatments

The tillage and cover crop treatments appear to have affected soil health properties over different time-scales. In the April 2016 sampling event, conducted ~7 months after the treatments were installed, tillage was the main factor that induced parameter differences within three of the sites (Figure 2.5). Treatment differences related to cover cropping started to appear during the April 2017 sampling, 1.5 years after introduction of the treatments. The more rapid response of parameters to tillage compared to cover crops likely reflects that tillage induced a more immediate and greater level of soil disturbance. These results reflect those of previous studies, such as Raper, et al. (2000), who also found that soil physical properties changed more rapidly in response to tillage compared to cover cropping, or Gabriel and Quemada (2011), who only observed N benefits from leguminous cover crops after the second year of planting.

In our second study year, the cover crop response was observed in two of the five sites (Sites 2 and 4; Figure 2.5). The cover crop treatment effect observed in Site 2 in April 2017 might be driven by the fact that site had the highest dry cover crop biomass among the five sites that year (Figure 2.4). This finding aligns with previous work suggesting soil health parameters may have greater response as cover crop biomass increases (Balkcom, et al., 2007, Roldán, et al., 2003). However, Site 4 also showed significant differences between cover and no cover crop treatments (Figure 2.5), even though that site had the lowest dry cover crop biomass in 2017 (Figure 2.4). This result may be explained by the complete lack of above-ground (i.e., weeds) in the no cover crop plots at this site (Figure 2.4), as weeds can cause similar improvements in soil health as a planted cover crops (Kabir and Koide, 2000, Oliveira, et al., 2016). Thus, even though cover crop biomass may be one of the key factors that determines whether cover crop

affect soil health, the presence or absence of weeds in the no cover plots can also alter the detection of cover crop effect.

2.5.2 Responsiveness of soil health parameters

The most responsive soil health indicators to the agricultural treatments (i.e., those parameters with a proportional response $PR \geq 0.4$) were mainly soil chemical and physical parameters (Figure 2.6). Soil biological parameters were not found to respond to our tillage and cover crop treatments, which is consistent with several recent studies (Abdollahi and Munkholm, 2014, Zuber, et al., 2017). Morrow, et al. (2016) also found that measures of active soil organic matter did not show high sensitivity to agroecosystems. However, a number of other studies have identified soil biological parameters as the fastest responding metrics (Cardoso, et al., 2013, Kibblewhite, et al., 2007, Ritz, et al., 2009). This discrepancy may be due to high temporal and spatial variability in soil biological measurements (Bastida, et al., 2008, Cardoso, et al., 2013, Morrow, et al., 2016, Zuber, et al., 2017, Zuber and Villamil, 2016), which can subsume any treatment effects (Degrune, et al., 2017, Hu, et al., 2018, Schwen, et al., 2011, Shi, et al., 2013, Spedding, et al., 2004). As a result, when conducted over seasonal or annual time-scales biological measurements may have limited usefulness to infer soil health.

The study results identified aggregate stability and hydraulic conductivity as highly responsive physical parameters (Figure 2.6), which is consistent with the meta-analysis results presented by Stewart, et al. (2018) and other studies on tillage (Bhattacharyya, et al., 2012, Roldán, et al., 2003, Schwen, et al., 2011) and cover crops (Hubbard, et al., 2013, Ramos, et al., 2010). Likewise, 6 out of 12 soil chemical parameters, including B and CEC, were also found to have *PR* values ≥ 0.4 (Figure 2.6). Previous studies have also noted high responsiveness of macro-nutrients (i.e., P, K, Ca, Mg) and CEC to tillage (Lienhard, et al., 2013, Lou, et al., 2012,

Zuber, et al., 2015, Zuber, et al., 2017) and cover crop (Dabney, et al., 2001, Nascente, et al., 2015, Sharma, et al., 2018) practices. One reason that the macro-nutrients may have shown greater treatment effects than other chemical parameters may be due to higher demands imposed by the cover crops and greater soil mixing due to disk tillage.

2.5.3 Consistency of soil health parameters

Consistency results for all the parameters across the two years show that some parameters can show high consistency (i.e., *CP* values; Figure 2.7) but show a low proportional response (Figures 2.6 and 2.7). For example, SIR and cellulose are among the parameters with the highest consistency values (*CP* = 0.3 for SIR and 0.6 for cellulose) yet have low responsiveness to the treatments (*PR* = 0.1 for SIR and 0.0 for cellulose). So, even though some parameters might show similar treatment ordering between years, as shown by the CP parameter, this may not translate in showing statistical treatment differences, as shown by the PR parameter.

Some parameters like 2 mm wet aggregate stability (AS_2mm) and Magnesium (Mg), displayed both higher responsiveness as well as consistency. Out of these two indicators, it is likely that Mg may represent effects of mixing due to tillage and uptake from cover crops. In contrast, previous studies have suggested that aggregate stability (AS_2mm) is a basis for a wide range of soil functions (An, et al., 2010), such as increasing carbon stabilization (Kong, et al., 2005), increasing water infiltration (Franzluebbers, 2002) and increasing resistance to erosion (Barthes and Roose, 2002).

The main objective of our study was to identify soil health indicators that consistently detected differences from conservation versus traditional agricultural practices. We conducted annual measurements to address this question, reflecting the frequency over which producers typically implement and modify practices (e.g., cover crops are typically planted once per year in

row crop systems). Our approach was therefore designed to identify indicators that have relatively low sensitivity to short-term (i.e., day to week) temporal dynamics, yet relatively high sensitivity on seasonal to annual timescales. Aggregate stability emerged from our study as having both high responsiveness and consistency, meaning that indicator may be the most useful for detecting effects of conservation agriculture practices on soil health.

2.6 Conclusion

The ability to objectively evaluate both existing and new agronomic practices is essential to build a sustainable food supply. In this study, we evaluated the responsiveness and consistency of 30 soil health parameters with respect to conservation practices like no-tillage and cover crops. This study presented two new metrics to quantify the overall responsiveness (Proportional Response, *PR*) and consistency (Consistency Parameter, *CP*) of various physical, chemical and biological parameters to these conservation practices. Using *PR* values, we saw that out of the 30 soil health parameters tested in this study, eight had high responsiveness to tillage and cover crop treatments: field-saturated hydraulic conductivity, aggregate stability, soil phosphorous, potassium, calcium, magnesium, boron, and cation exchange capacity (CEC). With regards to cover cropping, the responsive soil health parameters were similar to the ones mentioned above but also included some biological parameters like glucose and oxalic acid-aided soil respiration. Aggregate stability and magnesium also showed consistency in the relative ordering of the experimental treatments in two consecutive years, as shown by having *CP* values > 0.4.

By considering these two metrics (i.e., *PR* and *CP*) together, we were able to identify a small set of soil health indicators with appropriate sensitivity for evaluating conservation agricultural practices. Specifically, aggregate stability and soil magnesium showed responsiveness on annual timescales while also consistently differentiating between treatments.

Soil aggregate stability, on top of being responsive and consistent, is also a basis for wide range of soil functions. Here we note that our study installed similar treatments at five different sites, with underlying variations in soil type, climate, and cropping systems. Thus, the results of this study are likely to translate to row crop producers throughout the mid-Atlantic region of the United States. Having multiple sites also provides a more rigorous backing to the indicators identified here as having appropriate sensitivity and consistency.

Altogether, the results of this study provides a set of soil health indicators that respond consistently to conservation agriculture practices in Virginia. By focusing their data collection efforts to this subset of parameters, farmers and regulators can prioritize the type and frequency of measurements they collect to assess soil health, thereby saving both time and money.

Chapter 3. Identifying dynamic responses of soil health indicators to conservation agriculture practices

To be submitted to *European Journal of Soil Science*

3.1 Abstract

Concerns of increased costs and possible yield declines can hinder producer adoption of conservation agriculture practices such as reduced tillage and fallow-season cover crops. While conservation agriculture methods can cause long-term improvements in soil health, the short-term effects of such practices on soil properties remain poorly understood. The main study objective was to quantify temporal dynamics in eight soil health parameters under treatments representing conservation versus conventional agriculture. Treatments included reduced tillage with cover crops, reduced tillage without cover crops, disk tillage with cover crops, and disk tillage without cover crops. We collected measurements once or twice per year for three years using five sites across the state of Virginia, and examined variations in parameter values between treatments and through time. Our results showed that parameters can be grouped into consistent (e.g. aggregate stability) versus inconsistent (e.g. hydraulic conductivity) indicators of soil health. Even though none of the parameters detected treatment differences in all sites or at all times, samples collected after high biomass cover crops or after tillage in wet conditions tended to show significant treatment differences for multiple indicators. Treatment differences were also detected more often in fine-textured silty loam soils than in coarse-textured sandy soils. History of management may have affected trends in soil aggregate stability values through time, but did not consistently influence the other parameters. Altogether, reduced till and cover crops can induce positive changes in many of these soil health parameters, yet it is important to consider weather, soil, and management history when interpreting these indicators.

3.2 Introduction

Conservation agriculture practices such as reduced tillage and cover crops have been proposed to optimize the productive (in terms of yield) and protective (in terms of environment) aspects of agriculture, which are needed to sustainably support a rapidly growing and increasingly wealthy population (Foley, et al., 2011, Verhulst, et al., 2010). No-till is a common form of reduced tillage that can reduce erosion (Blevins, et al., 2018), decrease nutrient losses (Tiessen, et al., 2010), and mitigate greenhouse gas emissions (Maraseni and Cockfield, 2011). Despite these benefits, total acreage managed using no-till in the United States was fairly constant from 2005 to 2016. A similar story emerges for cover crops, which as of 2018 have been adopted in less than 5% of all planted acres in the United States, even though cover crops can help to control soil erosion, improve soil health, and reduce net greenhouse gas emissions (Baranski, et al., 2018).

Despite the high potential for increasing environmental protection, conservation agriculture practices offer less certain benefits in terms of cash crop yields. In some cases, practices like no-till can cause short-term declines in yield, which has limited the spread of that practice (Kladivko, et al., 1986, Ogle, et al., 2012, Pittelkow, et al., 2015). Planting cover crops also represent an additional expense in terms of costs and time to the producer, which means that many farmers will not plant them without clear benefit (Krueger, et al., 2011, Snapp, et al., 2005). Thus, it is important to understanding and quantify any benefits of practices such as reduced tillage and use of over-winter cover crop effects.

One potential advantage of conservation agriculture practices may be their effects on soil health, which refers to agroecosystem functions mediated by integrated biological, physical and chemical properties of the soil (Doran and Zeiss, 2000). Soil health can be measured using

parameters like soil hydraulic conductivity, aggregate stability, chemical concentrations, and biological indicators such as substrate induced respiration and microbial biomass carbon and nitrogen (Idowu, et al., 2009, Nair and Ngouajio, 2012). However, many of these soil health parameters can have high temporal (Hu, et al., 2018) and spatial (Cardoso, et al., 2013, Zuber and Villamil, 2016) variability, due to influences such as soil texture or local weather conditions. For instance, soil texture can affect the rate and form of soil carbon accumulation (Sprunger and Robertson, 2018), while differences in soil temperature and moisture can cause short-term fluctuations in many physical and biological properties (Bastida, et al., 2008, Cardoso, et al., 2013, Zuber and Villamil, 2016). Cover crop and tillage practices may therefore induce different responses in soil health parameters between measurements in the same location or between different locations at the same time.

The history of management of a soil may also affect its response to conservation agriculture practices. For example, a given soil that was previously maintained in forest or grass may have different values for soil health parameters compared to that soil managed using row crop agriculture with intensive tillage (Gajić, 2013, Jackson, et al., 2003, Lienhard, et al., 2014). These potential differences in soil health due to previous usage provide additional context that is often not considered when interpreting parameter values (Churchman, et al., 2010). This land use history effect might also affect the trends that these soil health parameters follow over time (Idowu, et al., 2009, Jangid, et al., 2011). Given these often-overlooked sources of variability, it is important to identify soil health indicators that are responsive to conservation agricultural practices yet otherwise demonstrate consistency between locations and through time.

To address these research gaps associated with locational and temporal dynamics of soil health parameters, we here focus on the set of parameters identified in Chapter 2 as having high

responsiveness: field-saturated hydraulic conductivity (K_{fs}), 2 – 4 mm aggregate stability (AS_2mm), phosphorus (P), potassium (K), calcium (Ca), magnesium (Mg), boron (B), and cation exchange capacity (CEC). For each parameter, we collected measurements once or twice per year for three years and examined variations in parameter values across treatments representing different management practices, and for the same treatments through time. Our objectives were to 1) evaluate the ability of each soil health parameter to detect treatment differences due to management practices, and 2) identify any consistent temporal trends for individual parameters within or across sites. For the first objective, our hypothesis was that reduced tillage and cover crop treatments would show significantly higher parameter values than disk tillage and no cover crop treatments. For the second objective, our hypothesis was that the soil health parameters would show trends specific to the history of the management of the site.

By quantifying dynamic responses of these indicators, our ultimate goal is to better identify potential benefits and any drawbacks of no-tillage and cover crop practices on soil health. This information may help encourage producers to adopt conservation agriculture practices despite the potential for short-term yield decreases that have been shown previously.

3.3 Methods and materials

The data in this chapter makes use of the same five sites (Sites 1-5) and the same experimental design as in Chapter 2. Our five sites had two different soil textures: Sites 1, 2 and 3 had silt loam soils and Sites 4 and 5 had sandy loam soils (Figure 3.1). The five sites also varied in their history of management, as Sites 1 and 2 were no-till cover crop fields, Sites 3 and 4 were grassland with fescue and Site 5 was an intensively cultivated potato field prior to installation of the treatments. The four experimental treatments were: 1) reduced tillage (RT) with cover crops (CC); 2) RT with no cover crops (NC); 3) conventional tillage (CT) with CC;

and 4) CT with NC. The specific practices in the reduced tillage treatments were no-till for the four sites with corn as the cash crop (Sites 1-3 and 5; Figure 3.1) and strip till for Site 4, which had tobacco as the cash crop. Conventional tillage was performed using a disk harrow every September and April starting 2015, with soil disturbance from the surface to a depth of between 15 and 20 cm. Cover crops were a three-way mixture of winter barley **(***Hordeum vulgare*), crimson clover **(***Trifolium incarnatum*) and tillage radish **(***Raphanus raphanistrum* subsp. *sativus***).**

Soil samples were collected from soil surface (0 – 10 cm) in all five sites in April 2016, April 2017, and April 2018. Additional samples were collected in Sites 1-3 in September 2016 and September 2017. Samples were analyzed for field-saturated hydraulic conductivity (K_{fs}), 2 – 4 mm aggregate stability (AS_2mm), phosphorus (P), potassium (K), Calcium (Ca), magnesium (Mg), Boron (B), and cation exchange capacity (CEC). Cover crop biomass was also measured in all sites every April. The protocols used for the measurement of soil health indicators and cover crop biomass were presented in Chapter 2. In addition, volumetric soil moisture content (0-20 cm) was measured using a Hydrosense II probe (Campbell Scientific, Logan, Utah, United States).

We performed statistical analyses for each of the five sites and at each sampling point to identify tillage, cover crop or interaction effects for each soil health indicator. Statistical analysis was conducted in R Version 3.5.0 (R Development Core Team, 2018). Analysis of Variance (ANOVA) with Tukey's HSD was used to test for differences in each of the eight soil parameters between management practices at each site for each sampling time. ANOVA with Tukey's HSD was also used to detect differences for soil water content and dry cover crop biomass between sites. The data were tested for normality and homoscedasticity prior to running ANOVA; non-

normal data were normalized either using a logarithmic or a box-cox transformation. $\alpha = 0.05$ was used to identify significance throughout the analysis.

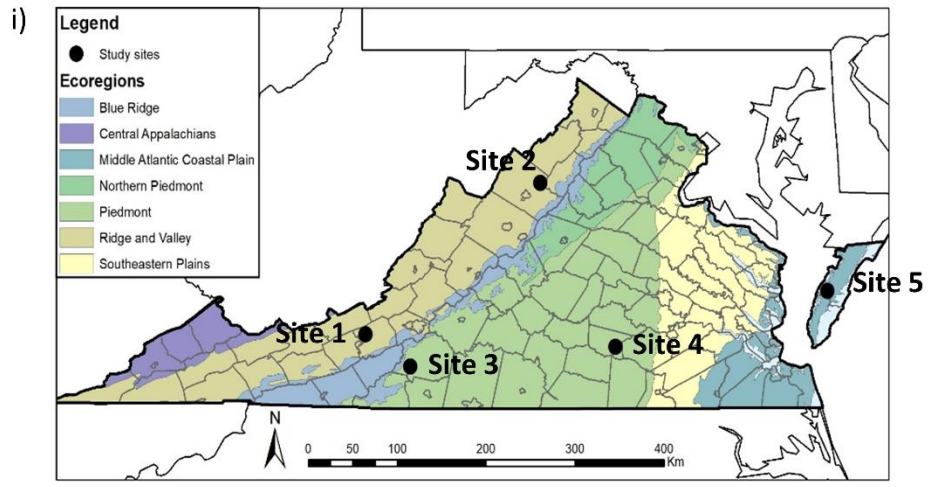

ii)

2014	2015			2016			2017			2018			2019
Sites	July	Sep	Oct	April	May	Sep	April	May	Sep	April	May	Sep	April
Site1			Cover crop		Corn		Cover crop		Corn		Corn		Cover crop
	*	T	*	*#	G T	#T	* #*	G T	#T	* #*	G T	#T	
Site 2			Cover crop		Corn		Cover crop		Corn		Corn		Cover crop
	*	T	*	*#	G T	#T	* #*	G T	#T	* #*	G T	#T	
Site 3			Fallow		Corn		Cover crop		Corn		Corn		Cover crop
		T		*	G T	#T	* #*	G T	#T	* #*	G T	#T	
Site 4			Cover crop		Tobacco		Cover crop		Tobacco		Tobacco		Cover crop
		T		T*#	G	T	#*	G T	T	T#*	G	T	
Site 5			Cover crop		Corn		Cover crop		Corn		Corn		Cover crop
		T		*#	G T	T	#*	G T	T	#*	G T	T	

* Soil sample taken
\# Plant sample taken
G Glyphosate application
T Tillage done on the tilled plots

Figure 3.1: i) Map of Virginia showing site locations, and ii) timeline of cover and cash crop planting, soil and plant sampling, herbicide application, and tillage.

To quantify temporal trends in parameters, we calculated the response ratio (RR) as:

$$RR = \ln[y_i(t)/y_{i,0}] \quad [3.1]$$

where $y_i(t)$ is the mean parameter value of treatment i at time t and $y_{i,0}$ is the median parameter value for that treatment from the initial measurement in April 2016 (i.e., the first sampling date after treatment installation).

3.4 Results

3.4.1 Cover crop biomass and soil water content across 5 sites

Dry cover crop biomass varied across the five sites as well as between the years (2016 – 2018) (Figure 3.2). Site 2 in 2017 and in 2018, and Site 5 in 2016 and 2017 had the highest dry cover crop biomass (ANOVA with Tukey's HSD; $P < 0.05$).

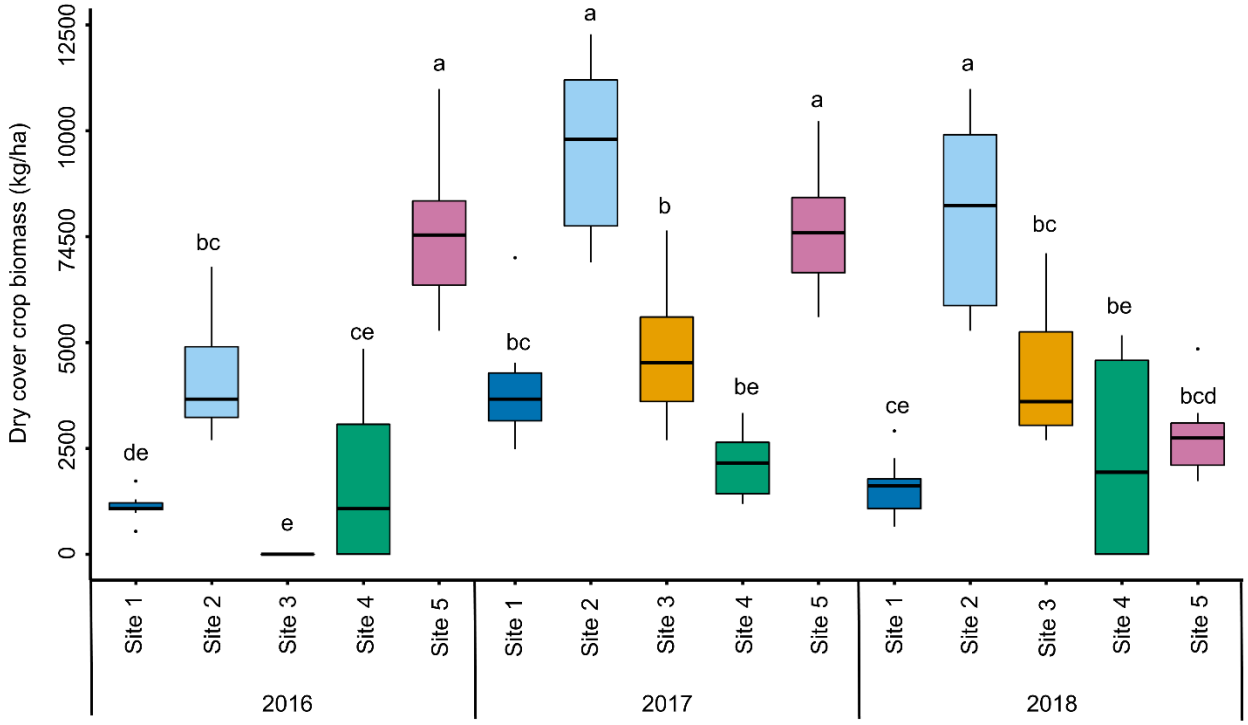

Figure 3.2: Dry cover crop biomass for all five sites for April 2016, 2017 and 2018. Different letters represent statistical difference for dry cover crop biomass ($P < 0.05$).

Soil water content measurements conducted in April 2017 and 2018 showed significant differences between sites (Figure 3.3). The relative order of the five sites (ranked from wettest to driest) was similar between both years. In both years Site 1 had the highest volumetric soil water contents and Site 4 had the lowest (ANOVA with Tukey's HSD; $P < 0.05$).

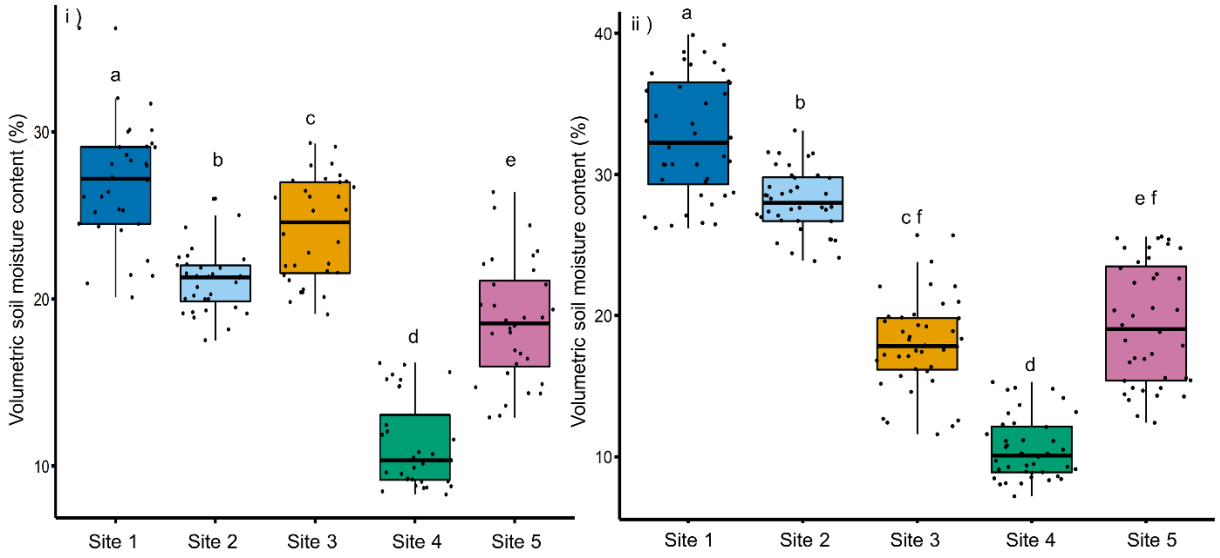

Figure 3.3: Volumetric soil moisture content for five sites measured in i) April 2017 and ii) April 2018. Sites with different lower case letters have statistically different volumetric soil water contents in each year ($P < 0.05$).

3.4.2 Tillage and cover crop effects on soil health indicators

All of the evaluated soil health indicators detected significant differences between treatments for at least one sampling time in at least one site (Table 3.1). Some of the indicators, such as field-saturated hydraulic conductivity (K_{fs}), wet aggregate stability of the 2 – 4 mm fraction (AS_2mm), and cation exchange capacity (CEC), showed significant differences more frequently than others, e.g., boron (B). Still, none of the indicators showed differences at every site, and only K_{fs} detected significant differences every time at one site (Site 4). The indicators can be grouped into two categories: those that had consistent responses in terms of which treatments had the highest and lowest values, versus those with inconsistent response. The first category includes AS_2mm, potassium (K), calcium (Ca), magnesium (Mg), and CEC, while the second category includes K_{fs} and phosphorus (P). Boron did not show a sufficient number of treatment differences to fall into either category.

Looking at specific parameters, AS_2mm was affected by the experimental treatments in Sites 1, 2 and 3, but not in Sites 4 or 5. Aggregate stability was higher for reduced till compared to conventional till (P = 0.03 in April 2016 and P = 0.02 in September 2017 for Site 1; P = 0.01 in September 2016 and P = 0.03 in September 2017 for Site 3) and for cover crop plots compared to no cover plots (P = 0.01 for Site 2 in April 2017).

K_{fs} showed significant differences between treatments in Sites 1, 3 and 4, but with inconsistent treatment effects. The reduced till plots had higher K_{fs} than conventional till plots in some cases (P = 0.04 for Site 1 in April 2018; P = 0.009 in April 2017 and P = 0.01 in April 2018 for Site 3), while in other instances the conventional till plots had higher K_{fs} than reduced till ones (P = 0.0004 in Site 1 for April 2017; P = 0.02 in Site 3 in September 2016; and P = 0.007 in April 2016 and P = 0.01 in April 2018 in Site 4). The cover crop treatments also showed inconsistency, with cover crop plots sometimes exhibiting significantly higher and other times significantly lower K_{fs} values than the no cover crop plots. As an example, in Site 1 the cover crop plots had significantly higher K_{fs} values in September 2016 (P = 0.03) and significantly lower values in April 2018 (P = 0.04).

Soil K showed treatment effects in Site 2, 4 and 5, and was the only parameter that significantly varied in Site 5. Even in that site, significant differences in K were only observed once (April 2017; P = 0.02). Soil Ca, Mg, CEC identified treatment differences in Sites 1, 2 and 3. Soil P was found to respond to treatments in Sites 1, 2 and 4. Moreover, P was the only indicator that showed significant interactions between treatments, with the reduced tillage with cover crop plots having higher P than the reduced tillage without cover crop plots in Site 4 (April 2018; P = 0.04).

Table 3.1: Soil health indicators with significant treatment differences through time (ANOVA with Tukey's HSD, $P < 0.05$). K_{fs}: field-saturated hydraulic conductivity, AS_2mm: 2 – 4mm wet aggregate stability, P: phosphorus, K: potassium, Ca: calcium, Mg: magnesium, B: boron, CEC: cation exchange capacity. RT = reduced tillage, CT = conventional tillage, CC = cover crops, NC = no cover crops.

Site	Time	K_{fs}	AS_2mm	P	K	Ca	Mg	B	CEC
1	Apr 2016		RT > CT			RT > CT	RT > CT		RT > CT
	Sep 2016	CC > NC							
	Apr 2017	CT > RT							RT > CT
	Sep 2017		RT > CT						
	Apr 2018	RT > CT; NC > CC		RT > CT		RT > CT	RT > CT	RT > CT	RT > CT
2	Apr 2016			CT > RT; NC > CC	NC > CC				
	Sep 2016								
	Apr 2017		CC > NC			CC > NC	CC > NC	CC > NC	CC > NC
	Sep 2017								
	Apr 2018								
3	Apr 2016								
	Sep 2016	CT > RT	RT > CT						
	Apr 2017	RT > CT					RT > CT; CC > NC		RT > CT; CC > NC
	Sep 2017		RT > CT						
	Apr 2018	RT > CT; CC > NC				RT > CT	RT > CT		RT > CT
4	Apr 2016	CT > RT							
	Apr 2017	NC > CC		CT > RT	NC > CC				
	Apr 2018	CT > RT; NC > CC		RT CC > RT NC	NC > CC				
5	Apr 2016								
	Apr 2017				NC > CC				
	Apr 2018								

3.4.3 Examples of site-level effects of cover crops and tillage on soil health indicators

In April 2017, five of the eight indicators at Site 2 had significantly higher values in the cover crop (CC) plots compared to no cover (NC) controls (Figure 3.4). Specifically, 2 - 4 mm aggregate stability (AS_2mm) had median values of CC = 14.2% versus NC = 5.39 % (P = 0.01); Ca had median values of CC = 403 mg/l versus NC = 322 mg/l ($P < 0.01$); Mg had median values of CC = 44.6 mg/l versus NC = 25.0 mg/l ($P < 0.01$); B had median values of CC = 0.20 mg/l versus NC = 0.13 mg/l ($P < 0.01$); and CEC had median values of CC = 2.81 meq/100g versus NC = 1.89 meq/100g ($P < 0.01$). The remaining three soil health indicators also had higher median values in the cover crop plots, though differences were not statistically significant.

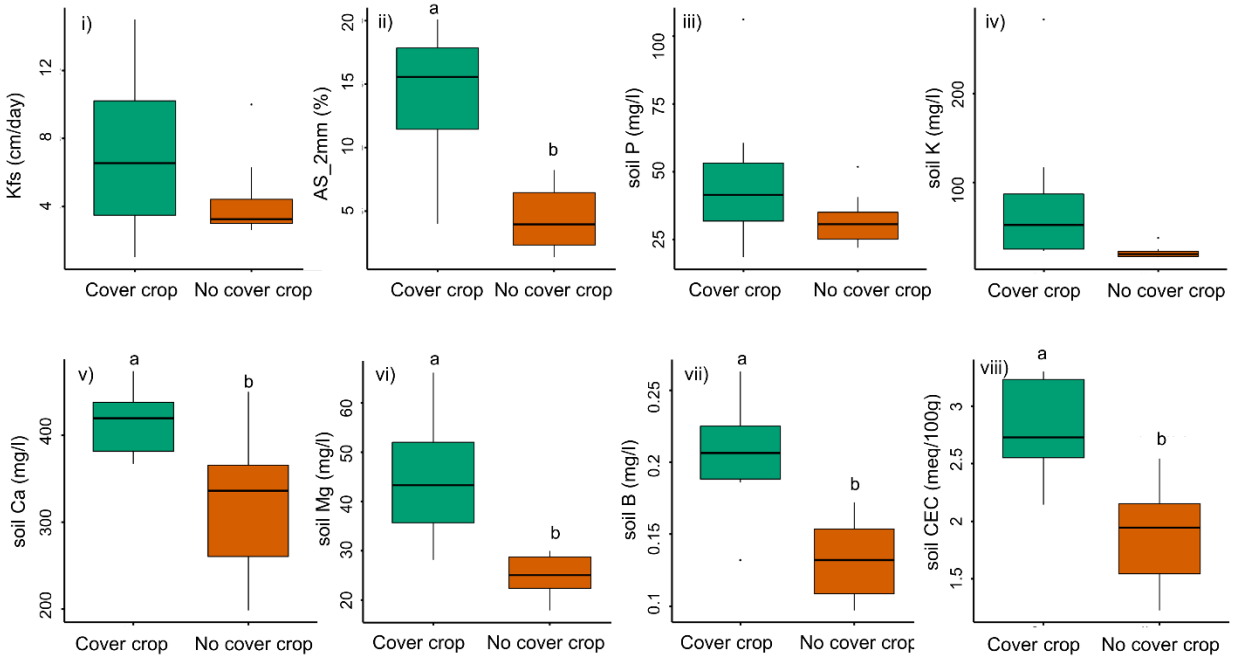

Figure 3.4: Soil health indicators in April 2017 at Site 2 in cover crop versus no cover crop plots. Different letters indicate statistical differences between treatments for each indicator (ANOVA with Tukey's HSD; $P < 0.05$). Kfs: Hydraulic conductivity, AS_2mm: 2 – 4 mm aggregate stability, P: Phosphorus, K: Potassium, Ca: Calcium, Mg: Magnesium, B: Boron, and CEC: Cation Exchange Capacity.

In April 2018, a site-wide tillage effect was observed in Site 1 (Figure 3.5). Here, six out of the eight soil health indicators were found to be higher for reduced till (RT) plots compared to the conventional till (CT) plots. Median K_{fs} values were RT = 0.88 cm/day compared to CT = 0.56 cm/day) (P = 0.04), soil P had median values of RT = 8.27 mg/l versus CT = 4.76 mg/l (P = 0.04), Ca had median values of RT = 412 mg/l versus CT = 324 mg/l (P = 0.01), Mg had values of RT = 105 mg/l versus CT = 80.1 mg/l (P = 0.02), B had median values of RT = 0.22 mg/l versus CT = 0.17 mg/l (P = 0.03), and CEC had median values of RT = 2.97 meq/100g compared to CT = 2.32 meq/100g (P = 0.01).

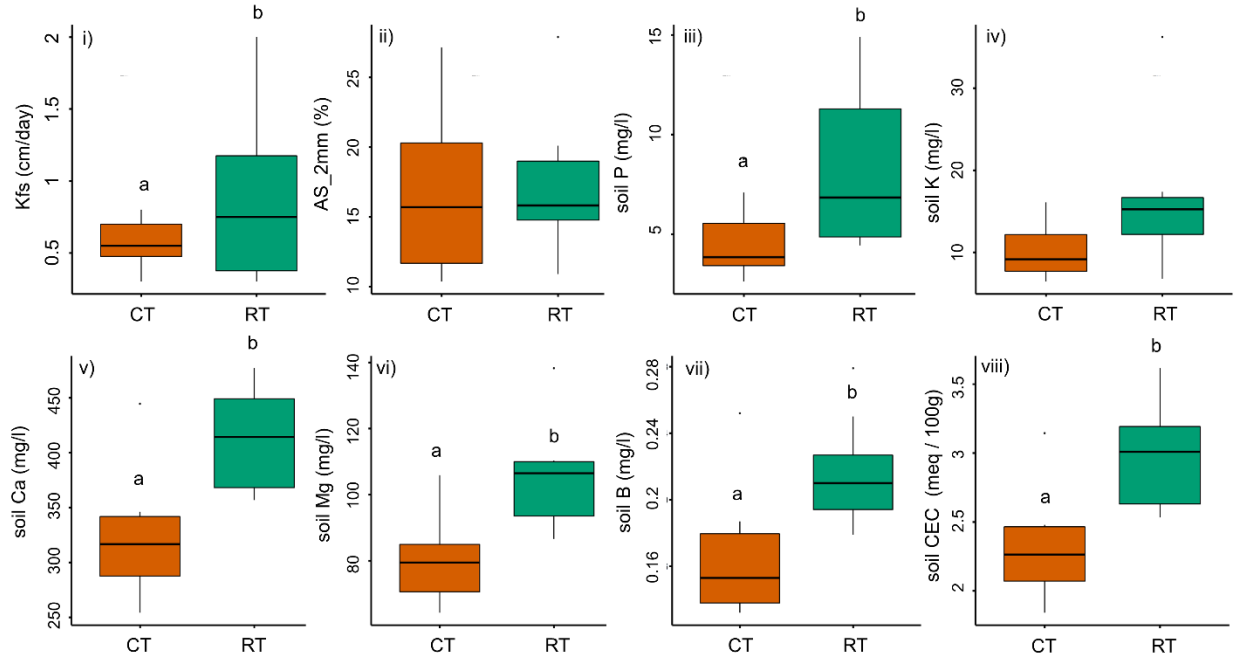

Figure 3.5: Soil health indicators in April 2018 in Site 1 in reduced till (RT) versus conventional till (CT) plots. Different letters indicate statistical differences between treatments for each indicator (ANOVA with Tukey's HSD; $P < 0.05$). Kfs: Hydraulic conductivity, AS_2mm: 2 – 4 mm aggregate stability, P: Phosphorus, K: Potassium, Ca: Calcium, Mg: Magnesium, B: Boron and CEC: Cation Exchange Capacity.

3.4.4 Site-specific trends in soil health indicators

We quantified response ratio (RR) through time for four soil health indicators using Equation 3.1. Two indicators – soil aggregate stability (AS_2mm) and cation exchange capacity (CEC) – were previously grouped as consistent indicators, while the other two – soil phosphorus (P) and field-saturated hydraulic conductivity (K_{fs}) – were grouped as inconsistent indicators for identifying treatment differences. Note that the aggregate stability response ratio trends are shown in Figure 3.6, while the other response ratios are shown in Appendix B (Figures B1-B3).

In Sites 1 and 2, aggregate stability was stable between April 2016 and April 2018 (Figure 3.6), as there were only fluctuations in the parameter values but not any consistent increasing or decreasing trends. In Site 3 and 4, aggregate stability decreased initially and then appeared to have stabilized in later measurements. Site 5 had a trend of increasing aggregate stability from April 2016 to April 2018 across all treatments.

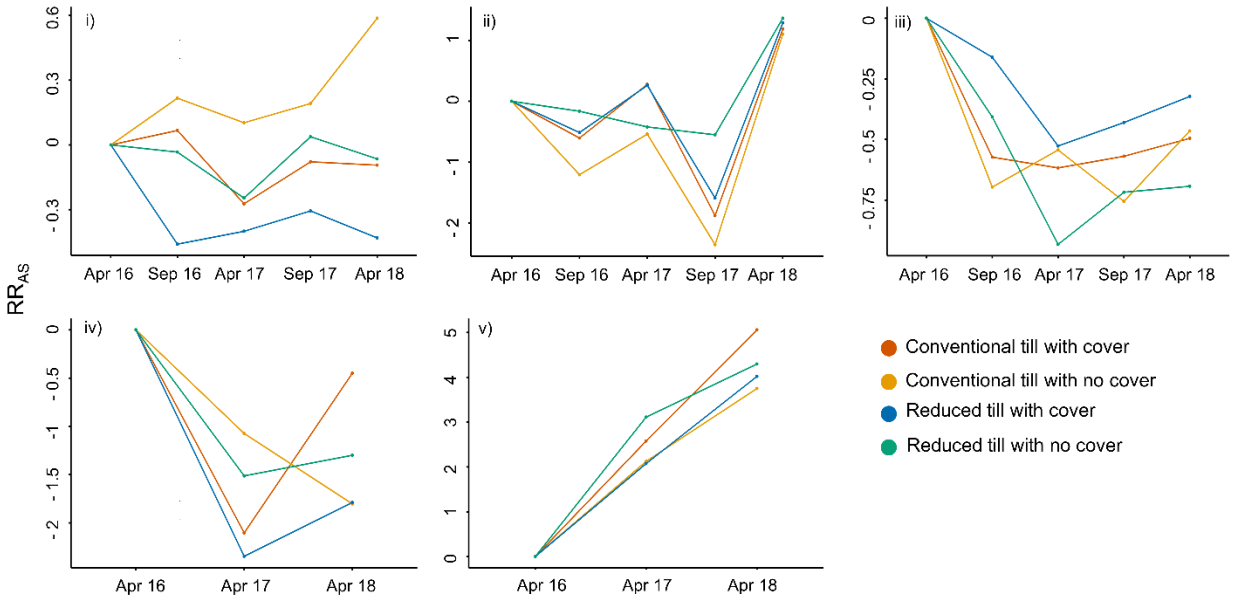

Figure 3.6: Response ratio for soil aggregate stability (RR_{AS}) through time for i) Site 1; ii) Site 2; iii) Site 3; iv) Site 4; and v) Site 5. Apr 16: April 2016, Sep 16: September 2016, Apr 17: April 2017, Sep 17: September 2017 and Apr 18: April 2018.

3.5 Discussion

In this study we examined the dynamic responses of soil health indicators to conservation agriculture practices across a set of treatments installed in five sites in Virginia that varied in texture (silt loam, sandy loam) and history of management (no-till row crop fields, deep plowed crop fields, grazed pasture, and non-grazed pasture). We installed four different treatments at each site, representing combinations of conventional versus conservational agriculture: reduced tillage (RT) versus conventional disk tillage (CT) and use of wintertime cover crops (CC) versus no cover crops (NC). Of the eight soil health indicators that we analyzed – field-saturated hydraulic conductivity (K_{fs}), 2 – 4 mm aggregate stability (AS_2mm), soil phosphorus (P), potassium (K), calcium (Ca), magnesium (Mg), boron (B) and cation exchange capacity (CEC) – all detected treatment effects in at least two different sites at least one time (Table 3.1). Based on their ability to detect treatment differences between sites and sampling times, we grouped indicators as being consistent (AS_2mm, K, Ca, Mg) or inconsistent (K_{fs}, P), with B having insufficient response to classify.

The inconsistency in K_{fs} and P may have several causes. K_{fs} values can vary through time, particular in conventionally tilled soils (Lampurlanés and Cantero-Martínez, 2006). In Site 4, tillage was done before the K_{fs} measurements in 2016 and 2018 (Figure 3.1), which may have caused K_{fs} of the conventionally tilled plots to be significantly higher during those measurements (Table 3.1). However, we also observed that conventional till plots sometimes had higher K_{fs} in April even when the tillage was done in the previous September (e.g., Site 1 - April 2017), showing that the tillage effects may persist throughout the non-growing season (Table 3.1). Increased K_{fs} values due to tillage have been shown to last until a soil crust forms from rainfall impact (Imeson, et al., 1990, Le Bissonnais, et al., 1995), yet crust formation can be delayed

when soils have high water contents (Bissonnais and Singer, 1992). As Site 1 had overall higher soil moisture content (Figure 3.3), crust formation in the conventional till plots may have been delayed relative to the other sites. Likewise, relative K_{fs} values varied between cover crop treatments, with no cover plots having higher K_{fs} than cover crops in certain sites and samples, and the opposite observed at other times. This inconsistency reflects the findings of other recent studies (Blanco-Canqui, et al., 2011, Carof, et al., 2007) and suggests that other sources of variability may be driving this parameter response. We also note that we quantified K_{fs} using a tension infiltrometer, which prevents water flow into large macropores (in this instance pores > 1 mm). Therefore, our analysis did not examine possible difference in macroporosity that may have resulted from cover crops, such as tillage radish.

For soil phosphorus, the reduced tillage treatments in Site 1 showed increased P concentrations in the surface soil (0 – 10 cm) compared to conventional tillage treatment, which may be due to mixing of soil in the conventional till plots (Abdollahi and Munkholm, 2014). However, the conventional tillage treatments had higher P levels in the surface soils in Sites 2 and 4. One possible mechanism for increased concentration of soil P in conventional tilled plots may be the higher uptake of P by corn in reduced tillage conditions (Fink and Wesley, 1974, Shear and Moschler, 1969). However, in Site 4 we had tobacco as a cash crop, so another mechanism where mineralization rates of organic P can become higher in conventionally tilled plots may also be playing a role there (Selles, et al., 1999). Higher concentration of P in the conventional tilled plots compared to reduced till plots was also observed by Nyakatawa, et al. (2001) and Hussain, et al. (1999).

As for the consistent soil health indicators, all except soil K showed treatment differences in the silt loam sites (Sites 1, 2 and 3). K, by contrast, showed the greatest treatment effect in the

sites with sandy soils (Sites 4 and 5). The reduced tillage plots had consistently greater amounts of 2-4 mm water stable aggregates (AS_2mm) than conventional till plots, and the cover crop plots had higher aggregate stability than no cover plots. Recent studies have also shown that cover crops can increase soil aggregate stability due to root exudates (Ramos, et al., 2010, Six, et al., 2004). Likewise, reduced tillage practices can increase aggregate stability by reducing soil organic matter turnover (Paul, et al., 2013, Six, et al., 1999). Other consistent soil health indicators like Ca, Mg, B and CEC also showed similar treatment differences, where reduced tillage had higher parameter values than conventional tillage practices and cover crop plots had higher values than no cover crop plots. It is likely that these results are inter-related, as soils with higher CEC will be able to retain more cationic nutrients such as Ca and Mg. Reduced tillage and cover crops can alter the concentration and type of organic carbon in near-surface soils (Mazzoncini, et al., 2011, Nascente, et al., 2013), which may increase CEC. The mixing effect of tillage might also alter nutrient concentrations in the surface soil in the conventional till plots (Abdollahi and Munkholm, 2014), while cover crops may be due to scavenging these nutrients from deeper layers (Gruver, et al., 2014). Soil K was also found to be a consistent indicator, but this nutrient had the opposite treatment response than the others, as no cover crops had higher K levels than cover crop plots. This result may reflect greater K uptake by cover crops.

In several of the samples, the same significant treatment effect was observed across the majority of indicators. In April 2017, Site 2 had significantly higher values in the cover crop plots for five of the eight parameters (Figure 3.4). Site 2 had the highest cover crop biomass during that time (Figure 3.2), which reflects the observation that many of the benefits of cover crops increase with biomass (Roldán, et al., 2003). In April 2018, Site 1 had significantly higher values for six of the eight parameters in the reduced tillage plots (Figure 3.5). This result may be

explained by the soil moisture data for all five sites (Figure 3.3), as higher soil moisture at the time of tillage can result in more soil disturbance (Allmaras, et al., 1967, Imeson, et al., 1990).

We also examined trends in parameter values through time at each site. Of the eight parameters, only aggregate stability showed consistent trends, though the trends differed between locations (Figure 3.6). Sites 1 and 2 had relatively consistent aggregate stability values through time, Sites 3 and 4 had initial decreases in values, and Site 5 had increasing values. These different trajectories may be attributable to history of management of each of the five sites. Sites 1 and 2 were row crop fields managed using no-till with cover crops prior to the study. Thus, the soils received similar inputs and levels of disturbance prior to and during the study, suggesting that aggregate stability was in a steady-state (Figure 3.6). Note that the spike in aggregate stability at Site 2 in April 2018 for all the treatments may be due to the addition of high organic matter bed pack manure in late 2017. The initial decreases in aggregate stability seen in Sites 3 and 4 may have been because both sites were planted in pasture grasses prior to our implementation of treatments. Row crop agriculture involves greater soil disturbance than non- or lightly-grazed pasture, and hence may have caused the initial decline in aggregate stability. In contrast, the soil in Site 5 was intensively cultivated with potatoes prior to our treatment installation. Thus, even our study treatment representing the greatest disturbance and lowest inputs (conventional tilled continuous corn with no cover crops) may have imposed less disturbance compared to the previous potato crop. As a result, aggregate stability increased with time. Some evidence of land use history effect on soil aggregate stability can also be found in Idowu, et al. (2009).

The results for aggregate stability suggest that parameter values may vary depending on the initial status of the soil, particularly for measurements collected in the first 1-3 years after

change in management. This finding implies that we may better understand soil health dynamics by providing additional context on whether we are trying to build or maintain soil health. In the former, the goal may be to increases parameter values such as aggregate stability and field-saturated hydraulic conductivity. In the latter, the goal may be to prevent changes (i.e., decreases) in the values of those indicators. Additional studies that better control for variability in terms of texture and land use history may be needed to better understand their potential effects on soil health parameters. Nonetheless, the results of this study suggest that the type and initial health of soils should be taken into consideration when evaluating possible effects of conservation agriculture and other management practices.

3.6 Conclusion

Conservation agriculture practices such as reduced tillage and use of over-winter cover crops can provide environmental benefits, but may pose short-term economic challenges to producers as a result of possible yield losses and the cost of new equipment, extra seeds, herbicides, etc. These costs have hindered widespread adoption of conservation agriculture practices. In order to more consistently evaluate whether reduced tillage and cover cropping practices render consistent improvements in soil health, we examined the short-term (i.e., 1-3 year) dynamics of eight soil health parameters after applying different agricultural management practices: reduced tillage versus disk tillage; winter cover crops versus no covers crops. By analyzing individual soil health parameters through time and across five sites in Virginia, we were able to divide those indicators into groups that had consistent (AS_2mm, K, Ca, Mg, and CEC) versus inconsistent (K_{fs}, P) capability to separate experimental treatments.

Though no single parameter identified treatment differences at every site or at every sampling time, there were several instances in which we observed significant effects of no-tillage

and cover cropping on the majority of soil health parameters. These instances were associated with either high cover crop biomass or high moisture content near the time of tillage, suggesting that weather and growing conditions can compromise the ability of even relatively sensitive parameters to detect treatment differences. We also observed possible differences corresponding to soil texture, where treatment differences were detected more consistently in the finer-textured silt loam soils than in the coarser-textured sandy soils.

As the five project sites varied in their previous management history, from non-grazed pasture to intensively cultivated row crops, the final objective of the study was to evaluate temporal trends in the various parameters at all sites. The effects of previous land management may have affected soil aggregate stability, which represents one of the most responsive and widely used indicators of soil health parameter. Specifically, sites that started with high aggregate stability saw a decrease through time in all treatments, while the site with the lowest aggregate stability saw an increase through time. These different trends suggest that parameter responses may vary in systems that are building soil health from a relatively depleted state versus those systems that are maintaining a relatively high level of soil health.

Altogether, conservation agricultural practices like reduced till and cover crops can induce changes in soil health parameters over a 1-3 year period. However, these soil health benefits may depend on factors like soil moisture, cover crop biomass, and prior land management. Of the eight parameters studied, aggregate stability may be the most useful for consistently detecting soil health changes due to management.

Chapter 4. An improved method for quantifying soil aggregate stability

Published in *Soil Science Society of America Journal*

Gyawali, A. J., & Stewart, R. D. (2019). An Improved Method for Quantifying Soil Aggregate Stability. *Soil Science Society of America Journal*. doi:10.2136/sssaj2018.06.0235

4.1 Abstract

Soil aggregate stability influences many biophysical and agronomic processes while acting as a key soil health indicator, yet current quantification methods suffer shortcomings including lack of repeatability, inadequate control over input energy, and inaccuracies in coarse-textured soils or those with multi-modal size distributions. In response, we propose a new method deemed integrated aggregate stability (IAS) to interpret aggregate stability using a laser diffraction machine. This method corrects for underlying particle size distributions and provides a comprehensive metric of aggregate stability. As verification, we presented repeatability tests that demonstrate the precision of the IAS method, and then compared IAS measurements to wet sieving results for three different soils. Overall, IAS showed higher correlation with the wet sieving method (R^2 = 0.49 to 0.59) than the median aggregate size (d50), which represents the most common current method for quantifying aggregate stability (R^2 = 0.09 to 0.27). Further, IAS can estimate the proportions of macro (> 0.25 mm) and micro (< 0.25 mm) aggregates, and thereby quantify shifts between those fractions under different applied energy levels. As an example, we compared IAS estimates of macro- and micro-aggregates from three different soils that due to differences in texture and previous land use showed varying levels of aggregation. While d50 identified some of the between-site differences in macro-aggregation, only IAS was able to consistently detect and quantify micro-aggregate fractions. Altogether, these results reveal that IAS can convey more consistent and relevant information about aggregate stability compared to traditionally used metrics.

4.2 Introduction

Soil aggregate stability influences biological activity and crop productivity by facilitating the movement of air and water (Amézketa, 1999, Karami, et al., 2012) and by reducing soil erosive and crusting potentials (Amézketa, 1999, Le Bissonnais and Arrouays, 1997). Among other factors, the size of an aggregate affects its stability, with larger aggregates typically having lesser stability than smaller aggregates (Dexter, 1988, Six, et al., 2004). For this reason, aggregates are often functionally grouped into micro- versus macro-aggregates, with a diameter of 0.25 mm used to distinguish between them (Amezketa, et al., 2003, Fristensky and Grismer, 2008, Tisdall and Oades, 1982). Most aggregate stability studies have focused on the macro-aggregate fraction, as these larger units tend to reflect soil structure and soil organic matter content, while also showing greater sensitive to disturbance (An, et al., 2010, Boix-Fayos, et al., 2001, Six, et al., 2004, Sparling, et al., 1994). Despite receiving relatively little attention, micro-aggregates can act as a carbon reservoir within the soil, making their stability an important factor in carbon sequestration (Six, et al., 2000, Skjemstad, et al., 1990). Thus, it is important to consider both size fractions when assessing soil aggregate stability.

Due to its influence on crop productivity, as well as its rapid response to changes in management practices (Laghrour, et al., 2016, Mulumba and Lal, 2008), aggregate stability has become commonly used as an indicator of soil health (Allen, et al., 2011, Arias, et al., 2005). Still, there exists an overall lack of consensus in how to appropriately quantify that property, with different methods typically showing low correlation to one another (Almajmaie, et al., 2017, Regelink, et al., 2015). A related complication arises because, even though it is often treated as constant, aggregate stability varies with the amount of applied stress (Amezketa, et al., 2003). In the field, soils are subjected to various levels of energy, particularly near the soil

surface, with light rainfall representing an example of low applied energy (Shin, et al., 2016) and vehicle traffic representing high applied energy (Ungureanu, et al., 2017). Some studies have attempted to connect this energy input with the breakdown of aggregates (Mayer, et al., 2011, Schomakers, et al., 2015), but there is still little consistency in how such methods are applied and interpreted (Almajmaie, et al., 2017).

Aggregate stability is typically measured using one of two general approaches: mechanical sieving or laser diffraction. Sieving can be done with wet or dry aggregates, using either a single sieve (e.g., to capture the 1-2 mm size fraction) or nested sieves (Arnold and Page, 1986, Kemper and Rosenau, 1986). Using a single sieve allows for determination of a mass fraction known as percentage of stable aggregates (De Leenheer and De Boodt, 1959, Yoder, 1936), while nested sieves can be used to calculate mean weight diameter (MWD), geometric mean diameter (GMD), and proportion of stable aggregates (Yoder, 1936). Sieve-based measurements suffer from several drawbacks, including a lack of repeatability, inadequate ability to quantify or regulate input energy, limited number of sieve sizes, and bias towards larger aggregates sizes (Amézketa, 1999, Rawlins, et al., 2013, Tisdall and Oades, 1982). In an attempt to address the first two drawbacks, researchers have explored using ultrasound waves (i.e., sonication) as a way to control the energy applied to the aggregates (Mentler, et al., 2004). Even with such modifications, sieving has limited capability to resolve micro-aggregate fractions.

Laser diffraction measurements can detect a wider distribution of aggregate sizes, though these data are typically summarized using only the median size (d50). Aggregate stability can then be described by analyzing shifts in d50 under different applied energy levels (Bieganowski, et al., 2010, Rawlins, et al., 2013, Virto, et al., 2011). While d50 has the advantage of being a single number, thus allowing comparison between different treatments and/or applied energy

levels, it does not account for textural differences between soils. In contrast, the corrected d50 ($d50_c$) corrects for the particle size distribution of the sample, and is calculated as (Rawlins, et al., 2013):

$$d50_c = d50 - d50_{psd} \quad [4.1]$$

where $d50_{psd}$ represents the median particle size. Still, $d50_c$ may not capture shifts between macro and micro aggregates, or even between aggregates and individual particles, particularly when applied to coarse-textured soils such as sands.

To overcome the shortcomings associated with current methods to quantify aggregate stability, we propose a new indicator deemed integrated aggregate stability (IAS). This indicator accounts for all aggregates < 2 mm in size, allows for controlled energy inputs, and corrects for the underlying particle size distribution of the soil. Further, IAS can be set to differentiate between micro- and macro-aggregates, allowing quantification of the dynamics of these fractions under different applied energies. Given its ability to consistently and accurately detect aggregate stability across size classes, the IAS method should serve as a standard by which to quantify and compare aggregate stability.

4.2.1 Theory

Integrated aggregate stability (IAS)

The cumulative size distribution function measured by a laser diffraction machine, $F(x)$, represents the integral of the measured density function, $f(x)$:

$$F(x) = \int_0^x f(s)ds \quad [4.2].$$

In the integrated aggregate stability (IAS) method, the cumulative distribution functions are measured for independent samples representing aggregated soils (hereafter "*a*") and dispersed samples composed of individual particles (hereafter "*p*"), such that:

$$F_a(x) = \int_0^x f_a(s)ds \quad [4.3]$$

$$F_p(x) = \int_0^x f_p(s)ds \quad [4.4].$$

$F(x)$ and $f(x)$ both represent relative volume fractions, with the former scaled between 0 and 1. However, due to the presence of internal porosity, aggregate formation often increases the specific volume of the soil, V, where V = volume of soil/mass of soil. In other words, a given mass of soil will have greater volume when its particles are aggregated as opposed to when they are dispersed. The total volume per mass of dispersed particles, $V_{t,p}$ [L^3 M^{-1}], and aggregated particles, $V_{t,a}$ [L^3 M^{-1}], can be used to convert the relative volume density functions into volume-corrected density functions, $v(x)$:

$$v_a(x) = V_{t,a} \cdot f_a(x) \quad [4.5]$$

$$v_p(x) = V_{t,p} \cdot f_p(x) \quad [4.6].$$

Likewise, we can combine Equations [4.3] and [4.5], and also Equations [4.4] and [4.6], to obtain the volume-corrected cumulative distribution functions for aggregates (V_a) and particles (V_p):

$$V_a(x) = V_{t,a}\int_0^x f_a(s)ds = V_{t,a}F_a(x) \quad [4.7]$$

$$V_p(x) = V_{t,p}\int_0^x f_p(s)ds = V_{t,p}F_p(x) \quad [4.8].$$

The two volume-corrected density functions, $v_a(x)$ and $v_p(x)$, will cross at some value x_1:

$$v_p(x_1) = v_a(x_1) \quad [4.9].$$

Further, because aggregation causes an overall shift of the volume distribution towards larger particle sizes, we can assume:

$$V_p(x_1) - V_a(x_1) = \int_0^{x_1} \left(v_p(s) - v_a(s) \right) ds \geq 0 \qquad [4.10].$$

For the entire range of particle/aggregate sizes ($0 < x \leq x_{max}$), the aggregated sample will have equal or higher specific volume than the dispersed particles, meaning that:

$$V_{t,p} - V_{t,a} = V_p(x_{\max}) - V_a(x_{\max}) = \int_0^{x_{\max}} \left(v_p(s) - v_a(s) \right) ds \leq 0 \qquad [4.11].$$

Equation [4.11] can also be written as:

$$V_{t,p} - V_{t,a} = \int_0^{x_1} \left(v_p(s) - v_a(s) \right) ds + \int_{x_1}^{x_{\max}} \left(v_p(s) - v_a(s) \right) ds \qquad [4.12].$$

Equation [4.12] can be rearranged as:

$$\int_{x_1}^{x_{\max}} \left(v_a(s) - v_p(s) \right) ds = V_{t,a} - V_{t,p} + \int_0^{x_1} \left(v_p(s) - v_a(s) \right) ds \qquad [4.13].$$

We now define the integrated aggregate stability, IAS, as (Figure 1):

$$\mathrm{IAS} = \frac{1}{V_{t,a}} \int_{x_1}^{x_{\max}} \left(v_a(s) - v_p(s) \right) ds \qquad [4.14].$$

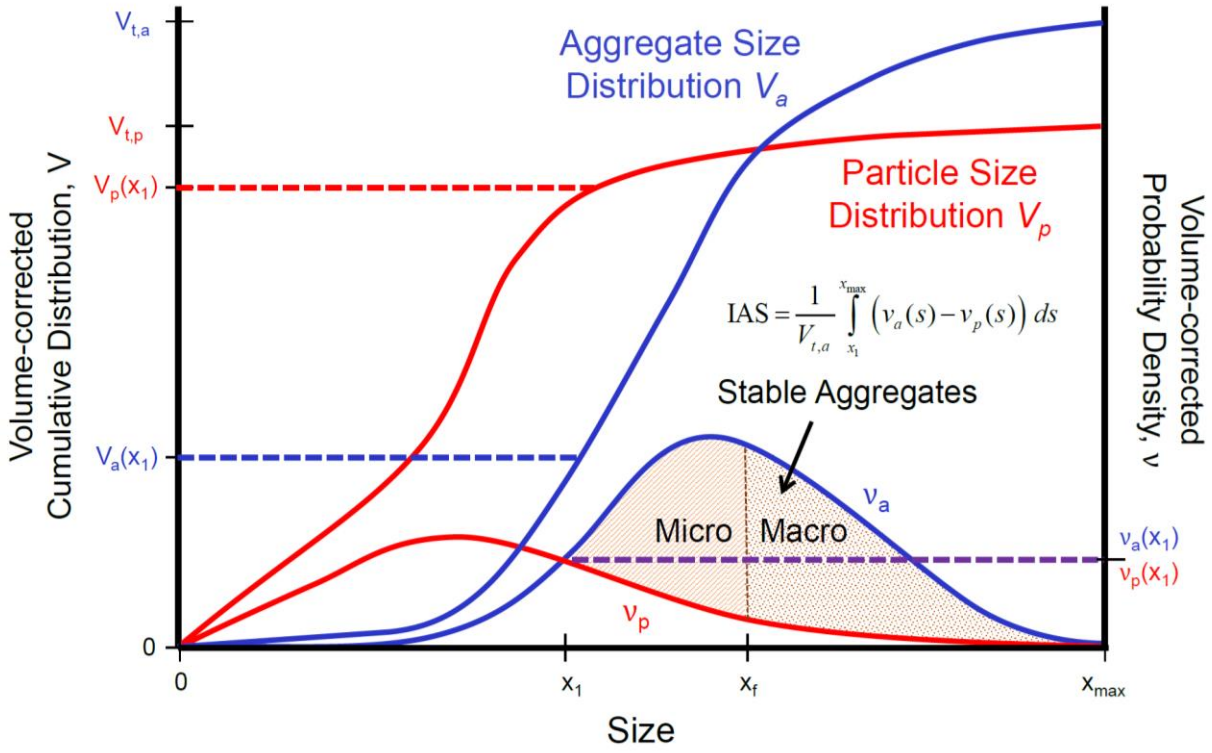

Figure 4.1: Schematic showing the integrated aggregate stability (IAS) metric, which is calculated as the area between the volume-corrected aggregate and particle density functions, respectively $v_a(x)$ and $v_p(x)$, over the range of diameters between x_1 and x_{max}.

Combining the Equations [4.13] and [4.14] we obtain:

$$IAS = 1 - \frac{V_{t,p}}{V_{t,a}} + \frac{1}{V_{t,a}} \int_0^{x_1} \left(v_p(s) - v_a(s)\right) ds \qquad [4.15].$$

We will use the symbol λ to define the ratio of specific volumes as:

$$\lambda = V_{t,p} / V_{t,a} \qquad [4.16].$$

Substituting Equation [4.16] into Equation [4.15]:

$$IAS = 1 - \lambda + \lambda F_p(x_1) - F_a(x_1) \qquad [4.17].$$

Bi- or multi-modal particle size distributions

Some soils, particularly coarse-textured ones, may have multiple crossings where the volume-corrected density functions $v_p(x)$ and $v_a(x)$ have identical values. We will call these crossings x_1, x_2, x_3… x_N, noting that $v_p(x)$ and $v_a(x)$ will have an odd number of crossings so long as the dispersed particles are smaller in size than the aggregated samples. In the case of a bimodal particle size distribution with three crossings, we can rewrite Equation [4.12] as:

$$V_{t,p} - V_{t,a} = \int_0^{x_1} \left(v_p(s) - v_a(s)\right) ds + \int_{x_1}^{x_2} \left(v_p(s) - v_a(s)\right) ds + \int_{x_2}^{x_3} \left(v_p(s) - v_a(s)\right) ds + \int_{x_3}^{x_{\max}} \left(v_p(s) - v_a(s)\right) ds \quad [4.18].$$

IAS in this instance will be defined as:

$$\mathrm{IAS}_{\mathrm{bimodal}} = \frac{1}{V_{t,a}} \int_{x_1}^{x_2} \left(v_a(s) - v_p(s)\right) ds + \frac{1}{V_{t,a}} \int_{x_3}^{x_{\max}} \left(v_a(s) - v_p(s)\right) ds \quad [4.19].$$

Substituting Equations [4.16] and [4.19] into Equation [4.18] yields:

$$\mathrm{IAS}_{\mathrm{bimodal}} = 1 - \lambda + \lambda F_p(x_1) - \lambda F_p(x_2) + \lambda F_p(x_3) - F_a(x_1) + F_a(x_2) - F_a(x_3) \quad [4.20].$$

Using the same approach, Equation [4.20] can be generalized for any multi-modal distribution as:

$$\mathrm{IAS}_{\mathrm{multimodal}} = 1 - \lambda + \lambda \sum_{\substack{i=1 \\ i \text{ odd}}}^{N} F_p(x_i) - \lambda \sum_{\substack{i=2 \\ i \text{ even}}}^{N-1} F_p(x_i) + \sum_{\substack{i=2 \\ i \text{ even}}}^{N-1} F_a(x_i) - \sum_{\substack{i=1 \\ i \text{ odd}}}^{N} F_a(x_i) \quad [4.21].$$

Separation between micro- and macro-aggregates

We will use x_f to represent the size fraction chosen to separate micro- versus macro-aggregates (e.g., 0.25 mm). In the case that the crossing point of the volume-weighted particle and aggregate density functions (x_1) is smaller than x_f, we can rewrite Equation [4.12] as:

$$V_{t,p} - V_{t,a} = \int_0^{x_1} \left(v_p(s) - v_a(s)\right) ds + \int_{x_1}^{x_f} \left(v_p(s) - v_a(s)\right) ds + \int_{x_f}^{x_{\max}} \left(v_p(s) - v_a(s)\right) ds \quad [4.22].$$

We can then define the micro-aggregate stability, IAS_{micro}, as:

$$IAS_{micro} = \frac{1}{V_{t,a}} \int_{x_1}^{x_f} \left(v_a(s) - v_p(s) \right) ds \qquad [4.23].$$

Substituting Equations [4.16] and [4.23] into [4.22], we obtain:

$$IAS_{micro} = \lambda F_p(x_1) - \lambda F_p(x_f) + F_a(x_f) - F_a(x_1) \qquad [4.24].$$

Likewise, we can define the macro-aggregate stability, IAS_{macro}, as:

$$IAS_{macro} = \frac{1}{V_{t,a}} \int_{x_f}^{x_{max}} \left(v_a(s) - v_p(s) \right) ds \qquad [4.25]$$

$$IAS_{macro} = 1 - \lambda + \lambda F_p(x_f) - F_a(x_f) \qquad [4.26].$$

Quantification of dispersive energy applied to the soil

During measurements of aggregated samples, ultrasonic energy may be applied. The total ultrasonic energy density applied to the soil suspension, J_s [E L^{-3}], can be estimated as:

$$J_s = P_s t_s / \upsilon_s \qquad [4.27]$$

where P_s is the applied power [E t^{-1}], t_s is the time over which sonication was applied [t], and υ_s is the volume of the ultrasonic chamber [L^3].

Using an energy balance, North (1976) quantified the fraction of applied energy consumed in dispersing the soil aggregates, β, as:

$$\beta = E_s / P_s t_s \qquad [4.28]$$

where E_s represents the ultrasonic energy adsorbed in dispersing soil [E].

Rearranging the full energy balance, β can be calculated as:

$$\beta = \left[1 - \frac{\Delta T'}{\Delta T} \left(1 + \frac{m_{sa} c_s}{m_w c_w + w_v} \right) \right] \cong 1 - \frac{\Delta T'}{\Delta T} \qquad [4.29]$$

where $\Delta T'$ is the change in temperature [T] of the soil and water suspension, ΔT is the change in temperature [T] for pure water under the same applied energy (Pt), m_{sa} is the mass of air dry soil [M], c_s is the specific heat of soil [E M^{-1} T^{-1}], m_w is mass of water [M], c_w is the specific heat of water [E M^{-1} T^{-1}] and w_v is the thermal capacity of the chamber [E T^{-1}].

4.3 Materials and methods

4.3.1 Soil descriptions

To demonstrate the IAS method and compare its estimated aggregate stability values with those estimated by other laser diffraction metrics (i.e., d50 and $d50_c$) and by wet seiving, we collected and analyzed soil samples from three locations. The first set of samples (deemed Site 1 hereafter) came from Blacksburg, Virginia, 6 km west of the Virginia Tech campus (37°12'25.3"N 80°29'12.0"W) in a long term no-till corn field. The soil was a silt loam composed of the Duffield-Ernest-Purdy undifferentiated group: Duffield - *Fine-loamy, mixed, active, mesic Ultic Hapludalfs*; Ernest - *Fine-loamy, mixed, superactive, mesic Aquic Fragiudults*; Purdy - *Fine, mixed, active, mesic Typic Endoaquults* (NRCS, 2017). Soil samples were taken from the surface (0-5 cm) layer in April 2016 with sixteen physical replicates collected (i.e., n = 16). A second set of surface samples were also collected in September 2016 (n = 16). The mean organic carbon content for these soils was 3.8 g kg^{-1} dry soil (n = 16).

The second set of soils (Site 2) came from a research farm in Ferrum, Virginia (36°55'13.6"N, 80°02'15.5"W). The soil was a silt loam classified as a Bluemount-Spriggs-Redbrush complex: Bluemount - *Fine-loamy, mixed, superactive, mesic Typic Hapludalfs*; Spriggs - *Fine-loamy, mixed, active, mesic Ultic Hapludalfs*; Redbrush - *Fine, mixed, superactive, mesic Typic Hapludalfs*. The soil had been in long-term grazed pasture before the grass was terminated in September 2015. The soil samples were collected in April 2016 from the

0-5 cm surface layer (n = 16). The mean organic carbon content for these soils was 6.2 g kg^{-1} dry soil (n = 16).

The third set of soils (Site 3) were collected near Blackstone, Virginia (37°05'44.0"N, 77°57'40.1"W), in a field that transitions between Appling (*Fine, kaolinitic, thermic Typic Kanhapludults*) and Durham (*Fine-loamy, siliceous, semiactive, thermic Typic Hapludults*) sandy loam soils (NRCS, 2017). The field was initially planted in fescue that was terminated in September 2015. In April 2016, soil samples were taken from the surface (0-5 cm) layer (n = 16). The mean organic carbon content for these soils was 2.6 g kg^{-1} of dry soil (n = 16).

4.3.2 Aggregate stability quantification

Particle size and aggregate size distributions were measured using a CILAS 1190 laser diffraction (LD) machine with a built-in 25 W ultrasound unit (CILAS Inc., Orleans, France). During analysis, samples were subjected to one of four applied energy levels: 1) 0 J ml^{-1}, where no sonication was applied; 2) 0.5 J ml^{-1}, where 13 seconds of sonication was applied; 3) 1 J ml^{-1}, where 26 seconds of sonication was applied; and 4) 5 J ml^{-1}, where 130 seconds of sonication was applied. For each run, soil was added to the LD machine until the sample obscurance reached 3-4%, at which time sonication was applied to the specified energy level. After the application of specified energy, the total measurement time to quantify $F_p(x)$ or $F_a(x)$ was ~3 minutes. To obtain particle size distributions, 0.2 grams of each sample was taken and mixed with a suspension of 1 ml sodium hexametaphosphate (5%) and 4 ml of DI water. This mixture was shaken on reciprocating shaker on low setting for 4 hours. The mixture was added to the LD machine and sonicated for 130 seconds before its size distribution was recorded.

After obtaining the aggregate and particle size distributions, aggregate stability was analyzed using d50 and the proposed method, IAS (Equation [4.17] or [4.20], depending on the

nature of each sample). The samples collected in April 2016 from Sites 1-3 were also evaluated for IAS_{micro} (Equation [4.24]) and IAS_{macro} (Equation [4.26]) with x_f = 0.25 mm (n = 16 per site). λ was assumed to equal 0.75 for all IAS calculations, as discussed in the following subsection.

4.3.3 Evaluation of the relative specific volume parameter λ

The IAS indicator requires an estimate for λ, which represents the specific volume of dispersed particle relative to those same particles when aggregated (i.e., Equation [4.16]). If the particles are spheres or ellipsoids of varying sizes, theoretical packing ratios suggest λ values of 0.64 to 0.74 (Donev, et al., 2004, Kyrylyuk and Philipse, 2011). For example, a sample composed to two different sphere sizes would have a λ value of ~0.74 (O'Toole and Hudson, 2011). Using laboratory measurements, Currie (1966) showed that λ varied between 0.69 and 0.79 for a variety of air-dried agricultural soils. For purposes of this study we assumed λ to equal 0.75, as this represents an average measured value also supported by theory.

To better understand the potential error associated with assuming a constant value for λ, we performed a sensitivity analysis using two soils from Site 1 and two from Site 3. IAS was estimated using Equation [4.17], assuming λ = 0.2, 0.5, 0.7, 0.9 and 1.0. Parameter sensitivity ratio (S_r) was then calculated as (Hamby, 1994):

$$S_r = \frac{I_o(O_m - O_0)}{O_o(I_m - I_0)} \qquad [4.30]$$

where I_o is the original parameter input (assumed for this analysis to be λ = 0.7), I_m is the modified parameter input, O_o is the original output (i.e., the calculated IAS value with λ = 0.7) and O_m is the IAS output with the modified parameter input.

4.3.4 Accuracy and precision of measurements

LD accuracy was stated by the manufacturer to be ± 3 x 10^{-3} mm; we verified this accuracy using polystyrene size standards of 10^{-4}, 10^{-3}, 0.01, and 0.1 mm (Sigma-Aldrich, Inc.,

St. Louis, USA). For each physical replicate analyzed on the LD machine, we ran two separate subsamples to check for measurement precision. So long as the two runs had higher precision than the LD machine accuracy, the first measurement was retained for subsequent analysis.

As a demonstration of the repeatability of LD-generated data, we homogenized a sample from Site 1 and another sample from Site 3, and then took four subsamples from each sample. The subsamples were then split for analysis within the LD machine under no sonication (0 J ml^{-1}) and 0.5 J ml^{-1} sonication, with another portion dispersed for particle size analysis. The resulting cumulative distribution data, $F(x)$, were plotted as mean values plus 95% confidence intervals.

4.3.5 Wet aggregate stability quantification

We investigated the relationship between the proposed IAS indicator, along with d50 (the traditional LD indicator), with water stable aggregation measured by wet sieving (Kemper and Rosenau, 1986). Samples were taken from Sites 1-3 (n = 32 for Site 1, representing the two sampling times there, and n = 16 for Sites 2 and 3). All samples were air-dried and then gently sieved to 4 mm. Subsamples were then passed through a 2 mm sieve for LD analysis, since the laser diffraction machine used in this analysis was limited to sizes < 2.5 mm. The LD analysis was run on all subsamples with no applied sonication (0 J ml^{-1} applied energy) and 13 seconds of applied sonication (0.5 J ml^{-1}). The particle size distribution was also measured for each subsample.

For the wet sieving, we placed 50 g of air-dry sample on top of nested sieves with openings of 2, 0.25, and 0.053 mm, with a collection tray on the bottom. This setup was lowered into water and submerged for 5 minutes. After 5 minutes, we vertically oscillated the sieves 50 times by hand. The soil remaining in each sieve was dried and weighed and corrected for small pebbles and sand content. The proportion of water stable aggregates 0.053 to 4 mm in size was

calculated as a sum of the water stable aggregates collected in the 0.053, 0.25, and 2 mm sieves, divided by the total dry mass of the sample.

Results from the three LD indicators (d50, $d50_c$, and IAS) were independently compared to the < 4 mm wet seive fraction using linear regression.

4.3.6 Dispersive energy quantification

To determine the fraction of dispersive energy consumed by the soil aggregates, β (Equation [4.29]), we measured ΔT using pure water, and $\Delta T'$ using suspension of soil plus water. The applied ultrasonic power P_s was fixed at 25 W, while the time of sonication was fixed at 130 seconds.

4.4 Results

Examples of cumulative distribution functions, $F(x)$, and probability density functions, $f(x)$, for two soils are shown in Figure 4.2. The first soil, from Site 2, was a fine-textured silt loam, and its size distribution consistently shifted to smaller sizes as the amount of applied ultrasonic energy increased (Figure 4.2a). The second soil, from Site 3, was a coarse-textured sandy loam. While the aggregated sample with no applied sonication (0 J ml^{-1}) had a unimodal distribution, the samples analyzed with higher ultrasonic energies (0.5, 1, and 5 J ml^{-1}) and as dispersed particles (psd) showed bimodal distributions (Figure 4.2b). Whereas the standard IAS equation (Equation [4.17]) was used to analyze the soil from Site 2, the samples from Site 3 required use of $IAS_{bimodal}$ (Equation [4.20]).

The repeatability test conducted on samples from Sites 1 and 3 showed that data generated from the laser diffraction (LD) machine had high precision (Figure 4.3). Further, applying ultrasonic energy to the samples caused consistent shifts in aggregate size distributions, as seen by the narrow confidence intervals for both soils with no sonication (0 J ml^{-1}) versus 13

seconds of sonication (0.5 J ml^{-1}). This consistency in quantifying aggregate and particle size distributions indicated that the LD machine provides repeatable measurements for aggregate and particle size distributions.

The proposed integrated aggregate stability (IAS) indicator requires an estimate of the relative specific volumes of the dispersed versus aggregated particles (λ; Equation [4.16]). As revealed by the sensitivity analysis, IAS has an inverse linear relationship with λ (Figure 4.4). Smaller λ values downscale the volume-corrected probability density function for the dispersed particles, $v_p(x)$, meaning that the aggregated particles will represent a higher proportion of the total aggregate sample as λ decreases. The four soils had mean sensitivity ratio S_r values (Equation [4.30]) that ranged from -0.49 to -0.075. Site 3 (sandy loam soil) had greater sensitivity to λ than Site 1 (silt loam soil), suggesting that coarse-textured soils may be more sensitive to λ than fine-textured soils.

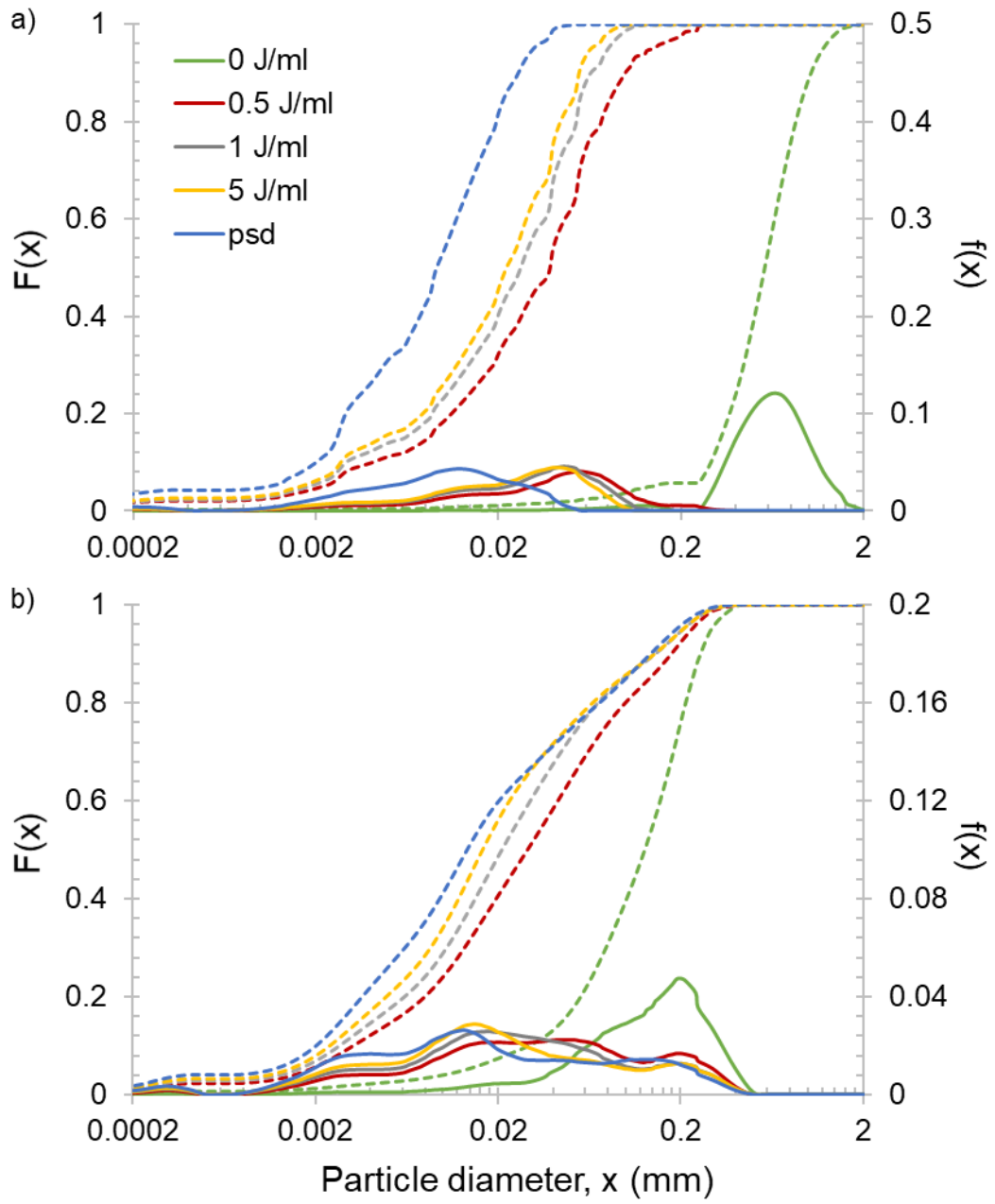

Figure 4.2: Examples of cumulative distributions, $F(x)$, and probability densities, $f(x)$, for soils from a) Site 2, and b) Site 3. Four different ultrasonic energies were applied to each set of soils: 0, 0.5, 1, and 5 J ml^{-1}; the underlying particle size distributions were also measured (psd). Solid lines show probability density functions, $f(x)$, and dotted lines show cumulative distribution functions, $F(x)$.

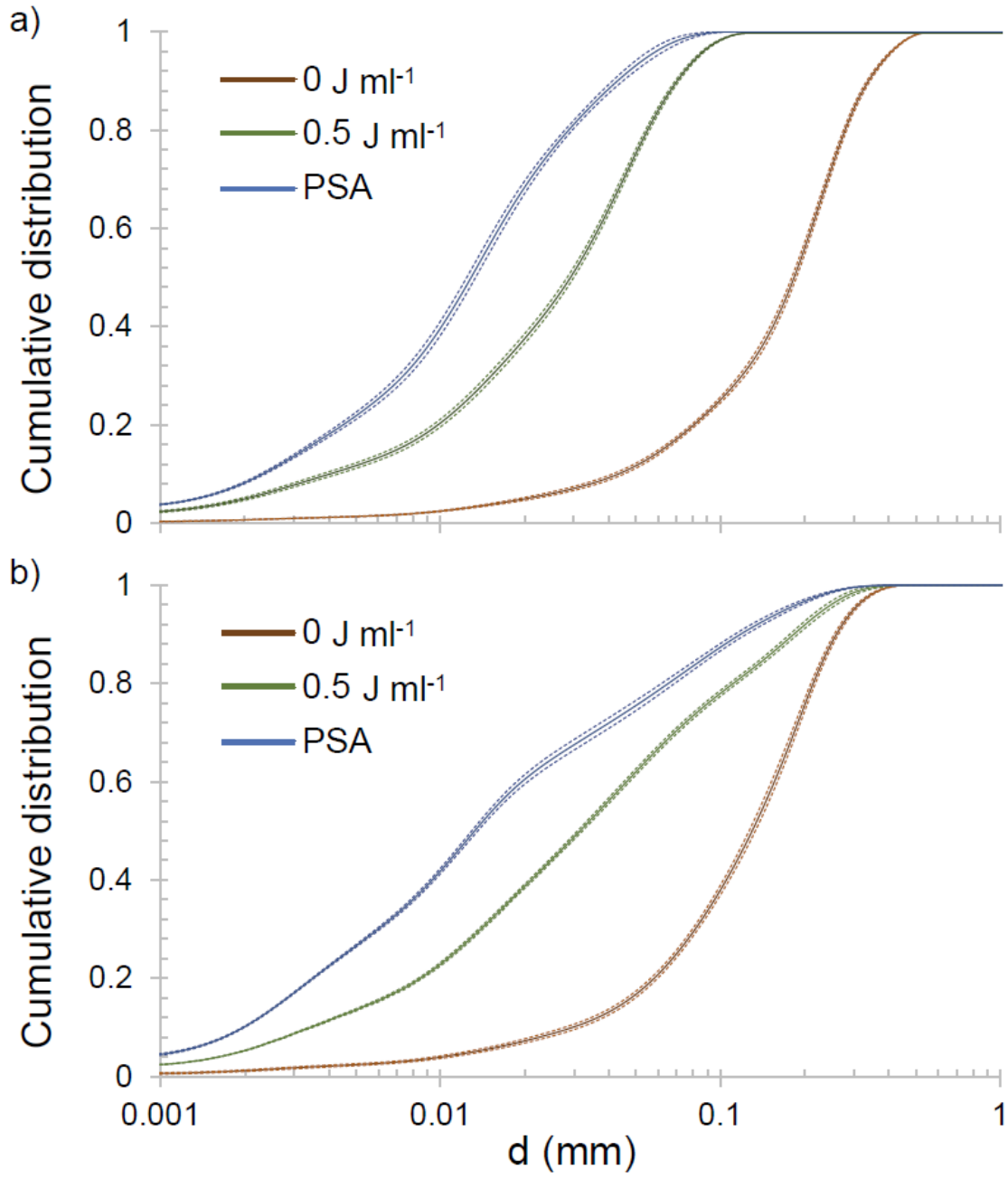

Figure 4.3: Repeatability test for cumulative distribution functions generated by laser diffraction measurements for two samples from a) Site 1, and b) Site 3. Four replicates of each sample were analyzed with no dispersion or applied sonication (0 J ml^{-1}), no dispersion with 13 seconds of sonication (0.5 J ml^{-1}), and full dispersion (particle size). Solid lines indicate mean values for each size class; dashed lines represent 95% confidence intervals.

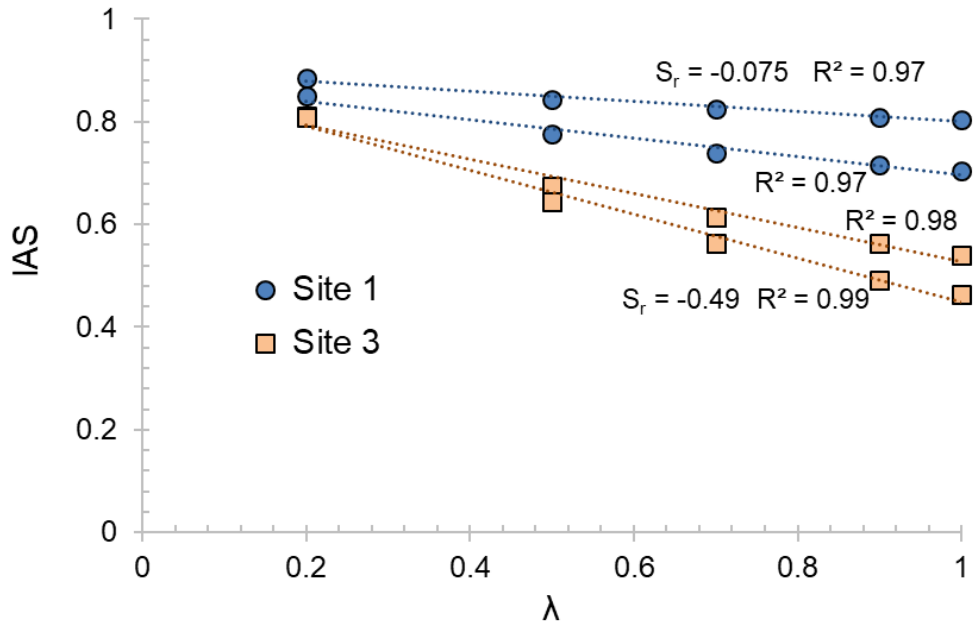

Figure 4.4: Sensitivity analysis of integrated aggregate stability (IAS) with the specific volume correction factor λ for two samples from Site 1 (blue and yellow points) and two samples from Site 3 (orange and gray points).

Near-surface soil samples collected from Sites 1-3 (n = 32 for Site 1 and n = 16 for Sites 2 and 3) were analyzed via LD and wet sieving (presented here as the proportion of total sample mass represented by water stable aggregates 0.053 – 4 mm). With no applied sonication (0 J ml^{-1}), the LD measurements as analyzed by IAS showed positive correlation with the wet sieving results (R^2 = 0.59; Figure 4.5a). The LD measurements with the input energy of 0.5 J ml^{-1} also showed relatively good correlation with the sieve-generated data when analyzed using IAS (R^2 = 0.49; Figure 4.5b). In contrast, the d50 metric traditionally used to interpret LD data showed low correlation with the wet sieving results (R^2 = 0.27 for 0 J ml^{-1} ultrasonic energy and R^2 = 0.09 for 0.5 J ml^{-1} applied energy; Figures 4.5c and 4.5d). The corrected $d50_c$ values (Equation [4.1]) had the same correlations with the wet sieving data as d50 (R^2 = 0.27 for 0 J ml^{-1} ultrasonic energy and R^2 = 0.09 for 0.5 J ml^{-1} applied energy; data not shown).

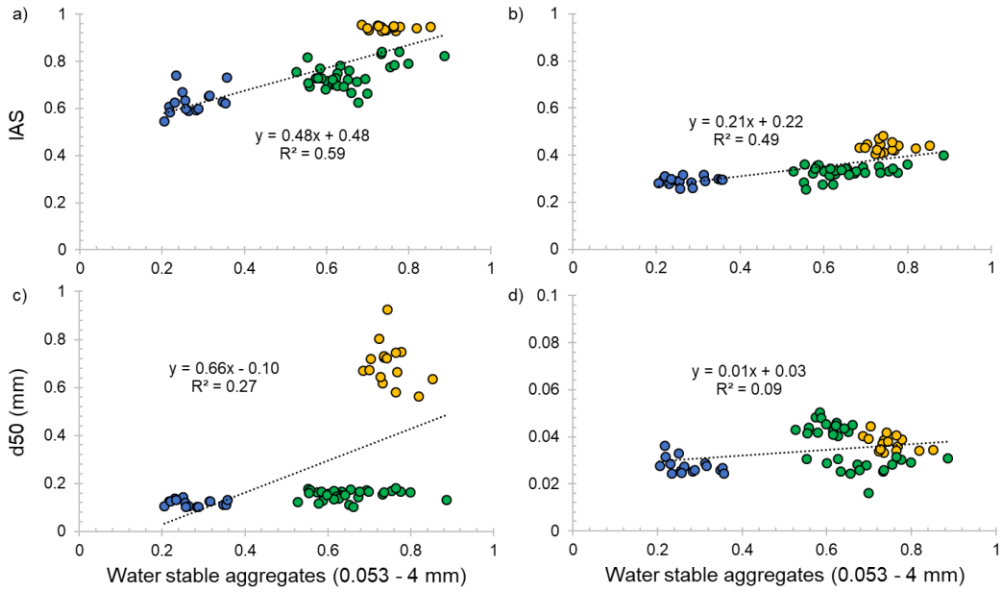

Figure 4.5: Relationship between water stable aggregates measured using wet sieving (values are presented as a proportion of total sample mass) versus integrated aggregate stability (IAS) for a) 0 J ml^{-1} and b) 0.5 J ml^{-1}; or versus median aggregate size d50 for c) 0 J ml^{-1} and d) 0.5 J ml^{-1}. Green points represent Site 1, yellow points represent Site 2, and blue points represent Site 3.

The soils from Sites 1-3 were also evaluated for IAS, IAS_{micro}, and IAS_{macro} under no sonication and the three applied ultrasonic energy densities (n = 16 per site and energy level). Site 2 had the highest IAS values for all energy densities, while Site 3 had the lowest IAS values (Figure 4.6a). When the aggregates were analyzed without sonication (0 J ml^{-1}), Site 2 primarily contained macro-aggregates > 0.25 mm in size. The application of ultrasonic energy dispersed most of the macro-aggregates from all three sites, though Site 2 retained some macro-aggregates at the 0.5 J ml^{-1} energy level. Site 3 (coarse-textured loamy sand) had non-zero values for IAS_{macro} at all applied energy levels, which may represent aggregates that formed around relatively large sand particles. Still, Site 3 had lower IAS values than the other two sites (fine-textured silt loams).

The LD measurements were also analyzed using d50 and $d50_c$ (Figure 4.6b), which both showed that Site 2 had greater aggregate stability than the other two sites at 0 J ml^{-1}. All sites had $d50/d50_c$ values < 0.05 mm for the other applied energy densities.

The quantification of dispersive energy contributing to soil aggregate breakdown showed that an average of 36 ± 11% of the applied ultrasonic energy was consumed in dispersing the soil aggregates (data not shown). Taking the applied energy levels of 0.5, 1, and 5 J m^{-1}, the soil aggregates experienced true dispersive energy levels of approximately 0.2, 0.4, and 2 J ml^{-1}.

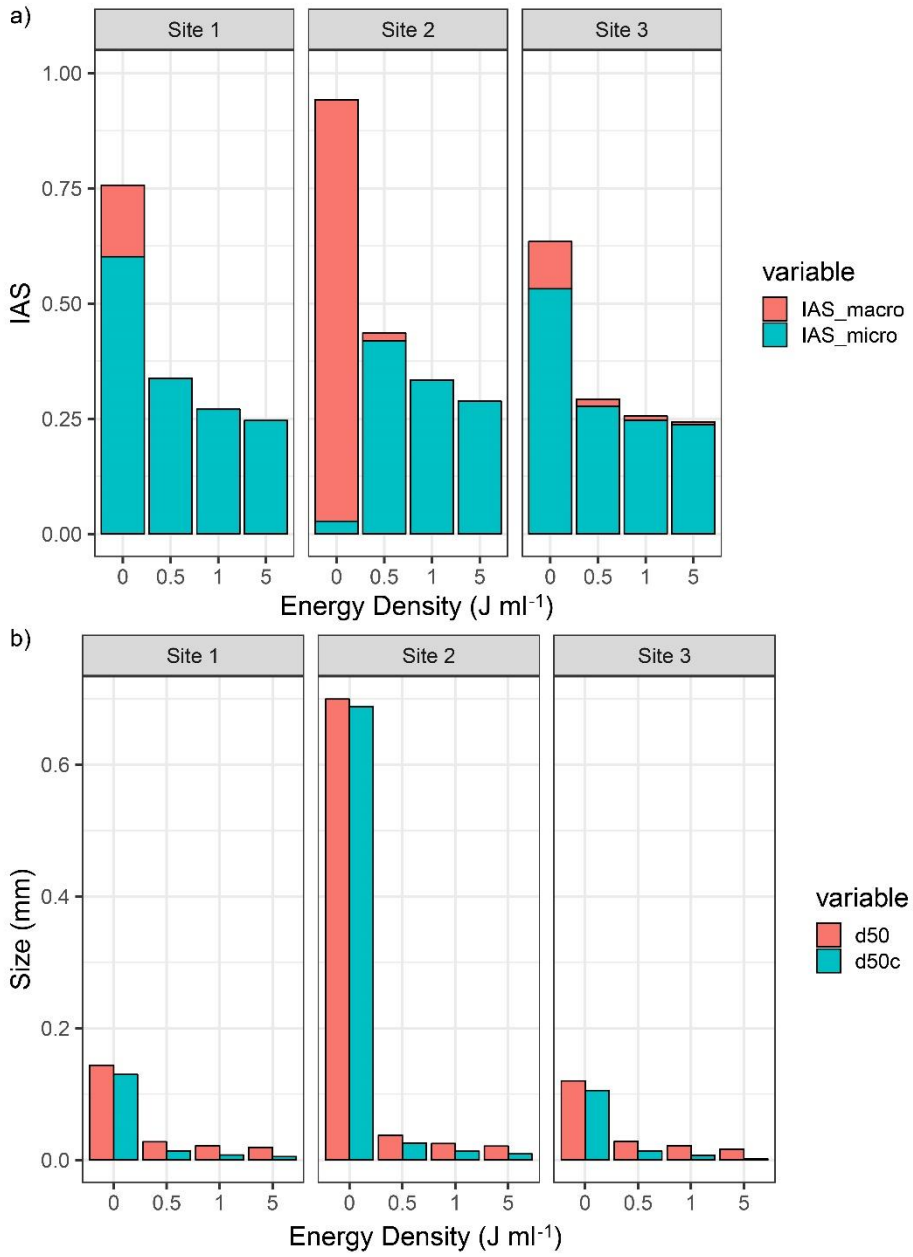

Figure 4.6: Laser diffraction measurements for soils from three sites and four applied sonication energies, 0, 0.5, 1, and 5 J ml^{-1}, as analyzed using a) IAS, including relative proportions of micro-aggregates IAS_{macro} (Equation [4.24]) and macro-aggregates IAS_{macro} (Equation [4.26]), and b) median aggregate size d50 and median aggregate size corrected for median particle size $d50_c$. Note that 0.25 mm was used to separate micro- from macro-aggregates, and that the figures show mean values from n = 16 replicates per site and applied energy.

4.5 Discussion and conclusion

In this paper we presented a new indicator that can quantify soil aggregate stability using laser diffraction (LD) measurements. In general, aggregate stability measurements using laser diffraction can overcome many of the shortcomings of traditional sieve methods, such as lack of repeatability, inability to quantify applied energy, and limited size range of aggregates that can be measured. Still, LD measurements have primarily been analyzed using median particle sizes (d50 or $d50_c$; Equation [4.1]). In contrast, our proposed integrated aggregate stability (IAS) indicator provides an estimate of the overall percentage of aggregates versus individual particles, e.g., an IAS value of 0.80 indicates that at least 80% of the total volume of the aggregated samples is made up of aggregates. At the same time, IAS had higher correlation with wet sieving data compared to the d50 and d50c indicators (Figure 4.5). As wet sieving represents a widely used method for determining aggregate stability (Almajmaie, et al., 2017, Kemper and Rosenau, 1986, Regelink, et al., 2015), the correlation shown here suggests that LD measurements may capture some of the same information when interpreted by IAS. Further, because the IAS presents LD data as a percentage of aggregated particles, it may be possible to set threshold values that can convey if a soil is resistant to aggregate breakdown, e.g., the 70% water stable aggregate threshold used by Amezketa, et al. (2003).

In its standard form (Equation [4.17]), IAS quantifies all aggregates < 2 mm in size, meaning that it integrates macro- and micro-aggregates together. Still, the IAS framework retains the capability to distinguish between micro-aggregate stability (IAS_{micro}; Equation [4.24]) and macro-aggregate stability (IAS_{macro}; Equation [4.26]). This flexibility means that IAS can quantify how soil aggregates shift between macro- and micro-aggregate fractions at different levels of dispersive energy. As an example, we caclulated IAS, IAS_{micro}, and IAS_{macro}, for three

different soils that differed in both their overall level of aggregation and in the distributions between macro and micro-aggregates (Figure 4.6). In this specific example, Site 2, which was a fine-textured silt loam soil that had previously been in pasture, had higher overall IAS values than Site 1 (silt loam in continuous row crop cultivation) or Site 3 (coarse-textured sandy loam previously in pasture). When the samples were analyzed without applied sonication (0 J ml^{-1}), Site 2 also showed a substantially higher proportion of aggregates within the macro-aggregate fraction, whereas most of the aggregates in Sites 1 and 3 existed within the micro-aggregate fraction. This result may be because Site 2 had higher organic carbon content (6.2 g kg^{-1}) than Site 1 (3.8 g kg^{-1}) or Site 3 (2.6 g kg^{-1}). The d50 and $d50_c$ metrics also reflected relative amounts of macro-aggregation at each site (i.e., higher $d50/d50_c$ for Site 2 compared to Sites 1 and 3 for 0 J ml^{-1}); however, those metrics proved incapable of differentiating between sites at higher levels of applied ultrasonic energy. The $d50/d50_c$ indicators therefore showed limited ability to detect micro-sized aggregates that were present in these soils. Taken altogether, these results reveal that IAS represents a superior option to study dynamics of different aggregate fractions when working with LD measurements, and demonstrate the potential for IAS_{macro} and IAS_{micro} to capture textural and land use effects on aggregation.

One primary advantage of LD measurements is that the amount of energy applied to the aggregates can be quantified (Mayer, et al., 2011, Schomakers, et al., 2015). Still, these calculations can suffer from some uncertainties. For example, while we focused our energy density calculations on the energy applied via the ultrasonic unit, the stirrer and pumps of the unit will also impart energy on the suspension (as detailed in the Appendix). There also exists uncertainty when translating these applied energies to those forces that a field soil might face. For example, a rainstorm with an intensity of 25 mm h^{-1} and a duration of 1 hour translates to an

energy density of approximately 0.1 J ml^{-1} if absorbed by the top 0.5 cm of soil (Shin, et al., 2016). The lowest applied ultrasonic energy (0.5 J ml^{-1}, translating to 0.2 J ml^{-1} of dispersive energy) thereby approximates the dispersive force of a typical heavy rainfall when quantified in volumetric terms, i.e., [E L^{-3}]. However, because of the dilute concentration of soil aggregates within the ultrasonic chamber (~0.001 g ml^{-1}), the corresponding energy densities on a gravimetric [E M^{-1}] basis were higher than those experienced by typical field soils. For example, assuming 1 g of soil was added to the ultrasonic chamber (which here had a volume of ~650 ml), the aggregates could have experienced more than 1000 J g^{-1} at the highest applied energy level. This value is two orders of magnitude larger than typical rainfall intensities (e.g., ~10 J g^{-1}; North, 1976); as a result, users should apply care when deciding whether to quantify energy inputs on a volumetric or gravimetric basis.

Another source of uncertainty in the IAS procedure resides in the λ parameter, which was used to account for specific volume differences between aggregated versus dispersed particles. In the calculations performed here, we assumed $\lambda = 0.75$, which represents a mean value supported by particle packing theory and experimental measurements of intra-aggregate porosity. To evaluate the effect of assuming a constant λ value, we performed a sensitivity analysis (S_r; Equation [4.30]). The four tested samples had mean values of $-0.5 \leq S_r \leq -0.075$. Previous studies have suggested that $|S_r| \leq 0.5$ or ≤ 1.0 represents a model parameter with low or damped sensitivity (Chaves, 2009, Gloe, 2011), meaning that the IAS calculation will be somewhat insensitive to the exact value of λ. Still, IAS accuracy will increase as λ becomes better constrained, particularly in coarse-textured soils, where the particle size and aggregate size distributions may have substantial overlap (i.e., $f_p(x)$ and $f_a(x)$ curves with similar shapes). At the same time, we assumed a constant λ regardless of applied energy, though in reality λ will likely

increase as the aggregated samples become more dispersed into individual particles (e.g., with the 1 and 5 J ml^{-1} ultrasonic energies). Numerous experimental procedures can be used to estimate the specific volume of aggregates, including measuring displacement when aggregates are added to non-wetting or non-mixing fluids (McIntyre and Stirk, 1954, Sarli, et al., 2001), or estimating aggregate volume using three-dimensional scanners (Sander and Gerke, 2007) or image reconstruction (Stewart, et al., 2012). Particle specific volumes can be estimated using pycnometers (Klute, et al., 1986). Thus, future work may therefore build on these methods to better constrain λ, and by extension improve the accuracy of IAS.

In conclusion, the integrated aggregate stability (IAS) indicator provides the ability to better interpret LD measurements, as it quantifies the total proportion of aggregated particles within a sample. Based on 64 samples collected from 3 sites, IAS showed relatively high correlation with water stable aggregation measurements collected by the wet sieving method ($R^2 \geq 0.5$). Further, IAS can be modified to quantify relative percentages of macro and micro aggregates within a sample. This capability means that future studies can better analyze soil resistance to failure under various applied stresses, which ultimately can be used to quantify and predict soil resilience. Based on these advantages, we conclude that IAS is altogether an improved method for quantifying soil aggregate stability.

Chapter 5: Talking SMAAC: a new tool to measure soil respiration and microbial activity

Accepted with moderate revisions in Frontiers in Earth Sciences

Ayush J. Gyawali*, Brandon J. Lester, and Ryan D. Stewart

5.1 Abstract

Soil respiration measurements are widely used to quantify carbon fluxes and ascertain soil biological properties related to soil microbial ecology and soil health, yet current methods to measure soil respiration either require expensive equipment or use discrete spot measurements that may have limited accuracy and neglect underlying response dynamics. To overcome these drawbacks, we developed an inexpensive setup for measuring CO_2 called the Soil Microbial Activity Assessment Contraption (SMAAC). We then compared the SMAAC with a commercial Infrared Gas Analyzer (IRGA) unit by analyzing a soil that had been subjected to two different management practices: grass buffer versus row crop cultivation with tillage. These comparisons were done using three configurations that detected 1) in situ soil respiration, 2) CO_2 burst tests, and 3) substrate induced respiration, a measure of active microbial biomass. The SMAAC provided consistent readings with the commercial IRGA unit for all three configurations tested, showing that the SMAAC can perform well as an inexpensive yet accurate tool for measuring soil respiration and microbial activity.

5.2 Introduction

Increased soil respiration due to warmer temperatures may exacerbate global climate change (Bond-Lamberty, et al., 2018, Davidson and Janssens, 2006, Rustad, et al., 2000), as soils currently have an gross efflux of ~60 Gt C yr^{-1} and represent one of the two largest terrestrial sources of carbon fluxes. Sequestering more carbon in soils has become a goal of climate mitigation efforts, such as the *four per mille* initiative (Minasny, et al., 2017), with particular emphasis on soils that have been degraded by human activities (Lal, 2004). Soil respiration measurements can help to inform such sequestration efforts, while also providing a means to monitor the health and function of agricultural soils (Allen, et al., 2011, Mondini, et al., 2010). In the laboratory, soil respiration measurements are used to interpret soil microbial characteristics, for example using assays like substrate induced respiration (Bradford, et al., 2010), carbon mineralization (Song, et al., 2014) and catabolic response profile (Casas, et al., 2011).

Soil respiration is often assessed by measuring changes in carbon dioxide (CO_2) concentration within a controlled volume over some period of time, and rely on either spot samples or integrated measurements. Spot samples are often analyzed using gas chromatography (GC) techniques (McGowen, et al., 2018). Multiple GC measurements can also be combined for integrated measurements. However, these GC measurements can be costly, particularly when many samples are required. Infrared gas analyzer (IRGA) devices provide integrated flux measurements, and have been widely used to quantify soil respiration in forest (Don, et al., 2009, Gaudinski, et al., 2000, Ladegaard-Pedersen, et al., 2005) and agricultural ecosystems (Smukler, et al., 2012). IRGA-based measurements have also been used to study microbial community composition (Fierer, et al., 2003), which represents one of the important properties related to soil function (Mukhopadhyay, et al., 2014). While IRGA-based devices provide the most accurate

flux data (Rowell, 1995), such sensors are often expensive, putting them beyond the means of many practitioners, and power-intensive, limiting their usefulness in the field.

Integrated measurements can also be collected using chemical titration with potassium hydroxide, KOH, or sodium hydroxide, NaOH (Haney, et al., 2008). While titration methods are straightforward and can be done without expensive devices, there are concerns over the accuracy of the titration process (Haney, et al., 2008). These methods often under-estimate soil respiration when compared to IRGA measurements (Ferreira, et al., 2018). To add to this, titration methods often require substantial labor and laboratory space to conduct.

Finally, both spot and integrated samples can be analyzed using colorimetric techniques. For spot samples, colorimetric tubes can be used (Patil, et al., 2010), while colorimetric paddles can provide integrated flux measurements (Norris, et al., 2018, Sciarappa, et al., 2016). Micro-respiration measurements, which quantify soil respiration and microbial community physiological profiles using indicator dyes in agar gel, also use colorimetric techniques (Campbell, et al., 2003, Renault, et al., 2013). Even though individual sampling units are relatively inexpensive, the materials are not re-usable and quickly become cost-prohibitive as the numbers of samples rise.

To address the above-mentioned shortcomings, we present an inexpensive Arduino-powered and IRGA-based CO_2 measurement device, called the Soil Microbial Activity Assessment Contraption (SMAAC). The SMAAC has considerable flexibility, as we demonstrate using three different configurations: 1) SMAAC-Field, where the device was used to quantify soil respiration in a field setting; 2) SMAAC-Burst, where the device was used to analyze CO_2 evolution upon rapid re-wetting of air-dried soil; and 3) SMAAC-Biomass, where the device was used to quantify substrate induced respiration. To validate these configurations,

we compared the measurements provided by the SMAAC with those from a commercial field-portable IRGA system. These examples reveal that the SMAAC can perform well as an inexpensive yet accurate tool to measure soil respiration.

5.3 Materials and methods

5.3.1 Soil Microbial Activity Assessment Contraption (SMAAC) Description and Calibration

The sensor platform consists of four main components (Figure 5.1).

1. Arduino Uno (Arduino LLC, Ivrea, Italy)
2. Adafruit Data Logger Shield (Adafruit Industries, New York, NY, United States)
3. Sandbox Electronics 10,000 ppm CO2 sensor (Sandbox Electronics, China)
4. 5V DC power source

The Arduino Uno is an open source/open hardware microcontroller based on the ATMEGA 328P. It has no storage space or accurate time-keeping abilities on its own, so the data logger shield contains a Real Time Clock (RTC) and additional circuitry to store data on a removable SD card. The SMAAC was powered using four 1.5 V AA batteries. This configuration provided up to 21 hours of readings at the rate of 20 readings per minute.

The CO_2 sensor requires only 4 wires to communicate with the Arduino (+V, RX, TX, and Ground). The sensor uses I2C (Intra Integrated Circuit) serial protocol and determines CO_2 concentration using non-dispersive infrared absorbance (NDIR). Example code for integrating this sensor with the Arduino is available at https://github.com/SandboxElectronics/NDIRZ16.

The CO_2 sensor has an option to calibrate itself to 400 ppm CO_2 based on ambient readings. To verify that this first-order calibration is accurate enough for scientific use, we checked the sensor accuracy using known CO_2 standards (n = 2). Here, the sensor was installed via a rubber stopper into a 1 L jar (Fig. 5.1a). The jar was filled with CO_2-free air, and then 0.1 L

of 1000 ppm CO_2 gas was replaced within the jar (providing a 100 ppm concentration within the jar). This process was repeated a second time with 1000 ppm CO_2 air, and also two times each with 2000 and 5000 ppm CO_2 air (providing concentrations of 200 and 500 ppm within the jar). The results obtained from SMAAC for these standards were repeatable within ±20 ppm and accurate within the ±50 ppm sensor limit.

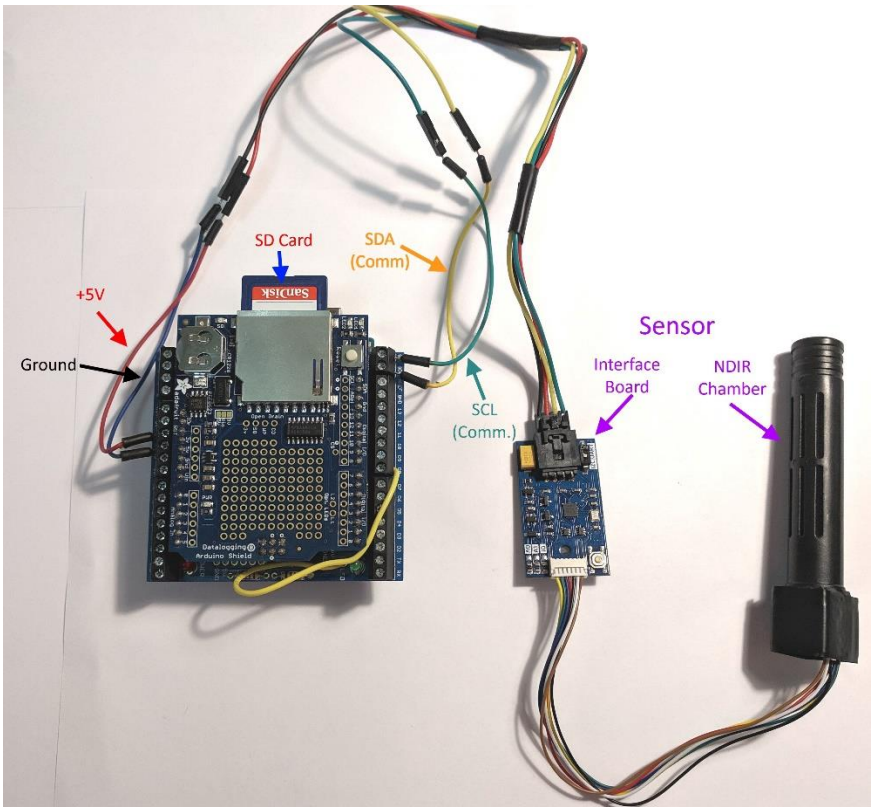

Fig 5.1: Schematic of the Soil Microbial Activity Assessment Contraption (SMAAC). NDIR = Non-dispersive infrared sensor used to detect CO_2; SCL = serial clock line, used to synchronize data and commands between the Arduino and the interface board; SDA= serial data line, used to send and receive serial data and commands to the interface board.

5.3.2 Soil description

We tested the SMAAC with a Weaver series silt loam soil (*Fine-loamy, mixed, active, mesic Fluvaquentic Eutrudepts*), located at Kentland Farm at Virginia Tech (37.198, -80.575). To include different soil microbial activity levels, we sampled two locations in adjacent fields that were managed using 1) perennial grass cover and 2) row crop cultivation with moldboard tillage. The pH of the grass-covered soil was 6.4 and of the tilled soil was 6.6, putting the soil at the upper pH limit for performing static chamber measurements (e.g., West and Sparling (1986) recommend pH ≤ 6.5). We performed three tests in which the SMAAC measurements were compared to a commercially available self-contained IRGA unit (LI-COR 8100 with 20 cm diameter 8100-103 survey chamber, LI-COR, Lincoln, NE, United States): SMAAC-Field, SMAAC-Burst, and SMAAC-Biomass.

5.3.3 Field and laboratory measurements

5.3.3.1 SMAAC-Field soil respiration test

We used 200 mm (diameter) by 150 mm (height) PVC columns for the field measurements. We collected a 2-minute CO_2 respiration measurement first using the SMAAC located within the LI-COR 8100-103 sampling chamber (i.e., SMAAC-simultaneous; Fig. 5.2b). Note that the sampling chamber provided an air-tight seal around the PVC column during measurements. Immediately after this first measurement the LI-COR unit was removed and the ring was capped with an airtight rubber cap (i.e., SMAAC-independent; Fig. 5.2b). The SMAAC then collected a second 2-minute measurement. The CO_2 flux (f_{CO_2}; [N L^{-2} t^{-1}] was estimated as:

$$f_{CO_2} = \frac{P_0 V_c}{R T_0 A} \frac{\Delta C}{\Delta t} \tag{5.1}$$

where P_0 is the pressure in the chamber [M L^{-1} t^{-2}], assumed to be equal to atmospheric pressure, V_c is the volume of the sampling chamber plus any tubing and pumps [L^3], R is the ideal gas law

constant [M L^2 N^{-1} T^{-1} t^{-2}], T_0 is the temperature of the air [T], A is the area of exposed soil [L^2], and ΔC is the change in CO_2 concentration on a molar basis [N N^{-1}] per change in time Δt [t].

Four rings were sampled for each of the grass-covered and tilled soils (n = 4).

5.3.3.2 SMAAC-Burst CO_2 test

For the CO_2 burst test, we placed 200 g of 4-mm sieved and air-dried soil from the two sites into a 200 mm diameter by 150 mm tall column. The water holding capacity for each soil sample was measured using the funnel method (Fierer, et al., 2006). Water was added dropwise to each soil sample using a syringe until the sample reached 50% water holding capacity. Once the soil samples were wetted, the SMAAC was placed on the soil surface (Fig. 5.2d). The LI-COR 8100 sampling hood was then placed on top. Both instruments collected readings several times a minute for at least 2 hours. For each instrument, the readings collected were averaged per minute for graphing purposes (n = 4 per soil).

5.3.3.3 SMAAC-Biomass substrate induced respiration (SIR)

We also compared LI-COR 8100 and SMAAC measurements during a test designed to mimic substrate induced respiration (SIR) measurements (Fierer, et al., 2003, Strickland, et al., 2010). Refrigerated soil samples from the fields were brought to room temperature overnight. We placed 80 g (equivalent dry mass) of 4-mm sieved soil samples into a 1 L glass jar (Fig 5.2a). We then added 0.16 L of autolyzed yeast solution made from 12 g of yeast extract (BD Biosciences, San Jose, United States) in 1 L of DI water as a substrate. The mixture of soil and substrate was then shaken with no cover for 10 minutes. We then sealed the jar using a rubber stopper that had the SMAAC sensor and a septum mounted through it. Using the septum, we flushed the headspace of the jar using CO_2 free air for 7 minutes. Then the jar was maintained at 20 °C for 4 hours. After 4 hours, we collected a gas sample through the septum using a syringe.

This sample was injected into the LI-COR 8100 unit to quantify the CO_2 concentration in the jar headspace. The 4-hour CO_2 reading from the SMAAC was also analyzed. Both measurements of headspace CO_2 were converted to SIR units (μg C g^{-1} dry soil h^{-1}) based on the dry mass of soil. Three replicates were analyzed for the grass buffer and moldboard plowed soils (n = 3).

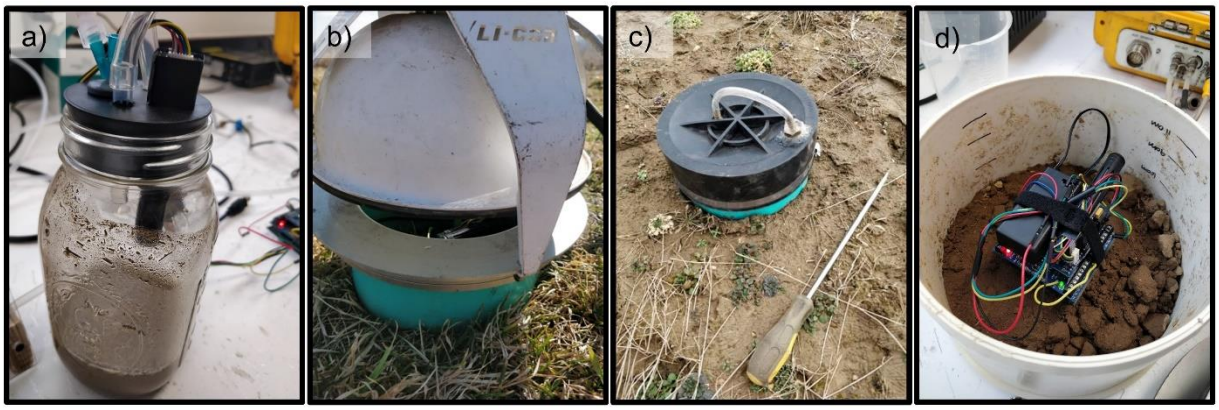

Fig 5.2: Measurement setups for: a) SMAAC-Biomass substrate induced respiration measurement; b) SMAAC-Field flux measurement with SMAAC simultaneously located within the LI-COR 8100 sampling chamber; c) SMAAC-Field flux measurement with SMAAC independent of the LI-COR unit; d) SMAAC-Burst laboratory CO_2 burst measurement.

5.3.4 Statistical Analyses

All statistical analysis and figures were done in R Version 3.5.0 (R Development Core Team, 2018). Analysis of Variance (ANOVA) was used to compare the three types of measurements performed in the SMAAC-Field configuration (i.e., LI-COR, SMAAC-simultaneous, SMAAC-independent). During the SMAAC-Burst and SMAAC-Biomass tests, the Student's t-test was used to compare results from the LI-COR versus the SMAAC. Measurements were analyzed separately for the grass-covered and tilled soils. $\alpha = 0.05$ was used to test for significance throughout this study.

5.4 Results

5.4.1 SMAAC-Field soil respiration test

For the SMAAC-Field respiration test, the LI-COR 8100 and SMAAC were used to quantify CO_2 flux over a 2-minute period, with the SMAAC both placed within (SMAAC-simultaneous) and without (SMAAC-independent) the LI-COR sampling chamber. Both instruments showed that the grass-covered soil had a higher CO_2 flux than the tilled soil (Fig. 5.3). The flux measured for the grass buffer soil by the LI-COR (4.1×10^{-4} μmol CO_2 cm^{-2} s^{-1} ± 9.9×10^{-5} standard deviation, SD) was not significantly different than fluxes determined via the SMAAC-simultaneous (5.6×10^{-4} μmol CO_2 cm^{-2} s^{-1} ± 2.7×10^{-4} SD) or SMAAC-independent (3.1×10^{-4} μmol CO_2 cm^{-2} s^{-1} ± 7.2×10^{-5} SD) tests. For the tilled soil, the LI-COR flux (5.9×10^{-5} μmol CO_2 cm^{-2} s^{-1} ± 1.9×10^{-5} SD) was again not significantly different from the fluxes measured during the SMAAC-simultaneous (5.9×10^{-5} μmol CO_2 cm^{-2} s^{-1} ± 1.5×10^{-5} SD) and SMAAC-independent (4.7×10^{-5} μmol CO_2 cm^{-2} s^{-1} ± 2.6×10^{-5} SD) tests.

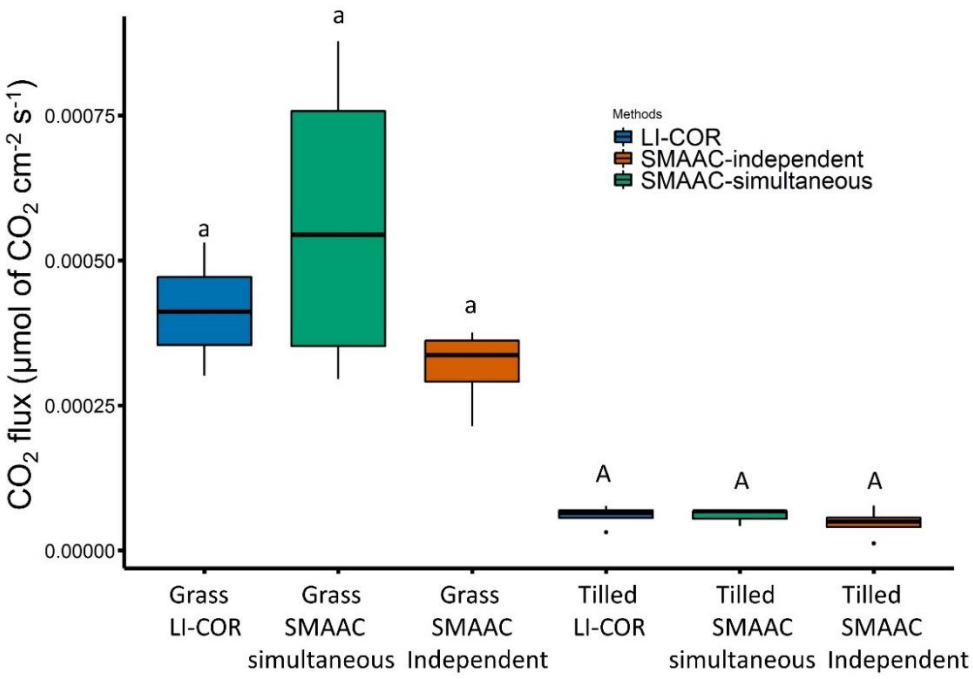

Fig 5.3: CO_2 fluxes measured in the field by the LI-COR (blue), SMAAC-simultaneous (green) and SMAAC-independent (orange). Different small letters indicate grass-covered soil fluxes are statistically different; different capital letters indicate tilled soil fluxes are statistically different (ANOVA with Tukey's HSD; $P < 0.05$).

5.4.2 SMAAC-Burst CO_2 burst test

The SMAAC-Burst configuration produced consistent results compared to the LI-COR 8100 unit for both the grass-covered and tilled soils (Fig 5.4), with similar mean values and standard deviations calculated from the four physical replicates for each soil (Fig 5.4a). We observed relatively large fluctuations in CO_2 emission rates, especially during the first 20 minutes of the experiment (Fig 5.4b). After this initial period, CO_2 emission rates fluctuated more for SMAAC compared to LICOR, though the mean rates were generally consistent between methods (Fig 5.4b). Both instruments showed that the CO_2 burst was larger in the grass-covered soil compared to the tilled soil (Fig 5.4).

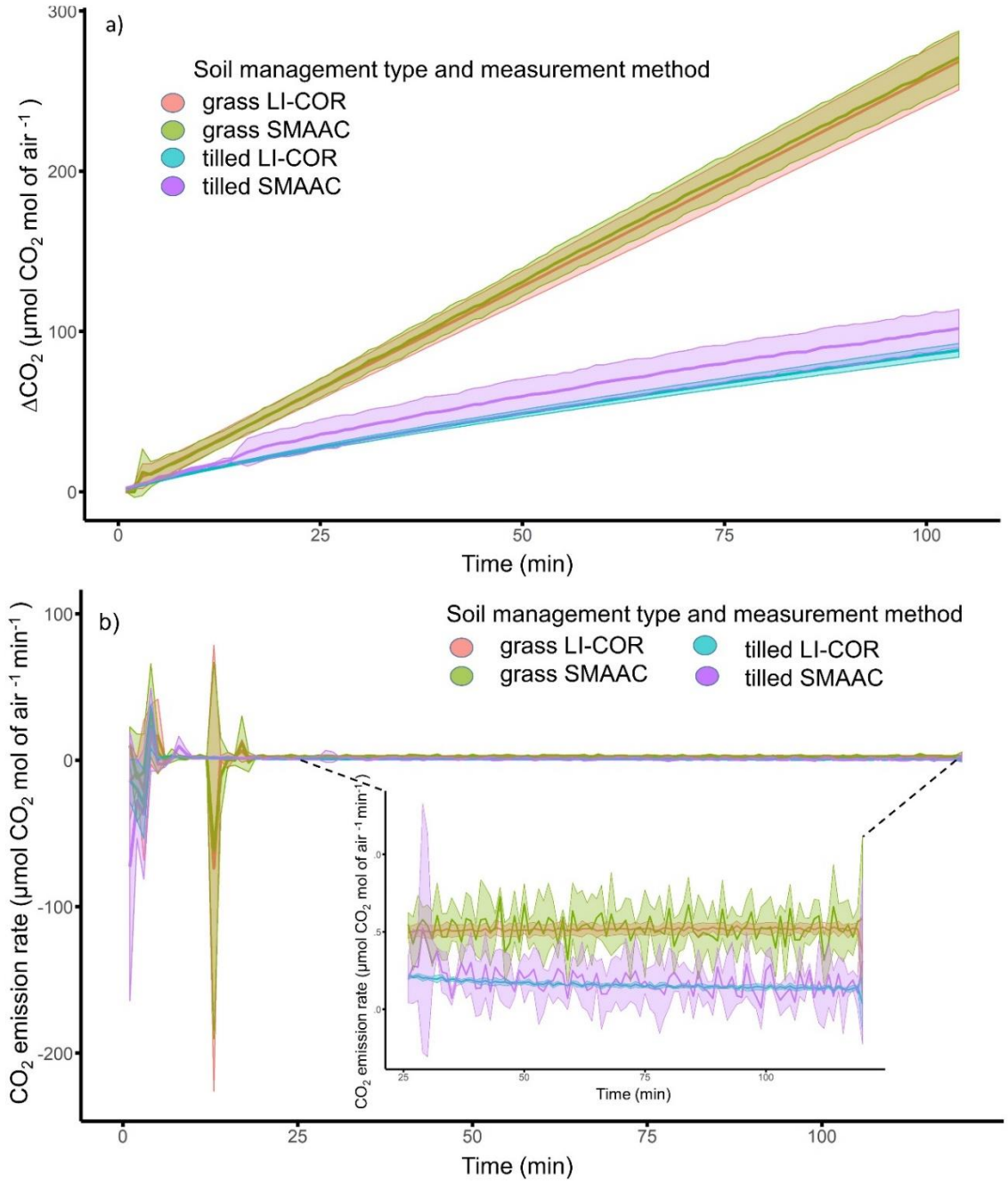

Fig 5.4: a) Laboratory measurement of change in CO_2 through time (min) for grass-covered and tilled soils, measured using a LI-COR 8100 and the SMAAC-Burst configuration. Solid lines represent mean values, and shaded areas represent standard deviations from the means. b) CO_2 emission rates for grass-covered and tilled soils, measured using the LI-COR and the SMAAC-Burst configuration.

5.4.3 SMAAC-Biomass substrate induced respiration test

Results generated using both the LI-COR 8100 and the SMAAC-Biomass consistently showed that the grass-covered soil had higher SIR values than the tilled soil (Fig. 5.5). The LI-COR (0.19 µg C g dry soil^{-1} h^{-1} ± 0.03 SD) and SMAAC (0.21 µg C g dry soil^{-1} h^{-1} ± 0.01 SD) measurements were not statistically different for the grass-covered soil ($P \geq 0.05$). However, the LI-COR SIR value (0.09 µg C g dry soil^{-1} h^{-1} ± 0.005 SD) for the tilled soil was significantly higher than the SMAAC SIR value (0.05 µg C g dry soil^{-1} h^{-1} ± 0.005 SD; $P = 0.0009$).

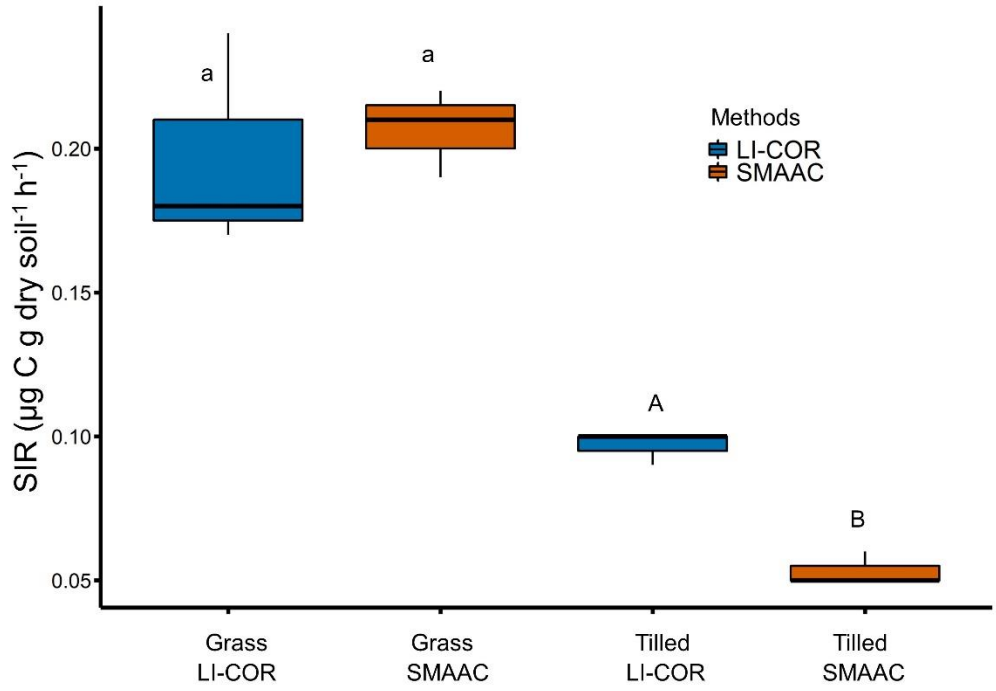

Fig 5.5: Substrate induced respiration (SIR) measured by a LI-COR 8100 (blue) versus the SMAAC-Biomass configuration (orange). Different small letters indicate grass-covered soil fluxes are statistically different; different capital letters indicate tilled soil fluxes are statistically different (Students t-test; $P < 0.05$).

5.5 Discussion

In this study we developed three configurations of an Arduino-based CO_2 sensor that allowed us to assess soil microbial activity. Our instrument, deemed the Soil Microbial Activity Assessment Contraption (SMAAC), was then compared against a commercial IRGA unit (LI-COR 8100). Overall, the SMAAC generated similar results to the commercial IRGA, with signficant differences only observed when substrate induced respiration (SIR) was quantified for the tilled soil (Fig. 5.5). In this example, the SIR value from the SMAAC-Biomass configuration was approximately half of the value estimated by the LI-COR. The reason for the discrepancy may relate to the accuracy of the SMAAC IRGA sensor (50 ppm per the manufacturer). Even though our calibration analysis determined that the instrument provided consistent readings for CO_2 concentrations between 100 and 500 ppm, the sensor accuracy implies that the error can exceed 10% for CO_2 concentrations < 500 ppm. Using the sensor to measure low CO_2 concentrations may therefore require extra precautions such as using longer run times, greater number of replicates, and more frequent calibration. We also note that we did not test the sensor beyond 1,000 ppm, so the calibration should also be assessed when using SMAAC to measure higher CO_2 concentrations.

The SMAAC tended to show more measurement noise than the LI-COR when assessing CO_2 fluxes, e.g., the field flux measurements from SMAAC-simultaneous versus LI-COR setups in the grass-covered soil (Figure 5.3), or the emissions rates calculated for both soils with the SMAAC-Burst (Figure 5.4b). However, during the field flux measurements, the SMAAC-independent test had a slightly lower median flux and a smaller standard deviation than either the LI-COR or SMAAC-simultaneous. This result may reflect the influence of the LI-COR pump unit, which provided continuous circulation of air in the chamber. At the same time, our flux

calculations (Equation 5.1) assumed that the volume of the air, V_c, for the LI-COR and SMAAC-simultaneous setups was equal to the LI-COR sampling chamber plus the internal pump volume of the LI-COR. We did not account for the volume or the exposed surface area of the soil occupied by the SMAAC itself, thus potentially introducing minor error into the flux calculations for those tests. We also note here that the SMAAC and LI-COR both showed high variability in emissions during the initial 20 minutes of the CO_2 burst test experiment. This result may reflect an equilibration period within the glass jar, particularly in response to the initial soil disturbance during wetting the soil and sealing the system.

The total cost of the SMAAC was ~$150, making it at least two orders of magnitude less expensive than commercial IRGA units. Despite the low cost, the SMAAC still maintained reasonable accuracy in all three configurations tested, and performed repeatable measurements when compared with CO_2 standards. The SMAAC is lighter weight and requires less power than commercial IRGA units, increasing its usefulness when performing extended measurements or working in remote locations. An additional benefit of the SMAAC comes from its small form factor: it can be placed directly inside the headspace of samples, thus eliminating the need to pull discrete gas samples using a syringe. Removing this step eliminates a potential source of error, particularly since many commercial IRGA pump units are not fully sealed.

The SMAAC may open new avenues of inquiry related to soil respiration measurements, both in terms of the configurations shown here as well as other possible configurations yet to be developed. For example, we focused our tests on closed chamber measurements, since those are commonly used to evaluate soil CO_2 fluxes and perform measurements such as SIR. The closed chamber measurements also lended themselves to direct comparison with the commercial IRGA unit. However, CO_2 can also be measured using open systems (Alterio, et al., 2006, Norman, et

al., 1997) or in continually flushed chambers (Chow, et al., 2006). Using the SMAAC in open/purged systems thus represents an area of possible future development.

Similarly, since the SMAAC system is inexpensive and easy to assemble, multiple sensors could be used concurrently to better quantify spatial and temporal variability in soil biological measurements, for example by analyzing multiple chambers simultaneously and thereby providing similar functionality as multiplexer units often offered with commercial IRGAs. Finally, direct continuous logging of CO_2 evoluation during measurements may help generate new insights. For example, the grass-covered versus tilled soil showed different temporal trends in the SMAAC-Burst test (Fig. 4b), where the grass-covered soil produced a constant CO_2 efflux rate over the 2-hour test period versus a decreasing CO_2 efflux rate for the tilled soil. While the underlying mechanisms controlling these different responses remain beyond the scope of this current paper, it is nonetheless worth noting that it would not be possible to observe such trends without the high measurement frequency offered by IRGA-based instruments such as SMAAC.

5.6 Conclusion

The Soil Microbial Activity Assessment Contraption (SMAAC) developed in this study represents an low cost yet reliable way to measure CO_2 fluxes from soils. The results obtained from the SMAAC were consistent with those from a commercial IRGA unit for both field and laboratory measurements. In this study we highlighted three SMAAC configurations that were designed to assess different aspects of soil microbial activity and function, yet the SMAAC also has the potential to generate additional applications and insights. As an example, by having the SMAAC-Burst and SMAAC-Biomass units placed inside the closed headspace above samples, we generated near-continuous measurements of CO_2 evolution through time. Such CO_2 trends

may provide new understanding of soil microbial processes that is not possible via traditional discrete measurements. In conclusion, the SMAAC is a promising tool for measuring soil respiration and microbial activity that warrants usage by the broader scientific community.

Chapter 6. Conclusion

The overarching objective of this dissertation was to better understand the effect of conservation agricultural practices on soil health dynamics, with the long-term goal of helping develop the tools and insights that will encourage producer adoption. The findings of this study make progress towards that goal. For example, a handful of parameters were found to consistently respond to conservation agriculture practices on seasonal timescales. These parameters included soil physical properties such as field-saturated hydraulic conductivity and 2-4 mm wet aggregate stability, and soil chemical parameters such as P, K, Ca, Mg, B, and CEC. However, none of these indicators were able to detect effects of conservation agricultural practices every sampling location and time. The ability of these identified responsive soil health parameters to detect the treatments may be compromised by weather (e.g., soil water content at tillage) and growing conditions (e.g., cover crop biomass). The effect of history of management of the field was also observed, particularly in soil aggregate stability. Specifically, sites that started with high aggregate stability saw a decrease through time in all treatments, while the site with the lowest aggregate stability saw an increase through time. These different trends suggest that parameter responses may vary in systems that are building soil health from relatively depleted conditions versus those systems that are maintaining relatively high levels of soil health (Figure 6.1). The possibility that soil health can take different trajectories based on previous management history was only detected by soil aggregate stability.

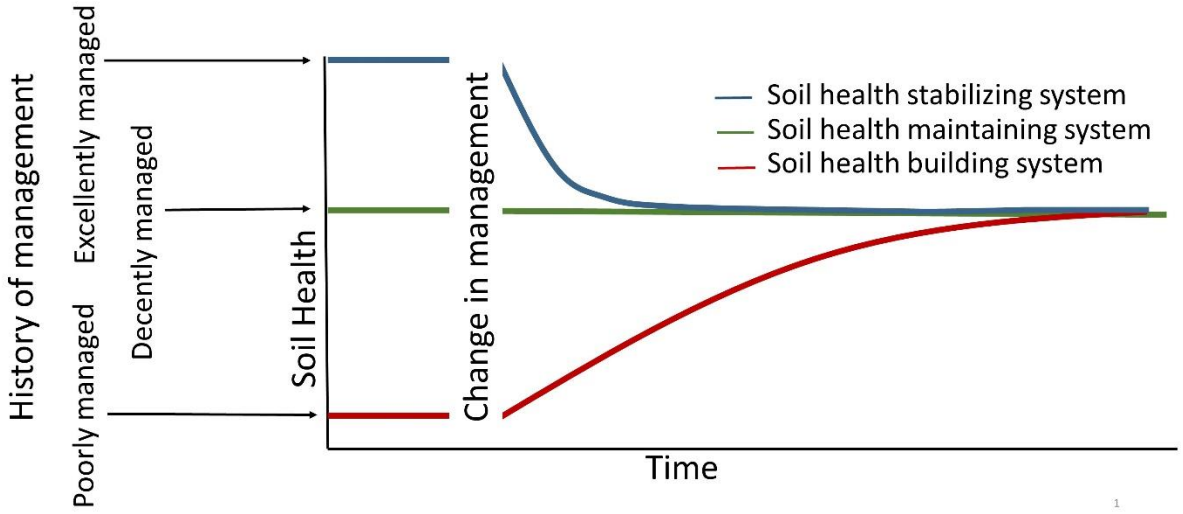

Figure 6.1: Conceptual figure showing various soil health trajectories related to the history of management of the field.

The results of these studies suggest that soil aggregate stability may be the most useful parameter for detecting seasonal or annual variations in soil health due to different management practices. Despite being one of the useful soil health parameters, methods for measuring soil aggregate stability suffer shortcomings including lack of repeatability, inadequate control over input energy, and inaccuracies in coarse-textured soils. Our proposed indicator Integrated Aggregate Stability (IAS) showed high precision and repeatability. When compared to the median aggregate size (d50), which is typically used to interpret laser diffraction data, IAS showed more consistent results with widely used wet sieving method. IAS also had much better ability than d50 to quantify the amounts and stability of soil micro-aggregates, which have high potential to stabilize and sequester carbon. Altogether, we determined that IAS can convey more consistent and relevant information about aggregate stability compared with traditionally used metrics and methods.

In contrast to soil physical and chemical properties, soil biological parameters did not show consistent treatment differences, which we attributed to temporal variability that was not captured by our seasonal sampling approach. For this reason, we developed the Soil Microbial Activity Assessment Contraption (SMAAC) as an inexpensive yet accurate tool to measure biological processes such as soil respiration and properties such as substrate induced respiration (SIR), a measure of active microbial biomass. Overall the SMAAC was found to be consistent with a commercial infrared gas analysis (IRGA) unit for quantifying various soil respiration based microbial assessments. Since the SMAAC is inexpensive (<$150) and easy to assemble, multiple sensors could be used concurrently to better address finer temporal scale response in soil biological measurements. The SMAAC may also open new avenues of inquiry related to soil respiration measurements, both in terms of the configurations that we tested as well as other possible configurations yet to be developed.

Some possible next steps of this research include developing a better understanding of the effect of history of management on soil health indicators using a replicated study. Better quantification of the temporal dynamics of soil biological properties with respect to conservation agricultural practices could also be a key since these biological properties have been proven to drive a wide variety of soil function.

Finally, the methods developed in these chapters ranged from highly complex (e.g., multivariate analyses using permutational analysis on 30 different indicators) to relatively straight-forward (e.g., measuring CO_2 fluxes using a ~$150 sensor). These methods will ultimately be judged useful if they can be translated to practitioners and producers in the real world. As an example, the multivariate approach we applied to all soil health indicators identified a small set of responsive soil health parameters that can be used by farmers in Virginia

and beyond to track soil health benefits from conservation agriculture practices. Likewise, the trends and findings regarding short term soil health benefits can be featured in demonstration days to encourage farmers to adapt conservation agriculture. Our method of measuring soil aggregate stability, IAS, can be useful in laboratory settings, as it can repeatedly and accurately quantify stability of various soil size fractions under a variety of applied energies. In particular, we recommend that commercial soil testing laboratories consider adopting this method in their soil health analyses. Finally, the SMAAC tool has great potential to accurately measure a large number of soil respiration based microbial assessments. Because the SMAAC is accurate, inexpensive, and has low power requirements and a small form factor, it is well suited for conducting a variety of measurements in resource-limited situations and remote locations.

References

Abdollahi, L. and L.J. Munkholm. 2014. Tillage system and cover crop effects on soil quality: I. Chemical, mechanical, and biological properties. Soil Science Society of America Journal 78: 262-270.

Abdollahi, L. and L.J. Munkholm. 2014. Tillage System and Cover Crop Effects on Soil Quality:I. Chemical, Mechanical, and Biological Properties. Soil Science Society of America Journal 78: 262-270. doi:10.2136/sssaj2013.07.0301.

Akram-Lodhi, A.H. 2008. (Re) imagining agrarian relations? The world development report 2008: Agriculture for development. Development and Change 39: 1145-1161.

Allen, D.E., B.P. Singh and R.C. Dalal. 2011. Soil health indicators under climate change: A review of current knowledge. Soil health and climate change. Springer. p. 25-45.

Allmaras, R., R. Burwell and R. Holt. 1967. Plow-Layer Porosity and Surface Roughness from Tillage as Affected by Initial Porosity and Soil Moisture at Tillage Time 1. Soil Science Society of America Journal 31: 550-556.

Almajmaie, A., M. Hardie, T. Acuna and C. Birch. 2017. Evaluation of methods for determining soil aggregate stability. Soil and Tillage Research 167: 39-45.

Alterio, G., P. Giorio and G. Sorrentino. 2006. Open-system chamber for measurements of gas exchanges at plant level. Environmental science & technology 40: 1950-1955.

Amézketa, E. 1999. Soil Aggregate Stability: A Review. Journal of Sustainable Agriculture 14: 83-151. doi:10.1300/J064v14n02_08.

Amezketa, E., R. Aragüés, R. Carranza and B. Urgel. 2003. Macro-and micro-aggregate stability of soils determined by a combination of wet-sieving and laser-ray diffraction. Spanish Journal of Agricultural Research 1: 83-94.

An, S., A. Mentler, H. Mayer and W.E. Blum. 2010. Soil aggregation, aggregate stability, organic carbon and nitrogen in different soil aggregate fractions under forest and shrub vegetation on the Loess Plateau, China. Catena 81: 226-233.

An, S., A. Mentler, H. Mayer and W.E.H. Blum. 2010. Soil aggregation, aggregate stability, organic carbon and nitrogen in different soil aggregate fractions under forest and shrub vegetation on the Loess Plateau, China. CATENA 81: 226-233. doi:https://doi.org/10.1016/j.catena.2010.04.002.

Andrews, S.S., D. Karlen and J. Mitchell. 2002. A comparison of soil quality indexing methods for vegetable production systems in Northern California. Agriculture, ecosystems & environment 90: 25-45.

Arias, M.E., J.A. González-Pérez, F.J. González-Vila and A.S. Ball. 2005. Soil health: A new challenge for microbiologists and chemists. International Microbiology 8: 13-21.

Arnold, K. and A. Page. 1986. Methods of soil analysis. pt. 1. Physical and mineralogical methods. Agronomy (USA). no. 9.

Balkcom, K., H. Schomberg, W. Reeves, A. Clark, L. Baumhardt, H. Collins, et al. 2007. Managing cover crops in conservation tillage systems. Managing cover crops profitably: 44-61.

Baranski, M., H. Caswell, R. Claassen, C. Cherry, K. Jaglo, A. Lataille, et al. 2018. Agricultural Conservation on Working Lands: Trends From 2004 to Present. Technical Bulletin Number 1950.

Barthes, B. and E. Roose. 2002. Aggregate stability as an indicator of soil susceptibility to runoff and erosion; validation at several levels. Catena 47: 133-149.

Bastida, F., A. Zsolnay, T. Hernández and C. García. 2008. Past, present and future of soil quality indices: a biological perspective. Geoderma 147: 159-171.
Bhattacharyya, R., M. Tuti, S. Kundu, J. Bisht and J. Bhatt. 2012. Conservation tillage impacts on soil aggregation and carbon pools in a sandy clay loam soil of the Indian Himalayas. Soil Science Society of America Journal 76: 617-627.
Bieganowski, A., M. Ryżak and B. Witkowska-Walczak. 2010. Determination of soil aggregate disintegration dynamics using laser diffraction. Clay Minerals 45: 23-34.
Bissonnais, Y.L. and M.J. Singer. 1992. Crusting, runoff, and erosion response to soil water content and successive rainfalls. Soil Science Society of America Journal 56: 1898-1903.
Blake, G.R. and K. Hartge. 1986. Bulk Density 1. Methods of Soil Analysis: Part 1—Physical and Mineralogical Methods: 363-375.
Blanco-Canqui, H., M.M. Mikha, D.R. Presley and M.M. Claassen. 2011. Addition of cover crops enhances no-till potential for improving soil physical properties. Soil Science Society of America Journal 75: 1471-1482.
Blevins, R., R. Lal, J. Doran, G. Langdale and W. Frye. 2018. Conservation tillage for erosion control and soil quality. Advances in soil and water conservation. Routledge. p. 51-68.
Boix-Fayos, C., A. Calvo-Cases, A.C. Imeson and M.D. Soriano-Soto. 2001. Influence of soil properties on the aggregation of some Mediterranean soils and the use of aggregate size and stability as land degradation indicators. CATENA 44: 47-67. doi:https://doi.org/10.1016/S0341-8162(00)00176-4.
Bond-Lamberty, B., V.L. Bailey, M. Chen, C.M. Gough and R. Vargas. 2018. Globally rising soil heterotrophic respiration over recent decades. Nature 560: 80.
Bradford, M.A., N. Fierer, R.B. Jackson, T.R. Maddox and J.F. Reynolds. 2008. Nonlinear root-derived carbon sequestration across a gradient of nitrogen and phosphorous deposition in experimental mesocosms. Global Change Biology 14: 1113-1124.
Bradford, M.A., B.W. Watts and C.A. Davies. 2010. Thermal adaptation of heterotrophic soil respiration in laboratory microcosms. Global Change Biology 16: 1576-1588.
Brejda, J.J., D.L. Karlen, J.L. Smith and D.L. Allan. 2000. Identification of regional soil quality factors and indicators II. Northern Mississippi Loess Hills and Palouse Prairie. Soil Science Society of America Journal 64: 2125-2135.
Brown, G.O. 2003. The history of the Darcy-Weisbach equation for pipe flow resistance. Environmental and Water Resources History. p. 34-43.
Campbell, C.D., S.J. Chapman, C.M. Cameron, M.S. Davidson and J.M. Potts. 2003. A rapid microtiter plate method to measure carbon dioxide evolved from carbon substrate amendments so as to determine the physiological profiles of soil microbial communities by using whole soil. Appl. Environ. Microbiol. 69: 3593-3599.
Cardoso, E.J.B.N., R.L.F. Vasconcellos, D. Bini, M.Y.H. Miyauchi, C.A.d. Santos, P.R.L. Alves, et al. 2013. Soil health: looking for suitable indicators. What should be considered to assess the effects of use and management on soil health? Scientia Agricola 70: 274-289.
Carof, M., S. De Tourdonnet, Y. Coquet, V. Hallaire and J. Roger-Estrade. 2007. Hydraulic conductivity and porosity under conventional and no-tillage and the effect of three species of cover crop in northern France. Soil Use and Management 23: 230-237.
Casas, C., M. Omacini, M.S. Montecchia and O.S. Correa. 2011. Soil microbial community responses to the fungal endophyte Neotyphodium in Italian ryegrass. Plant and soil 340: 347-355.

Chaves, H.M.L. 2009. Sensibilidade do modelo Hydrus aos parâmetros hidráulicos do solo em diferentes texturas. Revista Brasileira de Recursos Hídricos 14: 33-37.
Chow, A.T., K.K. Tanji, S. Gao and R.A. Dahlgren. 2006. Temperature, water content and wet–dry cycle effects on DOC production and carbon mineralization in agricultural peat soils. Soil Biology and Biochemistry 38: 477-488.
Churchman, G., R. Foster, L. D'Acqui, L. Janik, J. Skjemstad, R. Merry, et al. 2010. Effect of land-use history on the potential for carbon sequestration in an Alfisol. Soil and Tillage Research 109: 23-35.
Currie, J. 1966. The volume and porosity of soil crumbs. Journal of Soil Science 17: 24-35.
Dabney, S., J. Delgado and D. Reeves. 2001. Using winter cover crops to improve soil and water quality. Communications in Soil Science and Plant Analysis 32: 1221-1250.
Danielson, R. and P. Sutherland. 1986. Porosity. Methods of Soil Analysis: Part 1—Physical and Mineralogical Methods: 443-461.
Davidson, E.A. and I.A. Janssens. 2006. Temperature sensitivity of soil carbon decomposition and feedbacks to climate change. Nature 440: 165.
Davis, A.S. 2010. Cover-crop roller–crimper contributes to weed management in no-till soybean. Weed Science 58: 300-309.
De Leenheer, L. and M. De Boodt. 1959. Determination of aggregate stability by the change in mean weight diameter. Mededelingen van landbouwhogeschool en de opzoekingstations van de staat te Gent 24: 290-300.
Degens, B. and J. Harris. 1997. Development of a physiological approach to measuring the catabolic diversity of soil microbial communities. Soil Biology and Biochemistry 29: 1309-1320.
Degrune, F., N. Theodorakopoulos, G. Colinet, M.-P. Hiel, B. Bodson, B. Taminiau, et al. 2017. Temporal Dynamics of Soil Microbial Communities below the Seedbed under Two Contrasting Tillage Regimes. Frontiers in Microbiology 8. doi:10.3389/fmicb.2017.01127.
Dexter, A. 1988. Advances in characterization of soil structure. Soil and tillage research 11: 199-238.
Don, A., C. Rebmann, O. Kolle, M. SCHERER-LORENZEN and E.D. SCHULZE. 2009. Impact of afforestation-associated management changes on the carbon balance of grassland. Global Change Biology 15: 1990-2002.
Donev, A., I. Cisse, D. Sachs, E.A. Variano, F.H. Stillinger, R. Connelly, et al. 2004. Improving the density of jammed disordered packings using ellipsoids. Science 303: 990-993.
Doran, J.W. and M.R. Zeiss. 2000. Soil health and sustainability: managing the biotic component of soil quality. Applied soil ecology 15: 3-11.
Fageria, N., V. Baligar and B. Bailey. 2005. Role of cover crops in improving soil and row crop productivity. Communications in soil science and plant analysis 36: 2733-2757.
Ferreira, C.R.P.C., A.C.D. Antonino, E.V.d.S.B. Sampaio, K.G. Correia, J.R.d.S. Lima, W.d.A. Soares, et al. 2018. Soil CO2 Efflux Measurements by Alkali Absorption and Infrared Gas Analyzer in the Brazilian Semiarid Region. Revista Brasileira de Ciência do Solo 42.
Fierer, N., B.P. Colman, J.P. Schimel and R.B. Jackson. 2006. Predicting the temperature dependence of microbial respiration in soil: A continental-scale analysis. Global Biogeochemical Cycles 20.

Fierer, N., J.M. Craine, K. McLauchlan and J.P. Schimel. 2005. LITTER QUALITY AND THE TEMPERATURE SENSITIVITY OF DECOMPOSITION. Ecology 86: 320-326. doi:10.1890/04-1254.
Fierer, N. and J. Schimel. 2003. A Proposed Mechanism for the Pulse in Carbon Dioxide Production Commonly Observed Following the Rapid Rewetting of a Dry Soil.
Fierer, N. and J.P. Schimel. 2002. Effects of drying–rewetting frequency on soil carbon and nitrogen transformations. Soil Biology and Biochemistry 34: 777-787.
Fierer, N., J.P. Schimel and P.A. Holden. 2003. Variations in microbial community composition through two soil depth profiles. Soil Biology and Biochemistry 35: 167-176.
Fink, R.J. and D. Wesley. 1974. Corn Yield as Affected by Fertilization and Tillage System 1. Agronomy Journal 66: 70-71.
Foley, J.A., N. Ramankutty, K.A. Brauman, E.S. Cassidy, J.S. Gerber, M. Johnston, et al. 2011. Solutions for a cultivated planet. Nature 478: 337.
Franzluebbers, A.J. 2002. Water infiltration and soil structure related to organic matter and its stratification with depth. Soil and Tillage Research 66: 197-205.
Friedrich, T., R. Derpsch and A. Kassam. 2012. Overview of the global spread of conservation agriculture. Field Actions Science Reports. The journal of field actions.
Fristensky, A. and M.E. Grismer. 2008. A simultaneous model for ultrasonic aggregate stability assessment. CATENA 74: 153-164. doi:https://doi.org/10.1016/j.catena.2008.04.013.
Gabriel, J. and M. Quemada. 2011. Replacing bare fallow with cover crops in a maize cropping system: yield, N uptake and fertiliser fate. European journal of agronomy 34: 133-143.
Gajić, B. 2013. Physical properties and organic matter of Fluvisols under forest, grassland, and 100 years of conventional tillage. Geoderma 200: 114-119.
Gaudinski, J.B., S.E. Trumbore, E.A. Davidson and S. Zheng. 2000. Soil carbon cycling in a temperate forest: radiocarbon-based estimates of residence times, sequestration rates and partitioning of fluxes. Biogeochemistry 51: 33-69.
Gloe, M. 2011. Evaluating a Process-based Mitigation Wetland Water Budget Model. Virginia Tech.
Graham, M.H. 2003. Confronting multicollinearity in ecological multiple regression. Ecology 84: 2809-2815.
Gruver, J., R. Weil, C. White and Y. Lawley. 2014. Radishes: a new cover crop for organic farming systems. Michigan State University, MI.
Halde, C., K.C. Bamford and M.H. Entz. 2015. Crop agronomic performance under a six-year continuous organic no-till system and other tilled and conventionally-managed systems in the northern Great Plains of Canada. Agriculture, Ecosystems & Environment 213: 121-130.
Hamby, D. 1994. A review of techniques for parameter sensitivity analysis of environmental models. Environmental monitoring and assessment 32: 135-154.
Haney, R., W. Brinton and E. Evans. 2008. Soil CO 2 respiration: comparison of chemical titration, CO 2 IRGA analysis and the Solvita gel system. Renewable Agriculture and Food Systems 23: 171-176.
Haney, R.L., W. Brinton and E. Evans. 2008. Estimating soil carbon, nitrogen, and phosphorus mineralization from short-term carbon dioxide respiration. Communications in Soil Science and Plant Analysis 39: 2706-2720.
Hartwig, N.L. and H.U. Ammon. 2002. Cover crops and living mulches. Weed science 50: 688-699.

Hernanz, J., R. López, L. Navarrete and V. Sanchez-Giron. 2002. Long-term effects of tillage systems and rotations on soil structural stability and organic carbon stratification in semiarid central Spain. Soil and Tillage Research 66: 129-141.
Hu, W., F. Tabley, M. Beare, C. Tregurtha, R. Gillespie, W. Qiu, et al. 2018. Short-Term Dynamics of Soil Physical Properties as Affected by Compaction and Tillage in a Silt Loam Soil. Vadose Zone Journal 17. doi:10.2136/vzj2018.06.0115.
Hubbard, R.K., T.C. Strickland and S. Phatak. 2013. Effects of cover crop systems on soil physical properties and carbon/nitrogen relationships in the coastal plain of southeastern USA. Soil and Tillage Research 126: 276-283.
Hussain, I., K.R. Olson and S.A. Ebelhar. 1999. Long-term tillage effects on soil chemical properties and organic matter fractions. Soil Science Society of America Journal 63: 1335-1341.
Idowu, O., H. Van Es, G. Abawi, D. Wolfe, R. Schindelbeck, B. Moebius-Clune, et al. 2009. Use of an integrative soil health test for evaluation of soil management impacts. Renewable Agriculture and Food Systems 24: 214-224.
Imeson, A.C., J. Boardman, I.D. Foster and J. Dearing. 1990. The response of tilled soils to wetting by rainfall and the dynamic character of soil erodibilityWiley.
Jackson, L., F. Calderon, K. Steenwerth, K. Scow and D. Rolston. 2003. Responses of soil microbial processes and community structure to tillage events and implications for soil quality. Geoderma 114: 305-317.
Jangid, K., M.A. Williams, A.J. Franzluebbers, T.M. Schmidt, D.C. Coleman and W.B. Whitman. 2011. Land-use history has a stronger impact on soil microbial community composition than aboveground vegetation and soil properties. Soil Biology and Biochemistry 43: 2184-2193.
Jin, H., L. Hongwen and G. Huanwen. 2006. Subsoiling effect and economic benefit under conservation tillage mode in Northern China [J]. Transactions of the Chinese Society of Agricultural Engineering 10.
Kabir, Z. and R. Koide. 2000. The effect of dandelion or a cover crop on mycorrhiza inoculum potential, soil aggregation and yield of maize. Agriculture, ecosystems & environment 78: 167-174.
Karami, A., M. Homaee, S. Afzalinia, H. Ruhipour and S. Basirat. 2012. Organic resource management: Impacts on soil aggregate stability and other soil physico-chemical properties. Agriculture, Ecosystems & Environment 148: 22-28. doi:https://doi.org/10.1016/j.agee.2011.10.021.
Karlen, D., N.C. Wollenhaupt, D. Erbach, E. Berry, J. Swan, N.S. Eash, et al. 1994. Crop residue effects on soil quality following 10-years of no-till corn. Soil and Tillage Research 31: 149-167.
Kassam, A., T. Friedrich, F. Shaxson and J. Pretty. 2009. The spread of conservation agriculture: justification, sustainability and uptake. International journal of agricultural sustainability 7: 292-320.
Keesstra, S., P. Pereira, A. Novara, E.C. Brevik, C. Azorin-Molina, L. Parras-Alcántara, et al. 2016. Effects of soil management techniques on soil water erosion in apricot orchards. Science of the Total Environment 551: 357-366.
Kemper, W. and R. Rosenau. 1986. Aggregate stability and size distribution.
Kemper, W. and R. Rosenau. 1986. Aggregate stability and size distribution. In: A. Klute, editor Methods of Soil Analysis. Part 1. SSSA, Madison, WI.

Kibblewhite, M., K. Ritz and M. Swift. 2007. Soil health in agricultural systems. Philosophical Transactions of the Royal Society B: Biological Sciences 363: 685-701.
Kladivko, E.J., D.R. Griffith and J.V. Mannering. 1986. Conservation tillage effects on soil properties and yield of corn and soya beans in Indiana. Soil and Tillage Research 8: 277-287.
Klute, A., G. Blake and K.H. Hartge. 1986. Particle density. In: A. Klute, editor Methods of soil analysis. p. 377-382.
Kong, A.Y., J. Six, D.C. Bryant, R.F. Denison and C. Van Kessel. 2005. The relationship between carbon input, aggregation, and soil organic carbon stabilization in sustainable cropping systems. Soil science society of America journal 69: 1078-1085.
Krueger, E.S., T.E. Ochsner, P.M. Porter and J.M. Baker. 2011. Winter rye cover crop management influences on soil water, soil nitrate, and corn development. Agronomy journal 103: 316-323.
Kyrylyuk, A.V. and A.P. Philipse. 2011. Effect of particle shape on the random packing density of amorphous solids. physica status solidi (a) 208: 2299-2302.
Ladegaard-Pedersen, P., B. Elberling and L. Vesterdal. 2005. Soil carbon stocks, mineralization rates, and CO2 effluxes under 10 tree species on contrasting soil types. Canadian Journal of Forest Research 35: 1277-1284.
Laghrour, M., R. Moussadek, R. Mrabet, R. Dahan, M. El-Mourid, A. Zouahri, et al. 2016. Long and Midterm Effect of Conservation Agriculture on Soil Properties in Dry Areas of Morocco. Applied and Environmental Soil Science 2016: 9. doi:10.1155/2016/6345765.
Lal, R. 2004. Soil carbon sequestration impacts on global climate change and food security. science 304: 1623-1627.
Lampurlanés, J. and C. Cantero-Martínez. 2006. Hydraulic conductivity, residue cover and soil surface roughness under different tillage systems in semiarid conditions. Soil and Tillage Research 85: 13-26.
Le Bissonnais, Y. and D. Arrouays. 1997. Aggregate stability and assessment of soil crustability and erodibility: II. Application to humic loamy soils with various organic carbon contents

Stabilité structurale et évaluation de la sensibilité des sols à la battance et à l'érosion hydrique: II. Application à une série de sols limoneux à teneur en carbone organique variée. European Journal of Soil Science 48: 39-48. doi:10.1111/j.1365-2389.1997.tb00183.x.
Le Bissonnais, Y., B. Renaux and H. Delouche. 1995. Interactions between soil properties and moisture content in crust formation, runoff and interrill erosion from tilled loess soils. Catena 25: 33-46.
Lienhard, P., S. Terrat, N.C. Prévost-Bouré, V. Nowak, T. Régnier, S. Sayphoummie, et al. 2014. Pyrosequencing evidences the impact of cropping on soil bacterial and fungal diversity in Laos tropical grassland. Agronomy for sustainable development 34: 525-533.
Lienhard, P., F. Tivet, A. Chabanne, S. Dequiedt, M. Lelièvre, S. Sayphoummie, et al. 2013. No-till and cover crops shift soil microbial abundance and diversity in Laos tropical grasslands. Agronomy for sustainable development 33: 375-384.
Logan, B.E. 2012. Environmental transport processesJohn Wiley & Sons, Hoboken, NJ.
Lou, Y., M. Xu, X. Chen, X. He and K. Zhao. 2012. Stratification of soil organic C, N and C: N ratio as affected by conservation tillage in two maize fields of China. Catena 95: 124-130.
Lutz, W., W.P. Butz and K.e. Samir. 2017. World Population & Human Capital in the Twenty-First Century: An OverviewOxford University Press.

Magurran, A. 1988. Ecological Diversity and its Measurement Princeton University Press Princeton Google Scholar.
Maraseni, T. and G. Cockfield. 2011. Does the adoption of zero tillage reduce greenhouse gas emissions? An assessment for the grains industry in Australia. Agricultural Systems 104: 451-458.
Mayer, H., J. Schomakers, A. Mentler, N. Degischer and W.E. Blum. 2011. Measurement of soil aggregate stability using low intensity ultrasonic vibration Medición de la estabilidad de agregados de suelo utilizando vibración ultrasónica de baja intensidad Medição da estabilidade dos agregados do solo por vibração ultrasónica de baixa intensidade. Spanish Journal of Soil Science.
Mazzoncini, M., T.B. Sapkota, P. Bàrberi, D. Antichi and R. Risaliti. 2011. Long-term effect of tillage, nitrogen fertilization and cover crops on soil organic carbon and total nitrogen content. Soil and tillage research 114: 165-174.
McGowen, E.B., S. Sharma, S. Deng, H. Zhang and J.G. Warren. 2018. An Automated Laboratory Method for Measuring CO2 Emissions from Soils. Agricultural & Environmental Letters 3.
McIntyre, D. and G. Stirk. 1954. A method for determination of apparent density of soil aggregates. Australian Journal of Agricultural Research 5: 291-296.
Mentler, A., H. Mayer, P. Strauß and W. Blum. 2004. Characterisation of soil aggregate stability by ultrasonic dispersion. International agrophysics 18: 39-46.
Minasny, B., B.P. Malone, A.B. McBratney, D.A. Angers, D. Arrouays, A. Chambers, et al. 2017. Soil carbon 4 per mille. Geoderma 292: 59-86.
Mondini, C., T. Sinicco, M.L. Cayuela and M.A. Sanchez-Monedero. 2010. A simple automated system for measuring soil respiration by gas chromatography. Talanta 81: 849-855.
Morrow, J.G., D.R. Huggins, L.A. Carpenter-Boggs and J.P. Reganold. 2016. Evaluating measures to assess soil health in long-term agroecosystem trials. Soil Science Society of America Journal 80: 450-462.
Mukhopadhyay, S., S. Maiti and R. Masto. 2014. Development of mine soil quality index (MSQI) for evaluation of reclamation success: a chronosequence study. Ecological Engineering 71: 10-20.
Mulumba, L.N. and R. Lal. 2008. Mulching effects on selected soil physical properties. Soil and Tillage Research 98: 106-111. doi:https://doi.org/10.1016/j.still.2007.10.011.
Nair, A. and M. Ngouajio. 2012. Soil microbial biomass, functional microbial diversity, and nematode community structure as affected by cover crops and compost in an organic vegetable production system. Applied soil ecology 58: 45-55.
Nascente, A.S., Y.C. Li and C.A.C. Crusciol. 2013. Cover crops and no-till effects on physical fractions of soil organic matter. Soil and Tillage Research 130: 52-57.
Nascente, A.S., L.F. Stone and C.A.C. Crusciol. 2015. Soil chemical properties affected by cover crops under no-tillage system. Revista Ceres 62: 401-409.
Norman, J., C. Kucharik, S. Gower, D. Baldocchi, P. Crill, M. Rayment, et al. 1997. A comparison of six methods for measuring soil-surface carbon dioxide fluxes. Journal of Geophysical Research: Atmospheres 102: 28771-28777.
Norris, R., B.K. Chim, G. Evanylo, M. Reiter and W. Thomason. 2018. Assessment of In-Season Soil Nitrogen Tests for Corn Planted into Winter Annual Cover Crops. Soil Science Society of America Journal 82: 1428-1436.

North, P. 1976. Towards an absolute measurement of soil structural stability using ultrasound. European Journal of Soil Science 27: 451-459.
Nosrati, K. 2013. Assessing soil quality indicator under different land use and soil erosion using multivariate statistical techniques. Environmental monitoring and assessment 185: 2895-2907.
NRCS. 2017. Web Soil Survey. In: USDA, editor.
Nyakatawa, E., K. Reddy and K. Sistani. 2001. Tillage, cover cropping, and poultry litter effects on selected soil chemical properties. Soil and Tillage Research 58: 69-79.
O'Toole, P.I. and T.S. Hudson. 2011. New high-density packings of similarly sized binary spheres. The Journal of Physical Chemistry C 115: 19037-19040.
Ogle, S.M., A. Swan and K. Paustian. 2012. No-till management impacts on crop productivity, carbon input and soil carbon sequestration. Agriculture, Ecosystems & Environment 149: 37-49.
Oksanen, J., F.G. Blanchet, M. Friendly, R. Kindt, P. Legendre, D. McGlinn, et al. 2018. vegan: Community Ecology Package.
Oliveira, R.A.d., G. Brunetto, A. Loss, L.C. Gatiboni, C. Kürtz, V. Müller Júnior, et al. 2016. Cover crops effects on soil chemical properties and onion yield. Revista Brasileira de Ciência do Solo 40.
Patil, R.H., J.J. Colls and M.D. Steven. 2010. Effects of CO2 gas as leaks from geological storage sites on agro-ecosystems. Energy 35: 4587-4591.
Paul, B., B. Vanlauwe, F. Ayuke, A. Gassner, M. Hoogmoed, T. Hurisso, et al. 2013. Medium-term impact of tillage and residue management on soil aggregate stability, soil carbon and crop productivity. Agriculture, ecosystems & environment 164: 14-22.
Pittelkow, C.M., B.A. Linquist, M.E. Lundy, X. Liang, K.J. van Groenigen, J. Lee, et al. 2015. When does no-till yield more? A global meta-analysis. Field Crops Research 183: 156-168.
R Development Core Team. 2018. A language and environment for statistical computing. R Foundation for Statistical Computing, Vienna, Austria.
Ramos, M.E., E. Benítez, P.A. García and A.B. Robles. 2010. Cover crops under different managements vs. frequent tillage in almond orchards in semiarid conditions: Effects on soil quality. Applied Soil Ecology 44: 6-14.
Raper, R., D.W. Reeves, C. Burmester and E. Schwab. 2000. Tillage depth, tillage timing, and cover crop effects on cotton yield, soil strength, and tillage energy requirements. Applied Engineering in Agriculture 16: 379.
Rawlins, B., J. Wragg and R. Lark. 2013. Application of a novel method for soil aggregate stability measurement by laser granulometry with sonication. European journal of soil science 64: 92-103.
Regelink, I.C., C.R. Stoof, S. Rousseva, L. Weng, G.J. Lair, P. Kram, et al. 2015. Linkages between aggregate formation, porosity and soil chemical properties. Geoderma 247: 24-37.
Renault, P., M. Ben-Sassi and A. Berard. 2013. Improving the MicroResp™ substrate-induced respiration method by a more complete description of CO2 behavior in closed incubation wells. Geoderma 207: 82-91.
Ritz, K., H.I. Black, C.D. Campbell, J.A. Harris and C. Wood. 2009. Selecting biological indicators for monitoring soils: a framework for balancing scientific and technical opinion to assist policy development. Ecological Indicators 9: 1212-1221.

Roldán, A., F. Caravaca, M. Hernández, C. Garcıa, C. Sánchez-Brito, M. Velásquez, et al. 2003. No-tillage, crop residue additions, and legume cover cropping effects on soil quality characteristics under maize in Patzcuaro watershed (Mexico). Soil and Tillage Research 72: 65-73.

Rowell, M.J. 1995. Colorimetric method for CO2 measurement in soils. Soil Biology and Biochemistry 27: 373-375.

Rusinamhodzi, L., M. Corbeels, M.T. Van Wijk, M.C. Rufino, J. Nyamangara and K.E. Giller. 2011. A meta-analysis of long-term effects of conservation agriculture on maize grain yield under rain-fed conditions. Agronomy for sustainable development 31: 657.

Rustad, L.E., T.G. Huntington and R.D. Boone. 2000. Controls on soil respiration: implications for climate change. Biogeochemistry 48: 1-6.

Sander, T. and H.H. Gerke. 2007. Noncontact Shrinkage Curve Determination for Soil Clods and Aggregates by Three-Dimensional Optical Scanning. Soil Science Society of America Journal 71: 1448. doi:10.2136/sssaj2006.0372.

Sarli, G.O., R.R. Filgueira and D. Giménez. 2001. Measurement of soil aggregate density by volume displacement in two non-mixing liquids. Soil Science Society of America Journal 65: 1400-1403.

Schipper, L., B. Degens, G. Sparling and L. Duncan. 2001. Changes in microbial heterotrophic diversity along five plant successional sequences. Soil Biology and Biochemistry 33: 2093-2103.

Schoenholtz, S.H., H. Van Miegroet and J. Burger. 2000. A review of chemical and physical properties as indicators of forest soil quality: challenges and opportunities. Forest ecology and management 138: 335-356.

Schomakers, J., F. Zehetner, A. Mentler, F. Ottner and H. Mayer. 2015. Study of soil aggregate breakdown dynamics under low dispersive ultrasonic energies with sedimentation and X-ray attenuation. International agrophysics 29: 501-508.

Schwen, A., G. Bodner, P. Scholl, G.D. Buchan and W. Loiskandl. 2011. Temporal dynamics of soil hydraulic properties and the water-conducting porosity under different tillage. Soil and Tillage Research 113: 89-98. doi:https://doi.org/10.1016/j.still.2011.02.005.

2016. Assessing soil health in highbush blueberry with the Solvita® CO2 respiration test. XI International Vaccinium Symposium 1180.

Selles, F., B. McConkey and C. Campbell. 1999. Distribution and forms of P under cultivator- and zero-tillage for continuous-and fallow-wheat cropping systems in the semi-arid Canadian prairies. Soil and Tillage Research 51: 47-59.

Sharma, V., S. Irmak and J. Padhi. 2018. Effects of cover crops on soil quality: Part I. Soil chemical properties—organic carbon, total nitrogen, pH, electrical conductivity, organic matter content, nitrate-nitrogen, and phosphorus. Journal of Soil and Water Conservation 73: 637-651.

Shear, G. and W. Moschler. 1969. Continuous Corn by the No-Tillage and Conventional Tillage Methods: A Six-Year Comparison 1. Agronomy Journal 61: 524-526.

Shi, Y., R. Lalande, C. Hamel, N. Ziadi, B. Gagnon and Z. Hu. 2013. Seasonal variation of microbial biomass, activity, and community structure in soil under different tillage and phosphorus management practices. Biology and fertility of soils 49: 803-818.

Shin, S.S., S.D. Park and B.K. Choi. 2016. Universal power law for relationship between rainfall kinetic energy and rainfall intensity. Advances in Meteorology 2016: 1-11. doi:doi:10.1155/2016/2494681.

Shukla, M., R. Lal and M. Ebinger. 2006. Determining soil quality indicators by factor analysis. Soil and Tillage Research 87: 194-204.
Six, J., H. Bossuyt, S. Degryze and K. Denef. 2004. A history of research on the link between (micro) aggregates, soil biota, and soil organic matter dynamics. Soil and Tillage Research 79: 7-31.
Six, J., H. Bossuyt, S. Degryze and K. Denef. 2004. A history of research on the link between (micro)aggregates, soil biota, and soil organic matter dynamics. Soil and Tillage Research 79: 7-31. doi:https://doi.org/10.1016/j.still.2004.03.008.
Six, J., E. Elliott and K. Paustian. 1999. Aggregate and soil organic matter dynamics under conventional and no-tillage systems. Soil Science Society of America Journal 63: 1350-1358.
Six, J., E.T. Elliott and K. Paustian. 2000. Soil macroaggregate turnover and microaggregate formation: a mechanism for C sequestration under no-tillage agriculture. Soil Biology and Biochemistry 32: 2099-2103. doi:https://doi.org/10.1016/S0038-0717(00)00179-6.
Skjemstad, J., R. Lefeuvre and R. Prebble. 1990. Turnover of soil organic matter under pasture as determined by ¹³C natural abundance. Soil Research 28: 267-276. doi:https://doi.org/10.1071/SR9900267.
Smukler, S., A. O'Geen and L. Jackson. 2012. Assessment of best management practices for nutrient cycling: A case study on an organic farm in a Mediterranean-type climate. Journal of Soil and Water Conservation 67: 16-31.
Snapp, S., S. Swinton, R. Labarta, D. Mutch, J. Black, R. Leep, et al. 2005. Evaluating cover crops for benefits, costs and performance within cropping system niches. Agronomy journal 97: 322-332.
Song, Y., C. Song, B. Tao, J. Wang, X. Zhu and X. Wang. 2014. Short-term responses of soil enzyme activities and carbon mineralization to added nitrogen and litter in a freshwater marsh of Northeast China. European Journal of Soil Biology 61: 72-79.
Sparling, G., P. Hart, J. August and D. Leslie. 1994. A comparison of soil and microbial carbon, nitrogen, and phosphorus contents, and macro-aggregate stability of a soil under native forest and after clearance for pastures and plantation forest. Biology and Fertility of Soils 17: 91-100.
Spedding, T., C. Hamel, G. Mehuys and C. Madramootoo. 2004. Soil microbial dynamics in maize-growing soil under different tillage and residue management systems. Soil Biology and Biochemistry 36: 499-512.
Sprunger, C.D. and G.P. Robertson. 2018. Early accumulation of active fraction soil carbon in newly established cellulosic biofuel systems. Geoderma 318: 42-51.
Stewart, R.D., M.R. Abou Najm, D.E. Rupp and J.S. Selker. 2012. An Image-Based Method for Determining Bulk Density and the Soil Shrinkage Curve. Soil Science Society of America Journal 76: 1217-1221.
Stewart, R.D., J. Jian, A.J. Gyawali, W.E. Thomason, B.D. Badgley, M.S. Reiter, et al. 2018. What we talk about when we talk about soil health. Agricultural & Environmental Letters 3.
Strickland, M.S., M.A. Callaham, E.S. Gardiner, J.A. Stanturf, J.W. Leff, N. Fierer, et al. 2017. Response of soil microbial community composition and function to a bottomland forest restoration intensity gradient. Applied Soil Ecology 119: 317-326. doi:https://doi.org/10.1016/j.apsoil.2017.07.008.

Strickland, M.S., J.L. Devore, J.C. Maerz and M.A. Bradford. 2010. Grass invasion of a hardwood forest is associated with declines in belowground carbon pools. Global Change Biology 16: 1338-1350.
Sulc, R.M. and B.F. Tracy. 2007. Integrated crop–livestock systems in the US Corn Belt. Agronomy Journal 99: 335-345.
Tiessen, K., J. Elliott, J. Yarotski, D. Lobb, D. Flaten and N. Glozier. 2010. Conventional and conservation tillage: Influence on seasonal runoff, sediment, and nutrient losses in the Canadian prairies. Journal of Environmental Quality 39: 964-980.
Tilman, D., J. Fargione, B. Wolff, C. D'antonio, A. Dobson, R. Howarth, et al. 2001. Forecasting agriculturally driven global environmental change. science 292: 281-284.
Tisdall, J.M. and J.M. Oades. 1982. Organic matter and water-stable aggregates in soils. European Journal of Soil Science 33: 141-163.
2017. FEM modelling of soil behaviour under compressive loads. IOP Conference Series: Materials Science and Engineering, IOP Publishing.
Uri, N.D. 2000. Perceptions on the use of no-till farming in production agriculture in the United States: an analysis of survey results. Agriculture, ecosystems & environment 77: 263-266.
Verhulst, N., B. Govaerts, E. Verachtert, A. Castellanos-Navarrete, M. Mezzalama, P. Wall, et al. 2010. Conservation agriculture, improving soil quality for sustainable production systems. Advances in soil science: Food security and soil quality. CRC Press, Boca Raton, FL, USA: 137-208.
Virto, I., N. Gartzia-Bengoetxea and O. FernÁNdez-Ugalde. 2011. Role of Organic Matter and Carbonates in Soil Aggregation Estimated Using Laser Diffractometry. Pedosphere 21: 566-572. doi:http://dx.doi.org/10.1016/S1002-0160(11)60158-6.
Wardle, D.A. and A. Ghani. 1995. A critique of the microbial metabolic quotient (qCO2) as a bioindicator of disturbance and ecosystem development. Soil Biology and Biochemistry 27: 1601-1610. doi:https://doi.org/10.1016/0038-0717(95)00093-T.
West, A. and G. Sparling. 1986. Modifications to the substrate-induced respiration method to permit measurement of microbial biomass in soils of differing water contents. Journal of Microbiological Methods 5: 177-189.
Yoder, R.E. 1936. A direct method of aggregate analysis of soils and a study of the physical nature of erosion losses. Agronomy Journal 28: 337-351.
Zhang, R. 1997. Determination of soil sorptivity and hydraulic conductivity from the disk infiltrometer. Soil Science Society of America Journal 61: 1024-1030.
Zuber, S.M., G.D. Behnke, E.D. Nafziger and M.B. Villamil. 2015. Crop rotation and tillage effects on soil physical and chemical properties in Illinois. Agronomy Journal 107: 971-978.
Zuber, S.M., G.D. Behnke, E.D. Nafziger and M.B. Villamil. 2017. Multivariate assessment of soil quality indicators for crop rotation and tillage in Illinois. Soil and Tillage Research 174: 147-155. doi:https://doi.org/10.1016/j.still.2017.07.007.
Zuber, S.M. and M.B. Villamil. 2016. Meta-analysis approach to assess effect of tillage on microbial biomass and enzyme activities. Soil Biology and Biochemistry 97: 176-187.

Appendix A (Appendix for Chapter 2)

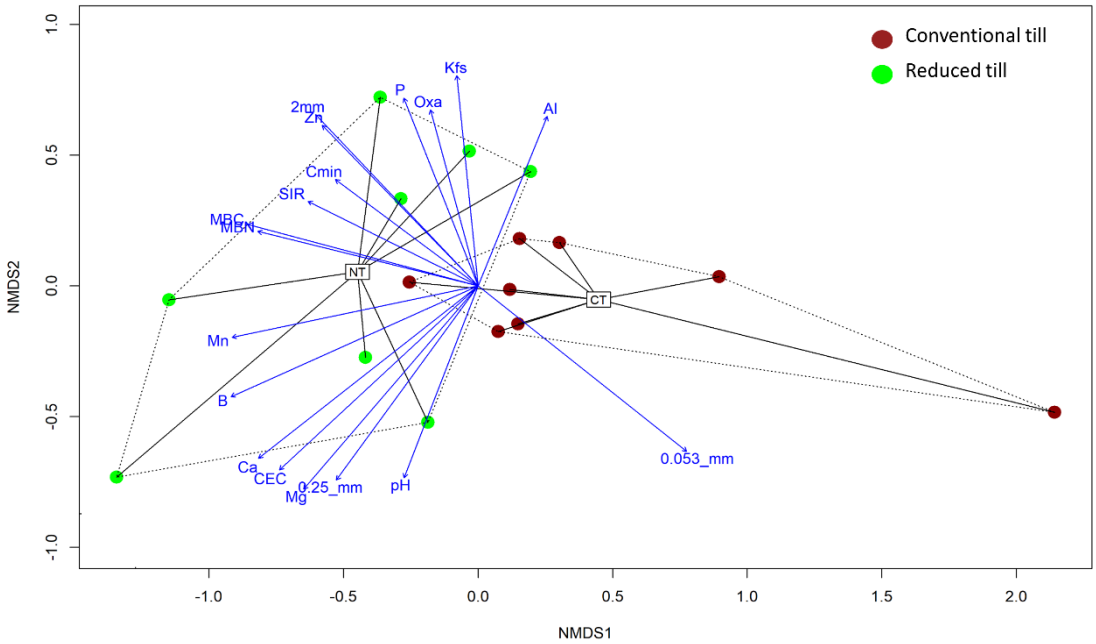

Figure A1: NMDS plot showing treatment differences as detected by perMANOVA ($P < 0.05$) and soil health parameters as shown by *envfit* ($P < 0.05$) for the surface soil in Site 1 during April 2016.

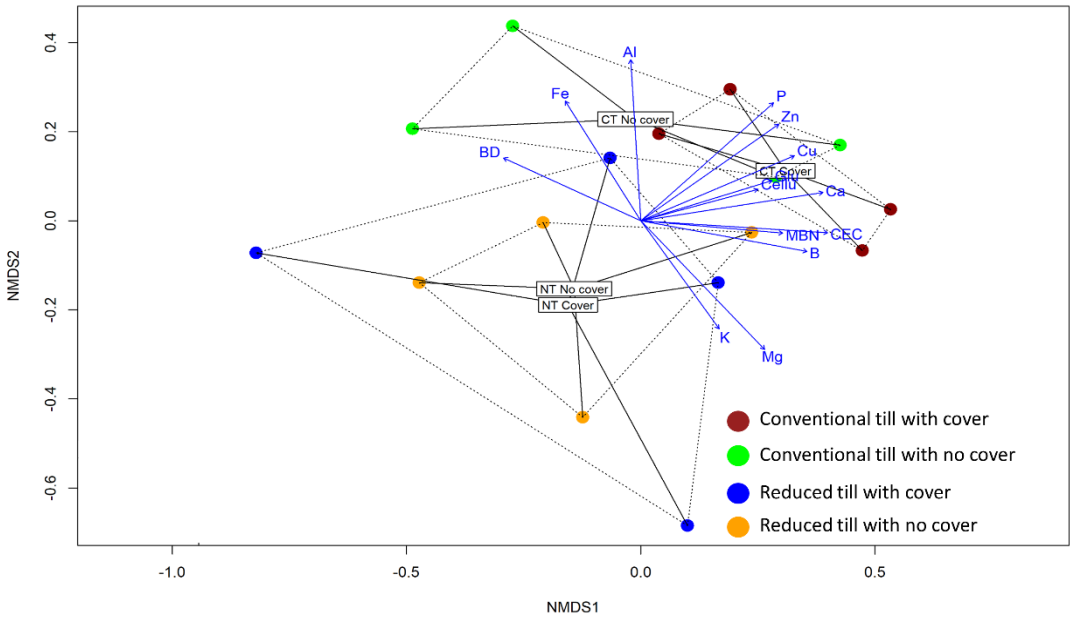

Figure A2: NMDS plot showing treatment differences as detected by perMANOVA ($P < 0.05$) and soil health parameters as shown by *envfit* ($P < 0.05$) for the subsurface soil in Site 2 during April 2016.

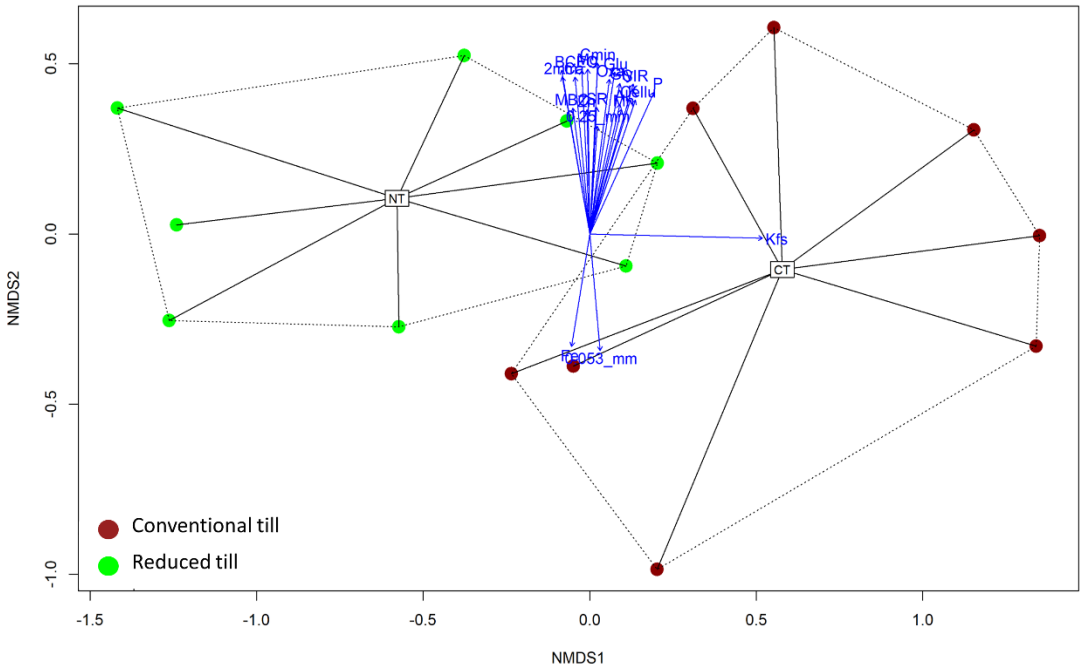

Figure A3: NMDS plot showing treatment differences as detected by perMANOVA (P < 0.05) and soil health parameters as shown by *envfit* (P < 0.05) for the surface soil in Site 4 during April 2016.

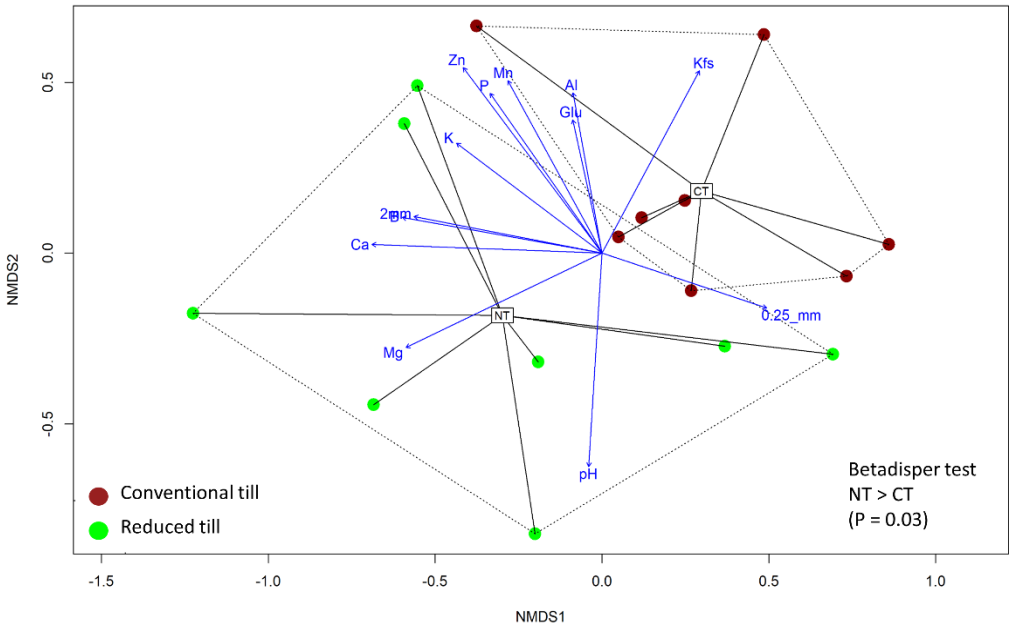

Figure A4: NMDS plot showing treatment differences as detected by perMANOVA (P < 0.05) and soil health parameters as shown by envfit (P < 0.05) for site 1 April 2017 for surface soil.

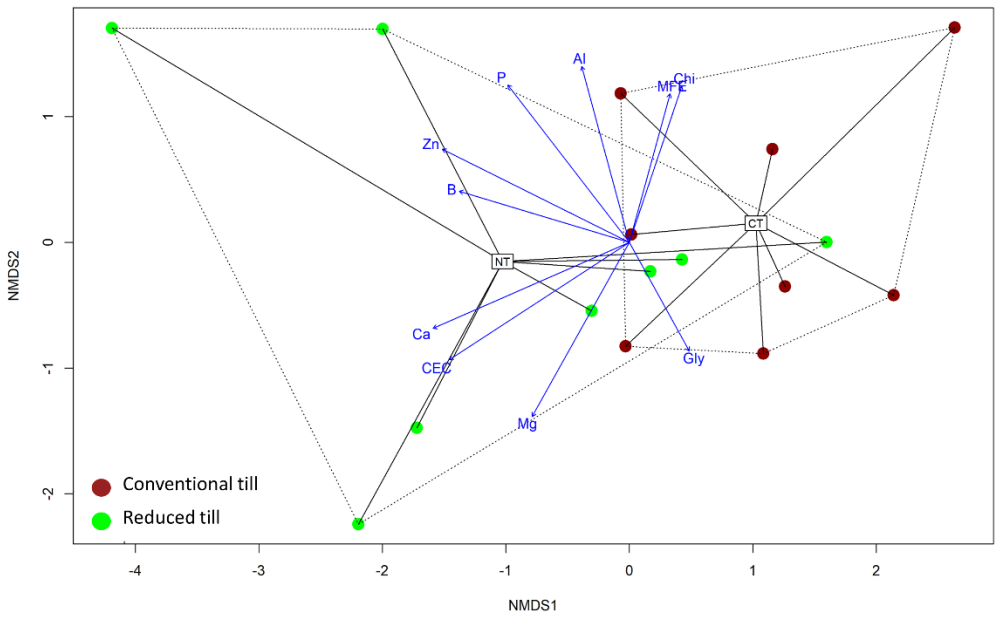

Figure A5: NMDS plot showing treatment differences as detected by perMANOVA ($P < 0.05$) and soil health parameters as shown by *envfit* ($P < 0.05$) for the subsurface soil in Site 1 during April 2017.

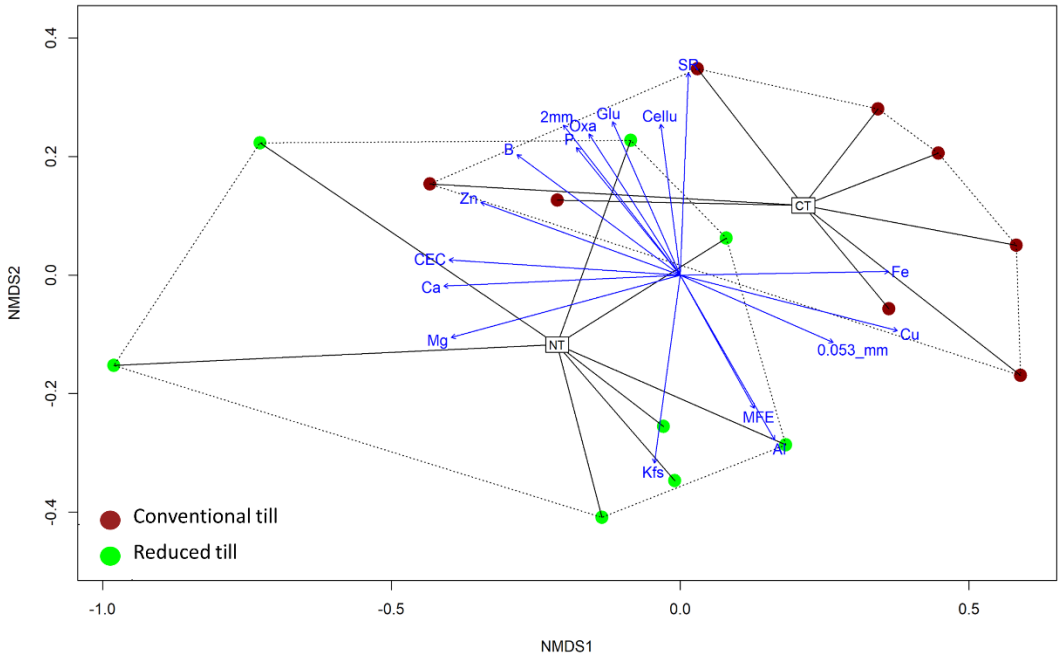

Figure A6: NMDS plot showing treatment differences as detected by perMANOVA ($P < 0.05$) and soil health parameters as shown by *envfit* ($P < 0.05$) for the surface soil in Site 3 during April 2017.

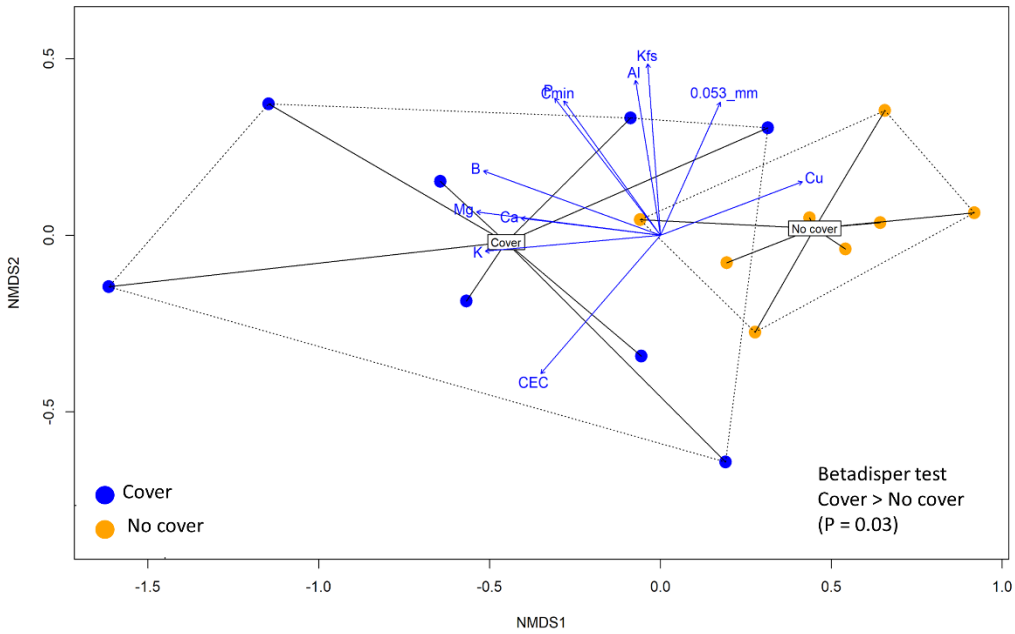

Figure A7: NMDS plot showing treatment differences as detected by perMANOVA (P < 0.05) and soil health parameters as shown by *envfit* (P < 0.05) for the surface soil in Site 2 during April 2017.

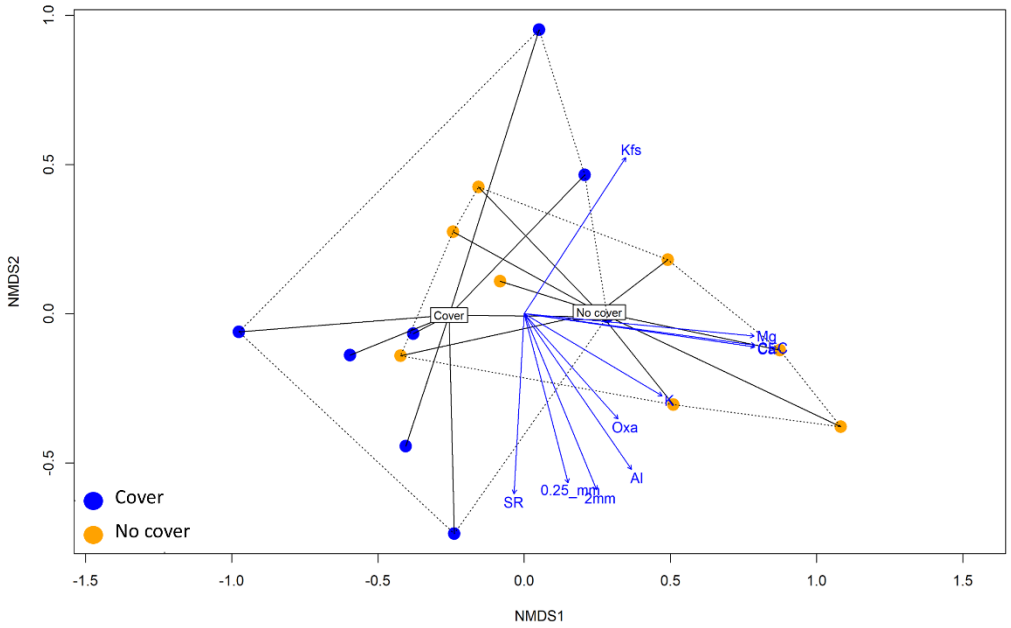

Figure A8: NMDS plot showing treatment differences as detected by perMANOVA (P < 0.05) and soil health parameters as shown by *envfit* (P < 0.05) for the surface soil in Site 4 during April 2017.

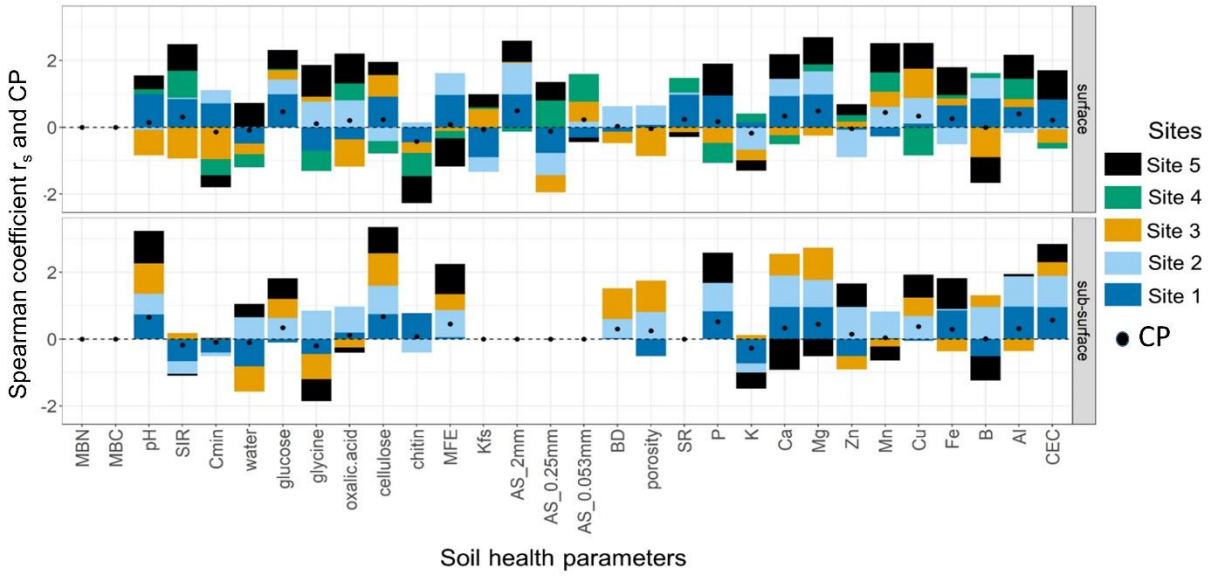

Figure A9: Spearman coefficient (r_s) and Consistency Parameter (*CP*) for all measured soil health parameters for all five sites, separated between surface and subsurface soil samples. The black dot for each parameter represents the consistency parameter (*CP*) for all five sites.

Appendix B (Appendix for Chapter 3)

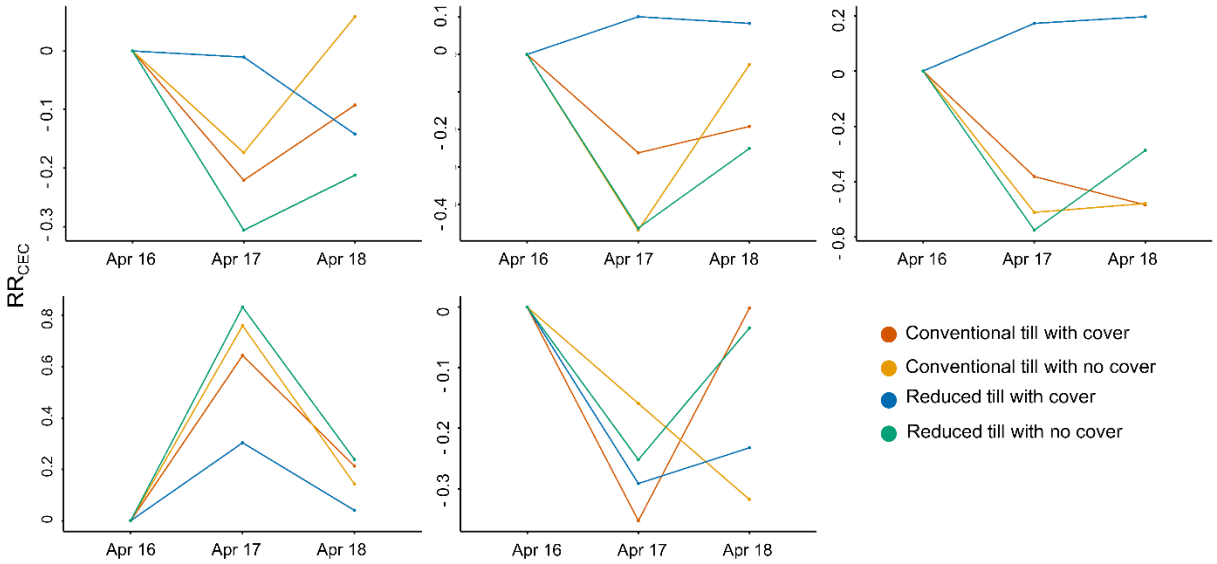

Figure B1: Response ratio for cation exchange capacity (RR_{CEC}) through time for i) Site 1; ii) Site 2; iii) Site 3; iv) Site 4; and v) Site 5. Apr 16: April 2016, Apr 17: April 2017 and Apr 18: April 2018.

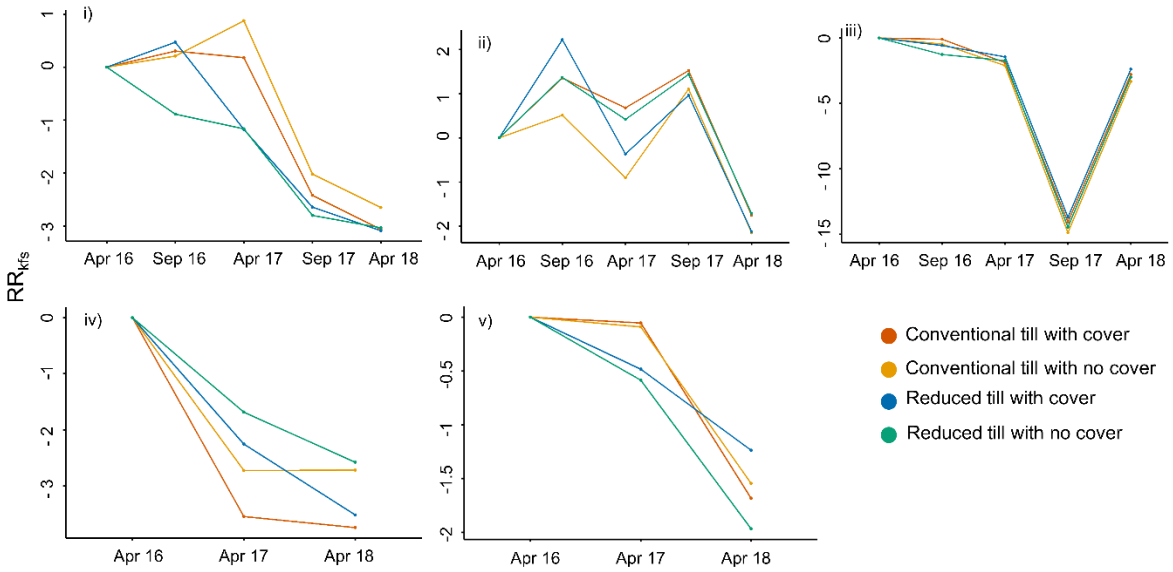

Figure B2: Response ratio for hydraulic conductivity (RR_{kfs}) through time for i) Site 1; ii) Site 2; iii) Site 3; iv) Site 4; and v) Site 5. Apr 16: April 2016, Sep 16: September 2016, Apr 17: April 2017, Sep 17: September 2017 and Apr 18: April 2018.

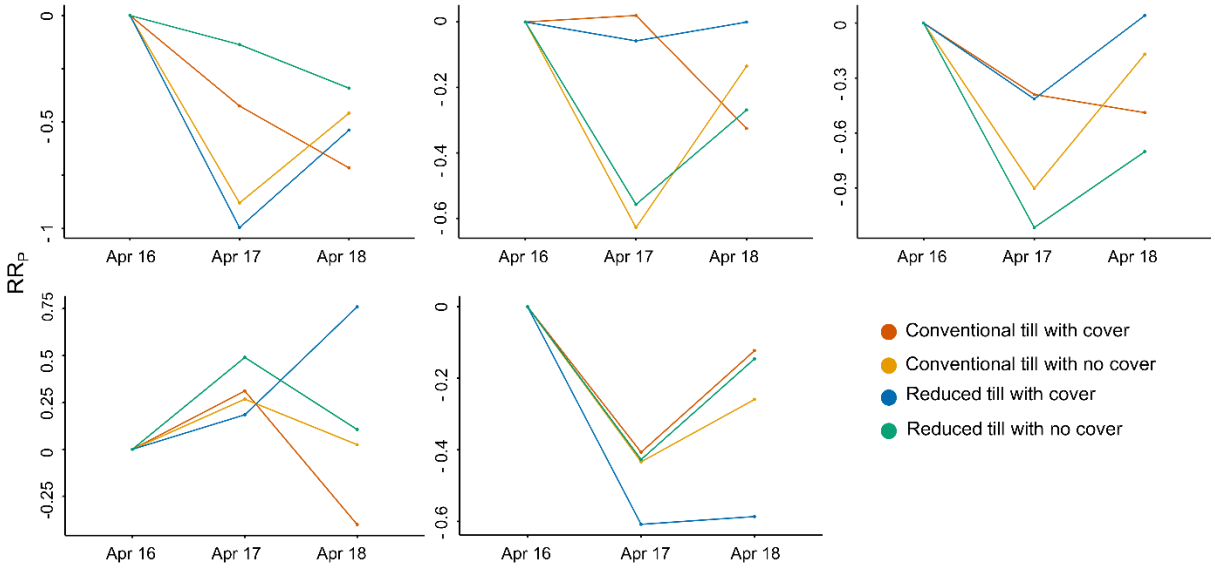

Figure B3: Response ratio for soil phosphorous (RR_P) through time for i) Site 1; ii) Site 2; iii) Site 3; iv) Site 4; and v) Site 5. Apr 16: April 2016, Apr 17: April 2017 and Apr 18: April 2018.

Appendix C (Appendix for Chapter 4)

The power input into a suspension by a stirring paddle, E_p [E], can be estimated as:

$$E_p = P_p t_p \quad [C1]$$

where P_p [E t^{-1}] is the power of the stirring paddle and t_p [t] is the time that the stirrer is operated.

The stirrer power can be estimated from the drag force of the paddle and the mean velocity of the stirrer paddle. Under the assumption that the mean stirrer velocity is 0.75 times the velocity at the end of the stirrer (Logan, 2012), E_p can be estimated as:

$$E_p = \frac{0.75^3}{2} b_{d,p} A_p \rho_w \omega^3 r_p{}^3 t_p \quad [C2]$$

where $b_{d,p}$ [-] is the paddle drag coefficient, A_p [L^2] is the cross-sectional area of the paddle, ρ_w [M L^{-3}] is the density of water, ω [L L^{-1} t^{-1}] is the angular velocity and r_p [L] is the radius of the paddle. For a paddle with a length-to-width ratio of 5, $b_{d,p}$ is ~1.2, while the maximum possible value of $b_{d,p}$ is 1.9 (Logan, 2012).

The CILAS 1190 laser diffraction unit used in this experiment has values related to the stirrer of A_p = 7.2 x 10^{-4} m^2, r_p = 0.029 m, ω = 36.6 rad s^{-1}. For 240 seconds of stirring and assuming $b_{d,p}$ = 1.2 and ρ_w = 1000 kg m^{-3}, the applied energy E_p is ~50 J. The total volume of suspension in the laser diffraction system is 620 ml, giving an energy density from the stirrer of 0.08 J ml^{-1}.

The pumping of the fluid also imparts energy to the suspension, due to friction losses within the tubing. The work applied by the pump, W_f [E], can be found as:

$$W_f = \Delta p \upsilon_t \quad [C3]$$

where Δp is the pressure drop within the tubing [M L^{-1} t^{-2}] and υ_t [L^3] is the total volume of the flow system, made up of tubing plus mixing chamber. Provided that the flow system and pump

represent a closed system, the work provided by the pump is equal to the energy absorbed by the suspension, E_f [E]. If we assume that the mixing chamber has a negligible contribution to the total volume and friction losses of the flow system, we can calculate the pressure drop in the tubing per unit length using the Darcy-Weisbach equation:

$$\frac{\Delta p}{L} = f \frac{\rho_w u_f^{\,2}}{2D_t} \qquad \text{[C4]}$$

where f [-] is a friction factor, D_t [L] is the diameter of the tubing, and u_f [L t^{-1}] is the velocity of the fluid.

The volume of tubing is equal to the area of tubing multiplied by the tubing length L_t [L], i.e., $\upsilon_{tubing} = \pi/4\ D_t^2 L_t$. Further, the total pressure drop depends on the total distance that the fluid has traveled, L_d [L], which is equal to the fluid velocity multiplied by the duration of pumping, t_d [t], i.e., $L_d = u_f t_f$. Assuming $\upsilon_t \approx \upsilon_{tubing}$, we can use these relationships in Equations [C3] and [C4] to obtain the energy associated with friction losses in the flow system:

$$E_f = f \frac{\pi \rho_w L_t D_t u_f^{\,3} t_d}{8} \qquad \text{[C5].}$$

The flow system of the unit also has values of L_t = 3.68 m, D_t = 6.4 x 10^{-3} m, u_f = 0.54 m s^{-1}. The Reynolds number is found by Re = $\rho_w u_f D_t/\mu$, where μ [M L^{-1} t^{-1}] is the dynamic viscosity of water (assumed here to equal 9 x 10^{-4} kg m^{-1} s^{-1}). For these flow conditions, Re = 3.84 x 10^3, which assuming a smooth pipe translates to a fraction factor of $f \approx 0.04$ (Brown, 2003). For 240 seconds of pumping, the applied energy E_f is ~14 J, which translates to an energy density of 0.02 J ml^{-1}. The combined energy of the pump and stirrer for four minutes is therefore ~0.1 J ml^{-1}, which represents approximately 1/5 of the energy provided by the ultrasonic unit at the lowest applied energy level (0.5 J ml^{-1}).

The limited effect of the stirrer and pump on aggregate stability measurements was verified by running an aggregated sample through the machine and collecting repeated measurements using four different homogenized subsamples. For the first subsample, the size distribution was measured immediately after adding the sample to the machine (0 seconds). The second subsample was measured after 240 seconds of continuous stirring and pumping. For the third subsample, the ultrasonic unit, stirrer, and pump were applied for 240 seconds before measurement, and the fourth subsample was allowed to run with sonication, pump, and stirrer for 480 seconds. The resulting data show that the pump plus stirrer caused a minor shift in the aggregate size distribution, whereas the initial 240 seconds of sonication caused a much larger shift towards smaller aggregates (Figure C1). Thus, the ultrasonic unit represents the dominant means by which energy is imparted onto the aggregates in this particular system. These calculations may prove useful to other users who either lack an ultrasonic unit or wish to apply lower levels of energy than sonication can provide.

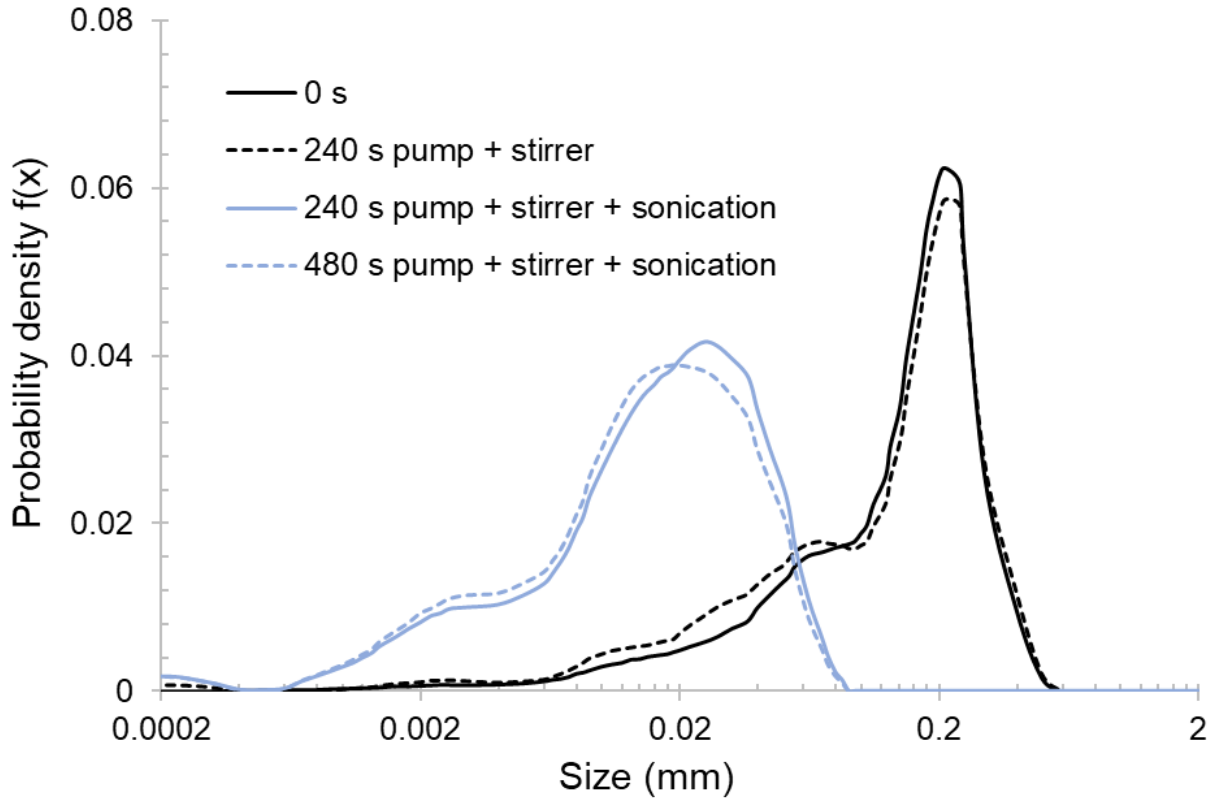

Figure C1: Probability density functions, *f*(*x*), for a soil sample from Site 2 that was analyzed immediately after addition to the laser diffraction machine (0 seconds), versus measured after: 240 seconds of pumping and stirring the sample; 240 seconds of pumping and stirring with ultrasonic; and 480 seconds of pumping and stirring with ultrasound.